Non-Markovian Epidemic Dynamics on Networks

Neil Sherborne

A thesis submitted for the degree of Doctor of Philosophy

University of Sussex

March 2018

Declaration

I hereby declare that this thesis has not been, and will not be, submitted in whole or in part to another University for any other academic award. Except where indicated by specific in the text, this thesis was composed by myself and the work contained therein my own.

Signature .....

Neil Sherborne

University of Sussex

NEIL SHERBORNE

THESIS SUBMITTED FOR THE DEGREE OF DOCTOR OF PHILOSOPHY

NON-MARKOVIAN EPIDEMIC DYNAMICS ON NETWORKS

SUMMARY

The use of networks to model the spread of epidemics through structured populations is widespread. However, epidemics on networks lead to intractable exact systems with the need to coarse grain and focus on some average quantities. Often, the underlying stochastic processes are Markovian and so are the resulting mean-field models constructed as systems of ordinary differential equations (ODEs). However, the lack of memory (or memorylessness) does not accurately describe real disease dynamics. For instance, many epidemiological studies have shown that the true distribution of the infectious period is rather centred around its mean, whereas the memoryless assumption imposes an exponential distribution on the infectious period. Assumptions such as these greatly affect the predicted course of an epidemic and can lead to inaccurate predictions about disease spread. Such limitations of existing approaches to modelling epidemics on networks motivated my efforts to develop non-Markovian models which would be better suited to capture essential realistic features of disease dynamics.

In the first part of my thesis I developed a pairwise, multi-stage SIR (susceptible-infected-recovered) model. Each infectious node goes through some $K \in \mathbb{N}$ infectious stages, which for $K > 1$ means that the infectious period is gamma-distributed. Analysis of the model provided analytic expressions for the epidemic threshold and the expected final epidemic size. Using available epidemiological data on the infectious periods of various diseases, I demonstrated the importance of considering the shape of the infectious period distribution.

The second part of the thesis expanded the framework of non-Markovian dynamics to networks with heterogeneous degree distributions with non-negligible levels of clustering. These properties are ubiquitous in many real-world networks and make model development and analysis much more challenging. To this end, I have derived and analysed a compact pairwise model with the number of equations being independent of the range of node degrees, and investigated the effects of clustering on epidemic dynamics.

My thesis culminated with the third part where I explored the relationships between

several different modelling methodologies, and derived an original non-Markovian Edge-Based Compartmental Model (EBCM) which allows both transmission and recovery to be arbitrary independent stochastic processes. The major result is a rigorous mathematical proof that the message passing (MP) model and the EBCM are equivalent, and thus, the EBCM is statistically exact on the ensemble of configuration model networks. From this consideration I derived a generalised pairwise-like model which I then used to build a model hierarchy, and to show that, given corresponding parameters and initial conditions, these models are identical to MP model or EBCM.

In the final part of my thesis I considered the important problem of coupling epidemic dynamics with changes in network structure in response to the perceived risk of the epidemic. This was framed as a susceptible-infected-susceptible (SIS) model on an adaptive network, where susceptible nodes can disconnect from infected neighbours and, after some fixed time delay, connect to a random susceptible node that they are not yet connected to. This model assumes that nodes have perfect information on the state of all other nodes. Robust oscillations were found in a significant region of the parameter space, including an enclosed region known as an 'endemic bubble'. The major contribution of this work was to show that oscillations can occur in a wide region of the parameter space, this is in stark contrast with most previous research where oscillations were limited to a very narrow region of the parameter space.

Any mathematical model is a simplification of reality where assumptions must be made. The models presented here show the importance of interrogating these assumptions to ensure that they are as realistic as possible while still being amenable to analysis.

Acknowledgements

I must start by thanking the people who, more than anyone else, made this thesis possible. I feel incredibly fortunate that both of my supervisors, Dr Konstantin Blyuss and Dr Istvan Kiss, have been so engaged and enthusiastic throughout the entirety of my studies. Their guidance, advice and support was never lacking over almost four years working together. They have set the standard for my future working relationships, and they have set it very high.

I would also like to thank Joel C Miller, who I had the privilege to collaborate with.

The EPSRC and the University of Sussex have provided the funding and support that enabled me to undertake this research and develop my knowledge and my skills. I would also like to thank the staff in the School of Mathematical and Physical Sciences for their kind support of all doctoral students.

Lastly, I would like to thank my friends, family and my partner for their consistent emotional support and encouragement.

List of publications and author contributions

1. **Dynamics of multi-stage infections on networks**

   Sherborne, N., Blyuss, K.B. and Kiss, I.Z., 2015. Bulletin of Mathematical Biology, Vol. 77, pp. 1909-1933.

   - N. Sherborne proved the final epidemic size relation and found the value of the epidemic threshold parameter R_0, produced all of the numerical solution and simulation results and wrote the bulk of the paper.
   - K.B. Blyuss conceived the goals of the study, assisted with the linear stability analysis and numerical solution to the system of ODEs, and wrote a portion of the paper.
   - I.Z. Kiss conceived the goals of the study, assisted with stochastic simulation, and wrote a portion of the paper.

2. **Compact pairwise models for epidemics with multiple infectious stages on degree heterogeneous and clustered networks**

   Sherborne, N., Blyuss, K.B. and Kiss, I.Z., 2016. Journal of Theoretical Biology, Vol. 407, pp. 387-400.

   - N. Sherborne derived the models for unclustered and clustered networks, performed the model analysis, numerical ODE solution and stochastic simulation, and wrote the bulk of the paper.
   - K. B. Blyuss assisted with the analysis of the epidemic threshold and wrote a portion of the paper.
   - I. Z. Kiss developed the compact moment closure approximation and assisted with network clustering algorithm.

3. **Mean-field models for non-Markovian epidemics on networks**

   Sherborne, N., Miller, J.C., Blyuss, K.B. and Kiss, I.Z., 2018. Journal of Mathematical Biology, Vol. 76, pp. 755-778.

   - N. Sherborne conceived the goals of the study, derived the pairwise-like model and all subsequent equivalences, and contributed to the proof of theorem 1. He produced all model solution and simulation results and wrote the bulk of the paper.
   - J.C. Miller derived the non-Markovian edge-based compartmental model and the final epidemic size result, and played a significant role in the proof of Theorem 1.
   - K.B. Blyuss conceived the goals of the study, assisted with and corrected some of the model equivalences, and edited the paper.
   - I.Z. Kiss conceived the goals of the study, played a significant role in the proof of Theorem 1, and edited the paper.

4. **Bursting endemic bubbles with adaptive rewiring**

   Sherborne, N., Blyuss, K.B., and Kiss, I.Z., 2018. arXiv preprint arXiv:1712.04536. Accepted for publication in Physical Review E

   - N. Sherborne developed the model and all analysis, the numerical solutions and comparisons to stochastic simulation.
   - K.B. Blyuss helped produce the figures and edited the paper.
   - I.Z. Kiss devised the subject of the paper and wrote a portion of it.

Contents

Chapter 1

Introduction

1.1 Background and motivation

There are many examples throughout history of the devastating impact that infectious diseases have had [110]. For centuries the causes of infection were poorly understood; until the 19th century many physicians believed in the miasma theory of disease which stated that the origin of an epidemic was a miasma or "bad air" given off by rotting organic material. With the discovery and development of germ theory, proposed by Fracastoro and later popularised by Pasteur [130], the bacterial and viral causes of many diseases were identified. In many cases this led to cures and vaccines being available. Despite this, infectious diseases have been a consistent danger to humans and their livelihoods, and are still a threat today, as evidenced by major outbreaks of foot-and-mouth disease [157], SARS [41, 97], influenza [50, 113], and Ebola [156] since the turn of the millennium. Naturally, therefore, people have long desired to understand how these diseases spread, so that preventative measures can be put in place and optimised to minimise the negative impact of infectious disease outbreaks.

The first attempt to model the spread of an infectious disease was the smallpox model of Bernoulli in the 18th century [40]. However, the field of mathematical epidemiology is generally accepted to have truly begun with the system of differential equations proposed by Kermack and McKendrick in 1927 [89]. They were the first to divide the population into compartments based on their disease status and to model infection as a result of contact between healthy and infected individuals.

As with any mathematical model, assumptions about the underlying processes must be made. In the case of infectious disease dynamics two major assumptions are the

timing and regularity of contact capable of transmitting the disease from an infectious individual to a healthy and susceptible person, as well as the length of time people remain infectious after they first become infected, known as the *infectious period*. Typically, for model simplicity and tractability, it is assumed that the infection and recovery processes are Markovian (memoryless), and thus, the inter-event times, i.e. the time between an infectious individual attempting to transmit the disease, or between infection and recovery, are exponentially distributed. However, this assumption does not accurately reflect true epidemic dynamics. In the case of human interactions, although it is difficult if not impossible to be precise, studies of various activities have suggested that our true behaviour is much more irregular and "bursty" [77, 153, 160]. For recovery processes the picture is clearer - the typical infectious period of a disease has a uni-modal shape centred around a mean duration [8, 152, 168]. Both of these true representations differ significantly from the Markovian assumption and thus, however useful Markovian models are, they are always flawed in this manner.

In this thesis I consider the modelling and analysis of the spread of infectious disease on networks, especially in cases where the epidemic dynamics are non-Markovian, in order to better understand how non-Markovianity impacts the dynamics of a disease and quantities, such as the epidemic threshold and final epidemic size, or long-term behaviour of the epidemic. In this introduction I provide an overview of networks and discuss some of their relevant properties, outline the main techniques for modelling epidemics on networks, and give an overview of the research presented in the subsequent Chapters.

1.2 Network/Graph theory and epidemic simulation

The use of networks to model the spread of epidemics through structured populations is widespread [35, 91, 131]. Using networks to model explicit contact structures has reinvented mathematical epidemiology and led to the development of a range of new techniques [84, 119, 162]. We begin by introducing the fundamental concepts of networks and their metrics.

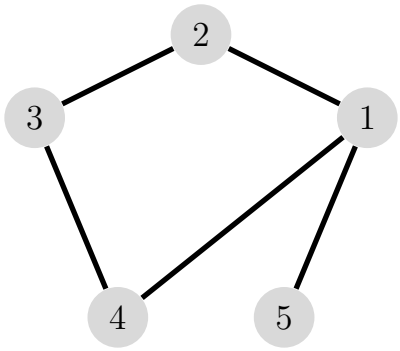

$$A = \begin{pmatrix} 0 & 1 & 0 & 1 & 1 \\ 1 & 0 & 1 & 0 & 0 \\ 0 & 1 & 0 & 1 & 0 \\ 1 & 0 & 1 & 0 & 0 \\ 1 & 0 & 0 & 0 & 0 \end{pmatrix}. \quad (1.7)$$

Figure 1.1: A toy undirected network of five nodes, with the corresponding adjacency matrix A.

1.2.1 Graph theory

A graph $\mathcal{G} = \{\mathcal{V}, \mathcal{E}\}$ is defined as a set of vertices (or nodes), $\mathcal{V}$, and edges, $\mathcal{E}$, which connect them. These edges describe the relationships between nodes. Assuming that $|\mathcal{V}| = N$ we have a network of N nodes. In an epidemiological context nodes usually denote individuals, and edges describe possible paths for disease transmission. An $N \times N$ adjacency matrix A is often used to describe the network. For a pair of nodes i and j we say that $a_{i,j} = 1$ if node i is connected to node j, and zero otherwise. On weighted networks some variable may be used in place of 1 to confer information about the closeness/weight of a relation between nodes. Since nodes cannot infect themselves, we set $a_{i,i} = 0$ for all i. In general we consider undirected networks, with $a_{i,j} = a_{j,i}$. Practically, this means that if node i can transmit a pathogen to j, then j also has the potential to transmit to i. Figure 1.1 shows an example of a network and its corresponding adjacency matrix.

The total number of neighbours of a node is known as its *degree*, which for any node i can be found as $k_i = \sum_j a_{i,j}$. The degree distribution, p_k, gives the probability that a randomly chosen node will have degree k. It is useful to define the moment generating function (MGF), G_0 for this distribution as follows

$$G_0(x) := \sum_k p_k x^k, \quad (1.1)$$

which gives the mean degree as $\langle k \rangle = G_0'(1)$.

Related to the degree distribution is the *excess degree distribution*, which gives the probability, q_k, that a node reached by traversing a randomly selected edge reaches a

node of remaining degree $k-1$ (i.e. excluding the initially selected edge) [126]. To find this distribution, we first note that there are $\langle k\rangle N$ edges in the network, for a given k there are $p_k N$ nodes with degree k and $kp_k N$ edges connecting to these nodes, and, therefore, $q_k = kp_k/\langle k\rangle$. Then the generating function for this distribution, $G_1(x)$, is given by

$$G_1(x) := \sum_k q_k x^{k-1} = \frac{1}{\langle k\rangle}\sum_k p_k k x^{k-1} = G_0'(x). \tag{1.2}$$

Equations (1.1) and (1.2) will play an important role for the analysis in Chapter 3.

Another network property that is relevant to epidemic spread is clustering, which measures the extent to which neighbours of a common node are likely to also be directly connected [166]. Data collected from real networks often identifies significant levels of clustering [51, 128, 167]. This makes intuitive sense, as friends and colleagues are likely to interact as part of a clique, and families that live together will all interact with each other. Clustering is defined as the ratio of closed three-node paths (triangles) to all triples in the network. This can be found for any network with the adjacency matrix A by calculating the clustering coefficient [84]

$$\varphi = \frac{\text{trace}(A^3)}{||A^2|| - \text{trace}(A^2)},$$

where $||\cdot||$ denotes the sum of all the elements of the matrix.

Generally, there are two options when using networks to model disease transmission. Firstly, we may use real-world data or, secondly, we can construct a synthetic network model that is designed with some tunable properties similar to those observed in real-world networks, e.g. heterogeneous degree or clustering. Next, I review a few algorithms which create such networks.

1.2.2 Constructing random graphs

The earliest known algorithm for generating random networks is known as the Erdős-Rényi model, or the random graph model [46]. This model is sometimes expressed as $G(N,p)$ where N is the number of nodes in the network, and p is the probability of any two nodes i, j ($i \neq j$) being connected. To construct the network, a Bernoulli trial with success rate p is performed for every possible pair of nodes. The resulting network has a binomial distribution with mean degree $\langle k\rangle = Np$.

Extensive studies of real-world social, biological and technological networks suggest that such networks do not conform to this structure and that, in reality, there is much

greater variance in the degree distribution [1, 99, 104, 167]. Motivated by the scale-free structure of the internet and the processes that dictate how new nodes join the network, Barabási and Albert introduced a new algorithm to construct random networks based on preferential attachment [1, 11]. The method which bears their names works as follows: a small fully-connected network of some m_0 nodes is created. Then at every step a new node is introduced to the network, and it draws $m \leq m_0$ edges to existing nodes in the network. The probability that an existing node i will be chosen for a connection, $\Pi(k_i)$, is based on its existing degree, such that $\Pi(k_i) = \frac{k_i}{\sum_j k_j}$. This process results in a network with scale-free degree distribution proportional to a power law $p_k \sim k^{-3}$.

In many cases, we wish to have total control over the degree distribution. Introduced by Bollobás [20], based on the work of Bender and Canfield [15], the configuration model (CM) is a method for generating networks with a desired degree distribution. The method starts by assigning a degree k_i to each node i according to the prescribed degree distribution. Then k_i half-edges (or stubs) are drawn. The half-edges are then randomly paired to form full edges connecting pairs of nodes. In order to successfully complete the algorithm there must be an even number of half-edges. In addition, there are several other limitations to the method. Multi-edges can occur when the same pair of nodes is selected multiple times, and self-loops emerge when two half-edges from the same node are paired. However, such occurrences are rare for large networks. So long as the network is sparse, CM networks are locally tree-like. This means that short cycles are rare, two connected nodes are unlikely to share any other neighbours. Thus, as it stands this method is unsuitable to generate clustered networks.

However, there are numerous algorithms available to generate clustered networks [61, 140]. One method is the so-called *big-V rewiring method* [10]. The algorithm takes an existing network and searches for chains of five nodes $u - v - w - x - y$, cuts the edges $u - v$ and $x - y$, and draws new edges $u - y$ and $v - x$, introducing a triangle to the network without changing the degree of any node, as shown in Fig. 1.2. If the local clustering is increased by the rewiring then it is accepted, otherwise it is rejected. The process continues until some target value of the clustering coefficient is achieved. When the CM and big-V rewiring methods are used in conjunction, the resulting random networks have tunable degree distribution and clustering.

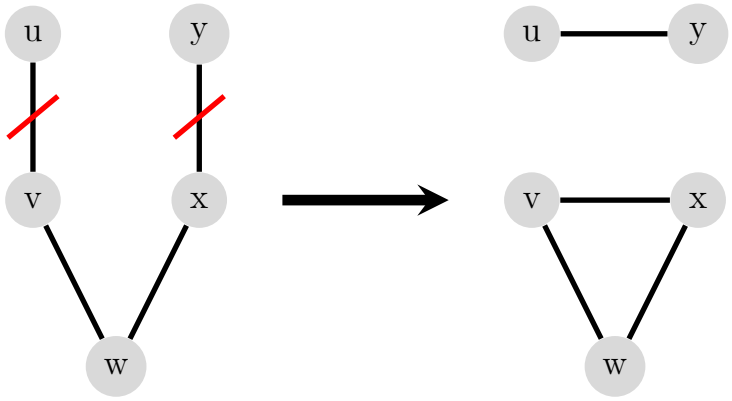

Figure 1.2: The central step of the big-V rewiring process. V-shaped chains are found, edges $u-v$ and $x-y$ are cut and replaced to form a triangle and an independent edge.

1.2.3 Simulation methods

The Gillespie algorithm

Once a network has been constructed, it is possible to simulate an epidemic spreading on that network. The Gillespie algorithm is a commonly used method to simulate statistically exact trajectories of large systems [55]. Although initially proposed to simulate systems of chemical reactions, it has subsequently been used to simulate stochastic dynamics in a variety of contexts, including infectious diseases. The algorithm relies on all processes being memoryless and uses the fact that, for any independent Poisson processes, the combined (or pooled) process is also Poisson, with the rate being equal to the sum of all the independent processes. This means that for each susceptible individual, the rate at which they will become infected is equal to the transmission rate multiplied by the number of infectious neighbours. Here we detail the algorithm in the case of a simple SIS (susceptible-infected-susceptible) epidemic on a network of N nodes, where τ is the per-contact transmission parameter, and γ is the recovery parameter. We also have an $N \times N$ adjacency matrix A, and an $N \times 1$ vector v holding the current state of all nodes. The algorithm then proceeds as follows.

1. Randomly select n nodes i_1, i_2, …, i_n to be the index cases of the epidemic, set $v(i_k) = 1$ for $k = 1, 2, \ldots, n$, all others zero.

2. For each node i calculate its rate λ_i at which it will either become infected or recover:

- If node i is susceptible, then $\lambda_i = \tau \sum_j a_{i,j} v(j)$.
- If node i is infected, $\lambda_i = \gamma$.

3. Generate two random numbers $u_1, u_2 \sim U(0,1)$.

4. Calculate
$$\Delta = \sum_{i=1}^{N} \lambda_i. \tag{1.3}$$

5. To determine the time of the next event, set $dt = 1/\Delta \ln(1/u_1)$. This is equivalent to randomly drawing from an exponential distribution with rate equal to Δ.

6. The node that is updated during this step is chosen uniformly at random, so that the probability that a node i is chosen is given by
$$P_i = \frac{\lambda_i}{\Delta}. \tag{1.4}$$

7. Let x denote the chosen node. Set $t = t + dt$ and update $v(x)$: if x is newly infected, then $v(x) = 1$, otherwise if it is newly recovered, set $v(x) = 0$. Update λ for node x and its neighbours according to step 2.

8. Return to step 3 and repeat until the infection dies out or some cut-off time is reached.

With some simple modifications this algorithm can be adapted to SIR-type infections, for instance, if node i is recovered/removed, then $\lambda_i \equiv 0$.

To get an idea of the typical dynamics of an epidemic it is often necessary to average across multiple iterations of a simulation. Care must be taken when this is done because the times of transmission and recovery events are irregular. Figure 1.3 shows how regular time intervals can be imposed.

The Gillespie algorithm with delays

In its classical formulation, the Gillespie algorithm is limited to Markovian processes. However, some modified versions of the algorithm exist that allow certain non-Markovian processes to be included as part of the dynamics [5]. Bratsun et al. [21] and Barrio et al. [13] developed an algorithm that incorporated time delays into chemical reactions, and this algorithm is used later in the thesis. For our purposes, suppose we wish to simulate an epidemic outbreak where the transmission process is memoryless, but the

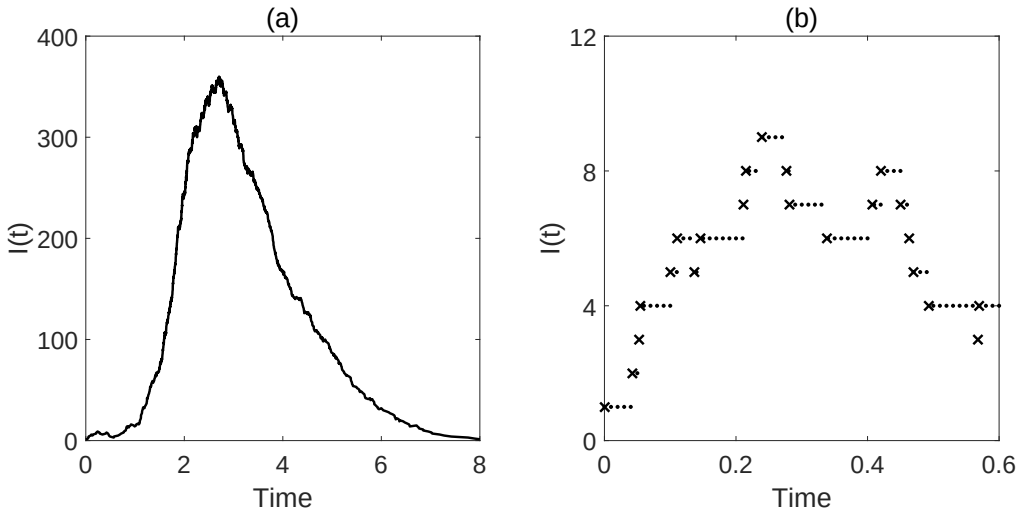

Figure 1.3: In (a) we show a realisation of a stochastic SIR epidemic on a random graph of 1000 nodes. The crosses in (b) show the early behaviour of the same epidemic, the dots show the number of infected individuals at regular time intervals.

infectious period is distributed according to some arbitrary, independent distribution $\rho(a)$. Whenever a node is infected, an infectious period is randomly selected according to this distribution and stored in an array; for all infected nodes we set $\lambda_i = 0$. The algorithm continues through the steps shown above up to and including step 5. Then the timestep dt is compared to the minimum time remaining in the delayed events (i.e. the node that will be next to recover), denoted dt_D. If $dt < dt_D$, the method in Step 6 is repeated to find the new node to infect, otherwise the recovery takes place, and dt is discarded. The overall time is then updated according to which event takes place, and $\min(dt, dt_D)$ is subtracted from the stored recovery waiting times.

Fully non-Markovian simulation methods

Due to the large number of realistic systems which exhibit non-Markovian behaviour, there is naturally a need for efficient algorithms to simulate their evolution. One such approach is the non-Markovian Gillespie algorithm (nMGA) derived by Boguñá et al. [19]. The steps of the algorithm remain largely the same as detailed above for the classical Gillespie algorithm, with changes made to (1.3) and (1.4).

As the authors discuss, one can no longer calculate the risk of infection for a susceptible node by simply summing across its infected neighbours, since the chance of being infected across an $S - I$ link depends on the age of infection of each infected

neighbour. In this case, the recovery of each infected node and the transmission across each $S-I$ edge are independent processes with their own inter-event time distributions. A susceptible node with more than one infected neighbour will be infected at the time of the first firing event of the active edges.

Suppose that the inter-event time for each process i is distributed according to $\psi_i(\tau)$, with survival function

$$\Psi_i(t_i) = \int_{t_i}^{\infty} \psi_i(t')\, dt'$$

where t_i is the time elapsed since i was last active. We also introduce Φ as the probability that no event occurs for an interval δt. For each i this is conditional on the last time it was active, so that we have the product

$$\Phi(\delta t|\{t_j\}) = \prod_j \frac{\Psi_j(t_j + \delta t)}{\Psi_j(t_j)}, \tag{1.5}$$

where $\{t_j\}$ is the set of times elapsed since the last occurrence of each process. This quantity is then equated to u_1 in Step 5 of the Gillespie algorithm above. Choosing which event is active is done in the same manner as step 6 of the Gillespie algorithm, although now for each i we have

$$\lambda_i(t_i + \delta t) = \frac{\psi(t_i + \delta t)}{\Psi_i(t_i + \delta t)}. \tag{1.6}$$

Finally, t_i must be updated for each event and the overall time is updated to $t + \delta t$.

In practice, $\Phi(\delta t|\{t_j\})$ is expensive to compute, and thus an approximation can be preferred. When the total size of the network N is large, this quantity is close to zero for all but very small δt, and can, therefore, be approximated by a Taylor expansion around $\delta t = 0$. Performing this expansion in (1.5) yields the following approximation

$$\Phi(\delta t|\{t_j\}) \approx e^{-\delta t \Delta},$$

where $\Delta = \sum_i \lambda_i(\{t_i\})$ [19].

A more efficient algorithm for simulating non-Markovian dynamics is the *Laplace Gillespie algorithm* of Masuda and Rocha [109]. The algorithm starts with a density function, $p_i(\lambda)$, for each process i, and then imposes the condition that the inter-event time distribution for process i is given by

$$\psi_i(a) = \int_0^{\infty} p_i(\lambda)\lambda e^{-\lambda a}\, d\lambda,$$

which then means that the survival function, $\Psi_i(a)$, is the Laplace transform of $p_i(\lambda)$. In terms of practical implementation, the algorithm is similar to the classical Gillespie

algorithm, but with the rate of the Poisson process λ_i for event i being drawn from the density $p_i(\lambda_i)$. This algorithm does not rely on an approximation to be efficient and is faster than the nMGA [109]. However, the inter-event time cannot be directly chosen, and the survival functions must be completely monotone, i.e.

$$(-1)^n \frac{d^n \Psi_i(a)}{da^n} \geq 0 \quad n \in \mathbb{Z}_0^+,\, a > 0,\, \forall\, i.$$

However, many inter-event time distributions are possible. The authors use this algorithm to simulate an SIR-type epidemic on networks using a node-centric approach.

Now, with networks in place modelling social contact and having discussed the stochastic epidemic process we are ready to present an overview of the main modelling techniques for epidemics on networks. However, we begin with simple compartmental models.

1.3 Modelling techniques

1.3.1 Compartmental models

The earliest mathematical models for the spread of an infectious disease commonly made the assumption that the population was fully mixed. This means that every individual has the potential to directly transmit the pathogen to any other member of the same population. This is equivalent to a fully connected network, or edges rewiring at an infinitely fast rate. One of the best known models of this type is that of Kermack and McKendrick [89]. Other standard models of this kind have been summarised by Anderson and May, Keeling and Rohani, and others [6, 83]. Typically, these models begin by splitting the population of size N into compartments based on the disease status of individuals at a given time. Individuals that are healthy but can be infected are considered susceptible, S, individuals that are infected and infectious are put into the infected compartment, I, and those who have recovered or died from the disease - or have been vaccinated - and have immunity are placed into the recovered/removed compartment, R. For some diseases it is desirable to have a compartment for individuals in the latent phase of infection, when they have acquired the infected but are not yet capable of transmitting the disease to others, this is usually referred to as the exposed compartment, E.

Diseases are then modelled as being either SIR (susceptible-infectious-recovered) or SIS (susceptible-infectious-susceptible) type (or SEIR, SEIS) according to the nature

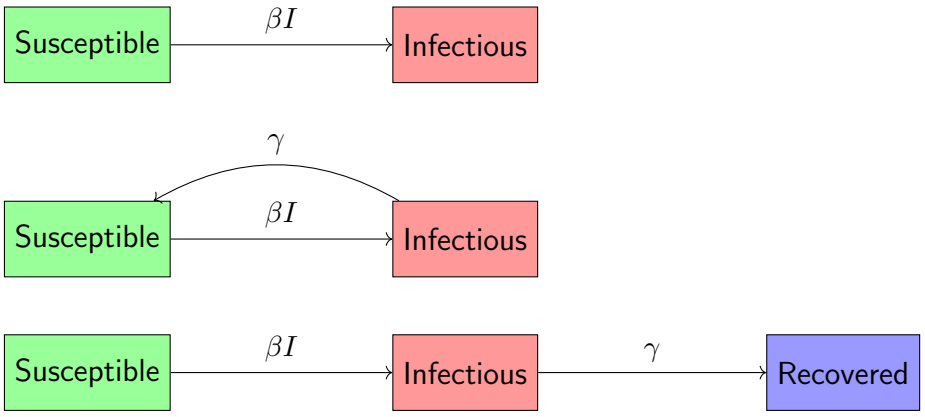

Figure 1.4: State changes and rates for SI, SIS and SIR models with Markovian transmission and recovery processes.

of the disease. For example, SIR models are used for diseases such as varicella where, typically, lifelong immunity is acquired after recovery [56]; whereas SIS models are appropriate for diseases where newly recovered individuals are still under threat of further infection, as is the case for some sexually transmitted diseases [171]. In rare cases it may be desirable to consider a disease where recovery is impossible, which can be modelled using SI dynamics. The transitions between different states for these models are illustrated in Fig. 1.4.

Under the above assumptions, the SIR and SIS models can be formulated as systems of ordinary differential equations (ODEs):

$$\begin{aligned} \frac{dS}{dt} &= \dot{S} = -\beta I \frac{S}{N}, \\ \frac{dI}{dt} &= \dot{I} = \beta I \frac{S}{N} - \gamma I, \\ \frac{dR}{dt} &= \dot{R} = \gamma I, \end{aligned} \tag{1.7}$$

for the SIR model, and

$$\begin{aligned} \frac{dS}{dt} &= \dot{S} = -\beta I \frac{S}{N} + \gamma I, \\ \frac{dI}{dt} &= \dot{I} = \beta I \frac{S}{N} - \gamma I, \end{aligned} \tag{1.8}$$

for the the SIS model, where γ is the rate at which an infected individual recovers, and β is the population-level transmission rate, i.e. the rate at which an individual makes contact with another random member of the population and, if they are infected, transmits the disease.

These models have been studied thoroughly, and several well-known results have emerged from their analysis. One of the most fundamental characteristics of epidemic dynamics is the *basic reproductive ratio*, $\mathcal{R}_0$, defined as the expected number of secondary infections caused by a single typical infectious individual in a completely susceptible population. If $\mathcal{R}_0 > 1$, then the initial outbreak will produce an epidemic, while if $\mathcal{R}_0 < 1$, the disease will die out. For these models, stability analysis of the disease free equilibrium (DFE) gives the value of the basic reproduction number as $\mathcal{R}_0 = \beta/\gamma$. This can also be seen directly from the equation for $I(t)$ taking $I(0) \approx 0$, $S(0) \approx N$, which shows that for a pathogen to spread beyond the initial number of infectives, and for $I(t)$ to grow, we need $\dot{I}(t) > 0$ for small t, which is satisfied iff $\mathcal{R}_0 > 1$. In the SIS model this transition also marks the point where the disease is expected to reach an endemic equilibrium within the population. By contrast, every SIR epidemic must reach a point where the infection dies out, having infected some fraction $R(\infty)/N$ of the population. This fraction, known as the *final epidemic size*, is given by $\frac{R(\infty)}{N} = \frac{(N-S(\infty))}{N} = 1 - e^{-\mathcal{R}_0 R(\infty)/N}$ [6, 105].

Whilst mathematically convenient, these models rely on the not entirely realistic assumption that disease transmission and recovery are both exponentially distributed processes. However, built on this framework, models have been proposed which no longer rely on this assumption and thus better reflect reality. These models can be represented as systems of integro-differential equations (IDEs) [86, 89], or systems of partial differential equations (PDEs) where the age of infection is explicitly included in the model [6]. Other models have included temporary immunity in the form of a system of delay differential equations (DDEs), where after some delay recovered individuals again become susceptible to the disease [17, 96].

A relatively simple methodology to overcome the non-exponentially distributed nature of infection and recovery is to employ a multi-stage approach to the infection [4, 102, 103, 168]. Let the number of disease stages be some positive integer K, the newly infectious individuals enter the compartment I_1, with rate $K\gamma$ they then transition into I_2, where they are still infectious, and this process repeats until they exit I_K and recover. The states and transition rates for this model are illustrated in Fig. 1.5. The total time spent being infected is then the sum of K exponentially distributed times, which obeys a well-known gamma distribution [42]. Modifying the transition rates to $K\gamma$ ensures that the mean infectious period of the underlying stochastic process remains $1/\gamma$. For $K \geq 2$ this gives a peaked distribution more closely resembling

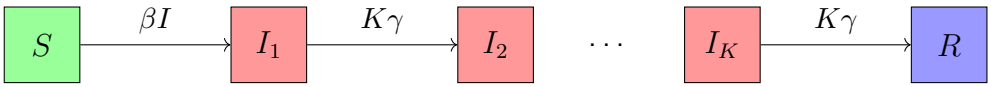

Figure 1.5: State transitions of the SI^{K}R model.

the distribution of infectious periods for many real diseases. The number of stages K provides a additional free parameter that can be tuned to better represent the disease being studied. Wearing et al. [168] showed that compared to a multi-stage SI^{K}R model using realistic data, the standard SIR model with the same disease parameters underestimates the speed of an epidemic but does not affect $\mathcal{R}_0$ or the final epidemic size. In Chapters 2 and 3 we extend this approach to network-structured populations.

Whilst these models can provide valuable insights into disease dynamics, they are limited by a fundamental assumption of a well-mixed population. In reality, however, social interactions between individuals are rather more structured, and most people only directly interact with a small fraction of the total population. This suggests the need for using network-based formulations of epidemic models.

1.3.2 Exact models on networks

Let us begin by defining an exact system using the forward Kolmogorov equations, also known as master equations [78]. The model gives the probability of the network being in each possible state. For SIS dynamics each node can be either susceptible or infected, for a network of N nodes this means that there are 2^N possible states. For SIR dynamics there are 3^N states. As an example of an exact model consider a fully connected network of three nodes, i.e. a triangle. Further, assume SIS dynamics and exponentially distributed inter-event times. Given these assumptions we can construct a continuous time Markov chain that will describe the probability of the network being in any state. The state space for this model is

$$\{SSS, SSI, SIS, ISS, SII, ISI, IIS, III\}.$$

Define $\mathcal{X}_{XYZ}$ as the probability of the network being in state XYZ where X represents the state of the first node, Y the second and Z the third, and $X, Y, Z \in \{S, I\}$. It is possible to write a system of differential equations to describe the transitions between different states. The epidemic spreads in the same manner as the stochastic model, recovery events occur with rate γ and transmission events occur with rate τ multiplied by the number of infected neighbours the node being infected has. For the given example

this yields

$$
\begin{aligned}
\dot{\mathcal{X}}_{SSS} &= \gamma\left(\mathcal{X}_{SSI} + \mathcal{X}_{SIS} + \mathcal{X}_{ISS}\right), \\
\dot{\mathcal{X}}_{SSI} &= \gamma\left(\mathcal{X}_{SII} + \mathcal{X}_{ISI}\right) - (2\tau+\gamma)\mathcal{X}_{SSI}, \\
\dot{\mathcal{X}}_{SIS} &= \gamma\left(\mathcal{X}_{SII} + \mathcal{X}_{IIS}\right) - (2\tau+\gamma)\mathcal{X}_{SIS}, \\
\dot{\mathcal{X}}_{ISS} &= \gamma\left(\mathcal{X}_{ISI} + \mathcal{X}_{IIS}\right) - (2\tau+\gamma)\mathcal{X}_{ISS}, \\
\dot{\mathcal{X}}_{SII} &= \gamma X_{III} + \tau\left(\mathcal{X}_{SSI} + \mathcal{X}_{SIS}\right) - 2(\tau+\gamma)\mathcal{X}_{SII}, \\
\dot{\mathcal{X}}_{ISI} &= \gamma X_{III} + \tau\left(\mathcal{X}_{SSI} + \mathcal{X}_{ISS}\right) - 2(\tau+\gamma)\mathcal{X}_{ISI}, \\
\dot{\mathcal{X}}_{IIS} &= \gamma X_{III} + \tau\left(\mathcal{X}_{SIS} + \mathcal{X}_{ISS}\right) - 2(\tau+\gamma)\mathcal{X}_{IIS}, \\
\dot{\mathcal{X}}_{III} &= -3\gamma X_{III} + 2\tau\left(\mathcal{X}_{SII} + \mathcal{X}_{ISI} + \mathcal{X}_{IIS}\right),
\end{aligned}
$$

as the exact model [91]. For this topology it is possible to reduce the size of the system if we only care about the probability of a given number of nodes having each status by introducing, for example, $\mathcal{Y}_0 = \mathcal{X}_{SSS}$, $\mathcal{Y}_1 = \mathcal{X}_{SSI} + \mathcal{X}_{SIS} + \mathcal{X}_{ISS}$ and so on [91]. However, this is not possible in general. For larger networks the system is prohibitively large and so we desire more manageable models which describe the dynamics at a coarser level. We now move on to give an overview of some of these modelling techniques.

1.3.3 Pairwise models

Pairwise approximation is a well-known tool for constructing epidemic models on networks, and has been successfully applied to both SIR and SIS dynamics [10, 35, 69, 82]. A comprehensive introduction into pairwise models for epidemic spread is found in [91]. Pairwise models successfully extend the scope and usefulness of classic compartmental models while in most cases still providing transparency and mathematical tractability. The total number of transmission events in a network is clearly proportional to the number of edges which connect susceptible and infectious nodes. Classical compartmental models assume that the number of such edges is proportional to the product of the number of nodes in susceptible and infectious states. Pairwise models instead introduce new relations that describe the expected number of connected pairs of nodes in each state. This gives an analytically tractable system of differential equations which capture the fact that individuals are limited in who they have contact with.

First, let us introduce the necessary notation. For each node $i \in N$ we say that if the node is in state X then $X_i = 1$, and zero otherwise. The total number of

nodes in state X across the whole network at time t is $[X] = \sum_{i=1}^{N} X_i$. A pair $X - Y$ describes a connected pair of nodes where one node is in state X, and the other node is in state Y. Across the whole network the expected number of such pairs is $[XY] = \sum_{i,j} X_i Y_j a_{i,j}$, where A is the adjacency matrix of the network. Since we assume an undirected network, this means that $[XY] = [YX]$, and any pairs $[XX]$ are counted twice, once in each direction. Finally, a triple $X - Y - Z$ describes a chain of three connected nodes, with the central node in state Y being connected to a node in state X and a node in state Y. The network-level count of triples is $[XYZ] = \sum_{i,j,k} X_i Y_j Z_k a_{i,j} a_{j,k}$. Applying these notions to the spread of infectious disease, and specifically SIR and SIS dynamics, we see that the different states satisfy $X, Y, Z \in \{S, I, R\}$. These quantities also become time dependent, that is $[S] = [S](t)$. It is common to write these quantities without highlighting time dependence, as will be done later. However, as an introduction it is useful to make this dependence explicit.

From these quantities it is possible to construct a pairwise model for an infectious disease on a static network with wholly Markovian dynamics. Defining τ as the per-edge transmission rate and γ as the recovery rate, in the case of SIR dynamics we have

$$\dot{[S]}(t) = -\tau[SI](t), \quad \dot{[I]}(t) = \tau[SI](t) - \gamma[I](t).$$

This system of differential equations is not closed, and in order to close it, we must obtain an evolution equation for $[SI](t)$ by deriving differential equations at the level of pairs. As an example consider the dynamics of $S - I$ edges. A new $S - I$ edge can only emerge from an $S - S$ pair where one of the nodes has become infected. Across the whole network the rate of such infections is $\tau[SSI](t)$. Destruction of an $S - I$ edge can occur in several different ways. Internally, i.e. within the pair, the infected node may transmit the disease to its susceptible neighbour or recover without transmitting the disease, with the rates of these events being given by $\tau[SI](t)$ and $\gamma[SI](t)$, respectively. Finally, a susceptible node can become infected by acquiring the infection from one of its infected neighbours outside the pair, which leads us to a consideration of triples of the form $I - S - I$. These arguments are presented visually in Fig 1.6. Applying the same process to the other pairs allows us to write the following full system of ODEs at

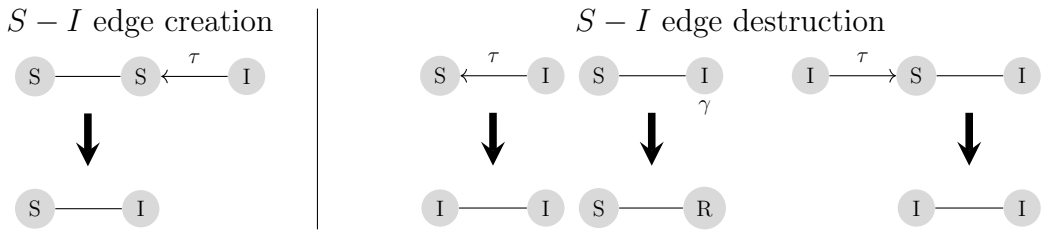

Figure 1.6: Illustration of different ways how $S-I$ edges can be created and destroyed.

the level of pairs

$$
\begin{aligned}
&[\dot{S}](t) = -\tau[SI](t),\\
&[\dot{I}](t) = \tau[SI](t) - \gamma[I](t),\\
&[\dot{R}](t) = \gamma[I](t),\\
&[\dot{SS}](t) = -2\tau[SSI](t),\\
&[\dot{SI}](t) = \tau([SSI](t) - [ISI](t) - [SI](t)) - \gamma[SI](t),\\
&[\dot{SR}](t) = -\tau[ISR](t) + \gamma[SI](t),\\
&[\dot{II}](t) = 2\tau([ISI](t) + [SI](t)) - 2\gamma[II](t),\\
&[\dot{IR}](t) = \tau[ISR](t) + \gamma([II](t) - [IR](t)),\\
&[\dot{RR}](t) = 2\gamma[IR](t).
\end{aligned}
\tag{1.9}
$$

A similar approach can be used to construct the full set of ODEs for an SIS-type epidemic.

Although these equations have been obtained by using a heuristic argument rather than a rigorous derivation, it has been proved using Kolmogorov equations, at least for SIS dynamics, that the unclosed system of equations is an exact representation of the expected dynamics of an outbreak [154]. The top 5 equations of (1.9) decouple, and since $[R](t) = N - [S](t) - [I](t)$ only 4 differential equations are needed to describe the dynamics of epidemic spread, namely $[\dot{S}], [\dot{I}], [\dot{SS}]$ and $[\dot{SI}]$.

A much more important issue to note is that this system is currently not closed, as it depends on the numbers of triples in various states. In theory, it is possible to write down differential equations for each of these triples, which would in turn depend on the number of connected quadruples, and so on. Instead, we choose to close the system by approximating triples in terms of the pairs and singles, known as a *moment closure*. To this point no knowledge of the network topology has been necessary. However, to close the model knowledge of the degree distribution and clustering is necessary. For the simplest case, a regular tree (or tree-like) network where every node has degree n,

the classical moment closure is [82]

$$[XYZ] \approx \frac{n-1}{n}\frac{[XY][YZ]}{[Y]}. \tag{1.10}$$

To see why this is appropriate, consider edges emanating from the central node. Assuming a uniform distribution, the probability of an edge reaching a node with status X can be approximated as $\frac{[XY]}{n[Y]}$ since $n[Y]$ is the total number of edges emanating from nodes with disease status Y. Similarly, we have $\frac{[YZ]}{n[Y]}$ for the probability of reaching a node with status Z. There are $n(n-1)$ choices for the two end nodes in the triple. Taking the product of these terms and multiplying by the expected number of nodes with disease status Y gives the result in (1.10).

When clustering is present, some of the triples will form closed loops, i.e. in an $X-Y-Z$ chain the nodes in state X and Z may also share an edge. Given the clustering coefficient φ, a fraction $(1-\varphi)$ of identified triples will not be closed triangles, and thus the standard closure can be applied, for the remainder the correlation between X and Z must be considered. This is $C_{XZ} = \frac{N[XZ]}{n[X][Z]}$, and therefore

$$[XYZ] \approx \frac{n-1}{n}\frac{[XY][YZ]}{[Y]}\left((1-\varphi)+\varphi\frac{N[XZ]}{n[X][Z]}\right),$$

is an appropriate extension for the closure [82]. Under the standard closure (1.10), Keeling [84] proposed the basic reproductive ratio

$$\mathcal{R}_0 = \frac{\tau(n-2)}{\gamma},$$

and the final epidemic size

$$R_\infty = 1-\left(1-\frac{\tau}{\gamma+\tau}+u\frac{\tau}{\tau+\gamma}\right)^n,$$
$$u = \left(1-\frac{\tau}{\tau+\gamma}+u\frac{\tau}{\tau+\gamma}\right)^{n-1}.$$

These closures are appropriate for regular networks, but fail when applied to networks with degree heterogeneity. A number of different approaches have been proposed that extend pairwise approximation to heterogeneous networks [69, 133]. Eames and Keeling [44] constructed a model where a separate differential equation is used for individuals and pairs of each type and each degree, i.e. $\dot{[X_k]}(t)$ describes the rate of change of nodes with degree k in state X. For networks with significant degree heterogeneity this approach can become infeasible due to the very large size of the resulting system of

equations. Numerous approaches have been made to overcome this limitation [70]. Simon and Kiss [151] proposed a super-compact SIS model. Using numerical simulation, they observed that the degree distribution of susceptible nodes, given by $[S_k]/[S]$, is approximately linearly related to the overall degree distribution. Using this, and other established approximations [44, 69], they derived the closure

$$[XYZ] \approx [XY][YZ]\frac{T_2 - T_1}{T_1^2},$$

where T_1 and T_2 are the first and second moments of the degree distribution of susceptible nodes. In Chapter 3 we extend this method to a multi-stage SI^{K}R model, and also to clustered networks.

Non-Markovian pairwise models

Recently, several non-Markovian pairwise models have been proposed. Kiss et al. [92] derived a DDE model for epidemics with an infectious period of fixed length, σ on a random regular network. Non-Markovianity requires a careful approach to the removal of $S-I$ edges created precisely σ time ago. This term is proportional to $\tau[SSI](t-\sigma)$ but one must realise that not all $S-I$ edges will survive that long, both external and internal transmission can destroy these edges before they reach age σ and the infected node recovers. To model this, the authors introduced $x(t)$ as a cohort of $S-I$ edges all created at the same time. The number of edges in this cohort evolves according to

$$\dot{x}(t) = -\tau\frac{k-1}{k}\frac{[SI](t)}{[S](t)}x(t) - \tau x(t). \tag{1.11}$$

The removal term for $S-I$ edges that were created precisely σ time ago is given by the solution of (1.11) over the interval $[t-\sigma, t]$, namely

$$\begin{aligned} x(t) &= x(t-\sigma)e^{-\int_{t-\sigma}^{t}\left(\tau\frac{k-1}{k}\frac{[SI](a)}{[S](a)}+\tau\right)da}, \\ &= \tau\frac{k-1}{k}\frac{[SS](t-\sigma)[SI](t-\sigma)}{[S](t-\sigma)}e^{-\int_{t-\sigma}^{t}\left(\tau\frac{k-1}{k}\frac{[SI](a)}{[S](a)}+\tau\right)da}. \end{aligned}$$

In Chapter 5 I consider a model with delayed rewiring of edges. The potential for nodes to change disease status while waiting to rewire, and therefore change the status of edges, is accounted for in a similar manner to that detailed above for delayed recovery.

This was later generalised to arbitrary infectious period by Röst et al. [143]. The authors assume Markovian transmission with per-edge transmission parameter τ and that the infectious period is distributed according to some $\rho(a)$ where a is the age of

infection, i.e. the time elapsed since infection was acquired. If $i(t,a)$ and $Si(t,a)$ are the numbers of infected nodes and $S-I$ edges with age a at time t, then with the hazard function $h(a)$ being defined as

$$h(a) = \frac{\rho(a)}{1 - \int_0^a \rho(a')\,da'},$$

they arrive at the unclosed system of PDEs

$$\begin{aligned}
&\dot{[S]}(t) = -\tau[SI](t),\\
&\left(\frac{\partial}{\partial a} + \frac{\partial}{\partial t}\right) i(t,a) = -h(a)i(t,a),\\
&\dot{[SS]}(t) = -2\tau[SSI](t),\\
&\left(\frac{\partial}{\partial a} + \frac{\partial}{\partial t}\right) Si(t,a) = -\tau ISi(t,a) - [\tau + h(a)]Si(t,a),
\end{aligned}$$

where $ISi(t,a)$ is the number of $I-S-I$ triples and the age of the first (external) infected node is unimportant. The total number of infected nodes can be found as $[I](t) = \int_0^\infty i(t,a)\,da$, and similarly, the number of $[SI]$ edges is given by $[SI](t) = \int_0^\infty Si(t,a)\,da$. In order to obtain a self-consistent system of equations they use the relations

$$[\dot{I}](t) = \int_0^\infty \frac{\partial}{\partial t} i(t,b)\,db \quad \text{and} \quad [\dot{SI}](t) = \int_0^\infty \frac{\partial}{\partial t} Si(t,a)\,da,$$

to reach a system of integro-differential equations.

Despite these advances, all of these models are limited to Poisson transmission processes, and it is currently unclear whether pairwise models could be extended beyond this assumption. We now turn our attention to a modelling technique which can incorporate general inter-event time distributions for the transmission process.

1.3.4 Bond percolation and the Message-passing method

Bond percolation models for infectious disease are concerned only with the epidemic threshold and the final epidemic size. As such, it is relatively straightforward to apply percolation to study diseases with arbitrary transmission and recovery processes, since the dynamics are not considered [88, 126]. The central notion is that of *transmissibility*, $\widetilde{\tau}$, defined as the overall probability that an infectious node will attempt to transmit the pathogen across a given network edge before it recovers. In bond percolation, each edge in the network is said to be *occupied* with probability $\widetilde{\tau}$ and empty with probability $(1-\widetilde{\tau})$ [23]. For the purposes of modelling the dynamics of an infectious disease, an

occupied edge means that, should the node at either end of the edge become infected, it will transmit the disease at some point before recovery, while empty edges will not transmit and thus can be removed with no effect. The size of the giant connected component, the largest subgraph where a path exists between any two nodes, then provides the final epidemic size.

Using this approach on the ensemble of large CM networks Newman [126] was able to find the epidemic threshold as the point where the size of the typical outbreak is a measurable fraction of the graph, even in the limit of large size. This divergence point can be found as

$$\widetilde{\tau}_c = \frac{1}{G_1'(1)}, \tag{1.12}$$

where $G_1(x)$ is defined in (1.2). The final epidemic size of a major outbreak is given by the size of the giant connected component (GCC), since a disease introduced anywhere in the GCC will eventually spread through all members. This gives

$$r_\infty = 1 - G_0(1 - \widetilde{\tau} + u\widetilde{\tau}), \tag{1.13}$$

where u satisfies an implicit equation

$$u = G_1(1 - \widetilde{\tau} + u\widetilde{\tau}). \tag{1.14}$$

On a regular network, this is equivalent to results found from pairwise models [84].

In some sense the message passing (MP) model of Karrer and Newman [80] can be seen as an attempt to reinstate time into the bond percolation models. Whereas percolation theory asks: *will this edge transmit the disease?*, MP asks *will this edge transmit the disease before a given time?* Given arbitrary independent transmission and recovery processes represented by distributions $\tau(a)$ and $q(a)$, where a is the age of the infection, the probability that an $S-I$ edge will carry a transmission in a small interval $(a, a+dt)$ is the transmission rate multiplied by the survival probability of the infected node. Formally, this can be written as

$$f(a) := \tau(a) \int_a^\infty q(x)dx. \tag{1.15}$$

In some sense, f acts a density function. For a node infected at time t_1 the probability that it will attempt to transmit the disease to a given neighbour before time t is $\int_{t_1}^{t} f(a)da$. It should be noted that the integral of this function over all time gives the transmissibility, $\widetilde{\tau}$, used in percolation models of disease spread, and introduced earlier.

The message, denoted $H^{i\leftarrow j}(t)$, is then defined as the probability that node j has *not* transmitted the disease to node i before time t. This can be calculated for each edge by considering two possibilities. Firstly, the age at which the node would transmit along the edge in question (if it would transmit at all) is larger than time t, and so regardless of when i became infected, it would not have transmitted the disease to j before time t, the probability of which is given by $1-\int_0^t f(a)da$. Alternatively, it could be that j is infected, but its age is not sufficient to have then also transmitted the disease to node i. More precisely, imagine j will transmit the disease at age a but was itself infected at some time $t_1 > t-a$. The probability of this event is equal to $z\prod_{l\in\mathcal{N}(j)\setminus i} H^{j\leftarrow l}(t-a)$, where z is the probability of a node being susceptible at $t=0$, and the product is taken across all neighbours of node j with the exception of i. This is equivalent to placing node i in a *cavity state* where it is unable to transmit the disease to its neighbours, on a tree-like network this does not alter the dynamics [118, 119]. These possibilities can now be combined to give

$$H^{i\leftarrow j}(t) = 1 - \int_0^t f(a)\left[1 - z\prod_{l\in\mathcal{N}(j)\setminus i} H^{j\leftarrow l}(t-a)\right]da, \tag{1.16}$$

and the overall state probabilities can then be written in terms of these messages as follows,

$$\begin{aligned} P(S_i) &= z\prod_{j\in\mathcal{N}(i)} H^{i\leftarrow j}(t), \\ \frac{dP(I_i)}{dt} &= -\frac{dP(S_i)}{dt} - (1-z)q(t) + \int_0^t q(t-t_1)\frac{dP(S_i)}{dt_1}dt_1, \\ P(R_i) &= 1 - P(S_i) - P(I_i). \end{aligned} \tag{1.17}$$

Alternatively, one can use the relation [170]

$$P(R_i) = \int_0^t q(a)\left[1 - S(t')\,dt'\right].$$

Theoretically, on a tree network, one can solve for $H^{i\leftarrow j}$ across all edges to find an exact solution to the problem of epidemic spread. When clustering is present, MP gives an upper bound on the size of epidemic at any time t [80]. Clearly, this approach becomes computationally expensive for large networks. However, on the ensemble of CM networks it is possible to find an average message $H_1(t)$ which can replace the edge-specific messages, so that, when weighted by the generating function of the degree

and excess degree distributions, we are left with a concise system of equations to model an SIR epidemic which is exact on the ensemble of CM networks of infinite size

$$\begin{aligned} H_1(t) &= 1 - \int_0^t f(a)\left[1 - zG_1(H_1(t-a))\right] da, \\ \langle S\rangle(t) &= zG_0(H_1(t)), \\ \langle R\rangle(t) &= \int_0^t q(a)\left[1 - \langle S\rangle(t-a)\right] da, \\ \langle I\rangle(t) &= 1 - \langle S\rangle(t) - \langle R\rangle(t). \end{aligned} \tag{1.18}$$

When the transmission process $\tau(a)$ is assumed to be Markovian and the network is a regular tree connections between MP and pairwise approximation models have been found by introducing new differential equations for the states of edges [169, 170]. In Chapter 4 we extend this methodology to networks with an arbitrary degree distribution.

1.3.5 Edge-based compartmental model

Another modelling technique that is able to consider arbitrary degree distribution is the Edge-based compartmental model (EBCM) [117, 119]. Initially designed only for diseases with Markovian dynamics, the EBCM shares certain elements of its approach with MP methods described above. The central quantity in the EBCM is $\theta(t)$, the probability that a randomly chosen neighbour of a test node i has not transmitted the disease before time t. Clearly this mirrors the message $H_1(t)$ in MP models. Given this, the probability that a representative test node i is susceptible at time t is the product of $\theta(t)$ across all neighbours. Then, given a recovery rate γ, it is easy to see that

$$S(t) = G_0(\theta), \quad \dot{R} = \gamma I, \quad I = 1 - S - R,$$

where $G_0(x)$ is defined in (1.1), and it is further assumed that $I(0) \approx 0$. The remaining difficulty lies in calculating $\theta(t)$. There are three distinct possibilities why a random neighbour may not have transmitted the disease: with probability ϕ_S the neighbour itself is susceptible, with probability ϕ_I it is infected and has not yet transmitted the disease, but may do in the future, or with probability ϕ_R it has already recovered from the disease, and did not transmit while infected. Thus, $\theta(t) = \phi_S + \phi_I + \phi_R$. Additionally, the rate of change of θ is determined by transmission events which occur with rate τ for each $S - I$ edge. Therefore, we have

$$\dot{\theta} = -\tau\phi_I. \tag{1.19}$$

Calculating ϕ_S is equivalent to finding the probability that this neighbour is susceptible, keeping in mind that it cannot have been infected by node i, that is, node i is once again in a cavity state. Thus, similarly to the MP we have

$$\phi_S = \frac{G_0'(\theta)}{G_0'(1)} = \frac{1}{\langle k \rangle} G_1(\theta).$$

Finally, ϕ_R is found by first noting that

$$\dot{\phi}_R = \gamma \phi_I = -\frac{\gamma}{\tau}\dot{\theta},$$

where the last step follows from (1.19). Integrating this equation from 0 to t gives $\phi_R = \gamma/\tau(1-\theta(t))$. This is enough to write the model as

$$\begin{aligned} \dot{\theta} &= -\tau\phi_I = -\tau\left(\theta + G_1(\theta) + \frac{\gamma}{\tau}(1-\theta)\right), \\ S &= G_0(\theta), \\ \dot{R} &= \gamma I, \\ I &= 1 - S - R. \end{aligned} \tag{1.20}$$

This system is equivalent to the so-called Volz equations [162]. Given the similarities in the models, it is not surprising that the same methods used to calculate the epidemic threshold and final epidemic size for MP methods are also applicable here [119]. In agreement with many previous studies, including Newman's work detailed above [88, 126, 162], they find the basic reproduction number as

$$\mathcal{R}_0 = \frac{\tau}{\tau+\gamma}\left(\frac{\langle k^2 - k \rangle}{\langle k \rangle}\right) \tag{1.21}$$

and the final epidemic size agrees with Newman's results stated earlier (1.13), (1.14).

Further work on this modelling technique has removed the assumption that the initial level of infection is infinitesimally small [117], applied the techniques to weighted networks [137, 165], and to multiplex networks that consider a clustered static network on one layer and a dynamic tree-like network on the other [12]. In Chapter 4, I extend the static EBCM to account for arbitrary, independent non-Markovian transmission and recovery processes and go on to prove that, on the ensemble of CM networks, the EBCM and MP frameworks are equivalent. This result forms the basis of a model hierarchy, the MP model is used to derive a general pairwise-like model (PLM) which reduces to existing models under the appropriate assumptions. These relationships are detailed here in Fig. 1.7.

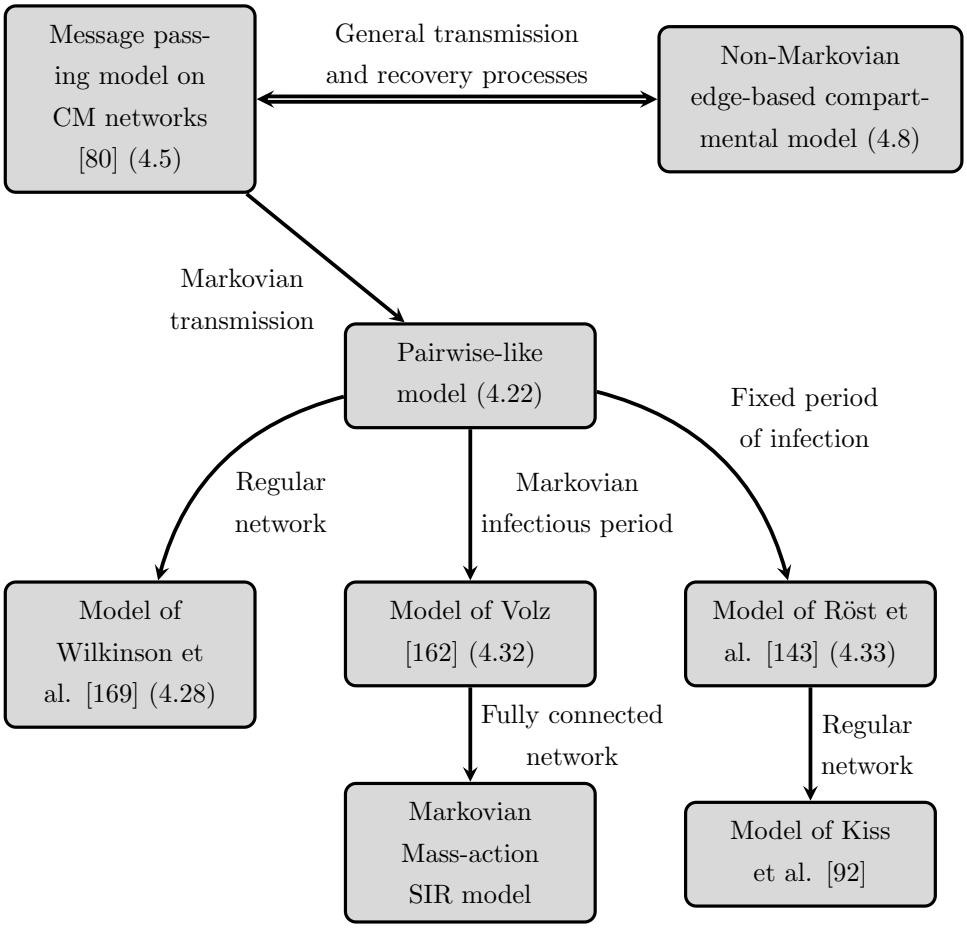

Figure 1.7: Hierarchy of models, full details of its derivation are given in Chapter 4.

1.3.6 Dynamic network models

Up to this point, it has been assumed that the contact network is static, and the connections between nodes do not change over time. We now relax this assumption by considering the network as dynamic. Dynamic network modelling encompasses all potential changes to a network over time, which involves edges being created, deactivated and reactivated, or destroyed, or nodes being introduced or removed. These changes in network topology may result in significant changes in the degree distribution, clustering and assortativity of the network. Dynamic networks are particularly relevant to the spread of disease because it is well-known that people alter their behaviour in response to the perceived threat of infection [53], which is a natural response taken by individuals [57, 134, 144], but it can also be dictated or influenced by governmental policy and/or media coverage [111, 142].

In dynamic network models the state of the network changes, either as an ongoing natural process [108, 119], or as a response to the threat of infection [52, 53, 62, 63, 64]. Due to their transparency, pairwise models have been a popular choice when modelling the spread of infectious diseases on temporal networks [63, 64, 158]. Gross et al. [64] introduced a simple SIS model for edge rewiring. Susceptible nodes which share an edge with infectious nodes break the edge with rate ω and immediately draw a new edge to an unconnected susceptible node selected uniformly at random. They were able to identify an $\mathcal{R}_0$-like threshold parameter, and found that rewiring makes epidemic outbreaks less likely if they are starting from an initial seed which is vanishingly small. The dynamics of the epidemic were much richer than in the standard model, with bistability and stable oscillatory behaviour observed in certain regions of the parameter space.

Besides pairwise models, other approaches have examined the effects of decisions based on available information about the prevalence of disease [172]. The delay in an individual's response reflects poorer quality information and can cause oscillatory dynamics. Risau-Gusman and Zanette [139] consider the case where, with a given probability, it is the infectious node that rewires rather than the susceptible one, reflecting that people infected with a disease change their behaviour, as well as those trying to avoid infection.

In Chapter 5, I present an SIS epidemic spreading on an adaptive network where susceptible nodes can rewire at rate ω but must wait for a fixed period of time before creating a new edge.

1.4 Thesis overview

The remainder of this thesis is based on four published papers, with each Chapter corresponding to one paper.

In Chapter 2, I consider how a multi-stage approach can be used to analyse an SIR epidemic on a random regular network. After summarising results from the classical homogeneously mixed model, I introduce a new pairwise model with multiple stages of infection, with the overall infectious period being gamma distributed. Through linear stability analysis I identify the epidemic threshold, using the transmissibility of the disease I make an argument for the appropriate formulation of the $\mathcal{R}_0$-like threshold parameter. I also analytically find the final epidemic size directly from the system of ODEs and observe that it is in agreement with previous findings [126]. Both the final epidemic size and $\mathcal{R}_0$ are found to increase with the number of stages. This is in contrast to the equivalent well-mixed models, where final epidemic size remains constant [4, 105]. The model is compared to numerical simulation, and it shows excellent agreement. Results from numerical solution and simulation are used to highlight the impact of including the true distribution of the infectious period in a case study based on data for SARS, smallpox, and influenza.

In Chapter 3, the multi-stage model derived in Chapter 2 is extended to heterogeneous and clustered networks. Using the super-compact approach of Simon and Kiss [151], I derive a new model whose size is independent of the heterogeneity of the network. Comparison with numerical simulation remains favourable. I obtain an $\mathcal{R}_0$-like threshold parameter through two methods: a linear stability analysis and a generational approach. Although it does not prove possible to extend the method used in Chapter 2 to find the final epidemic size directly from the system of ODEs, I do show that the final epidemic size obtained from the numerical solution is approximately equal to theoretical results from percolation theory. I discuss how the proposed mode interpolates between the limiting cases of the classical pairwise methods equivalent to a single infectious stage and the model of Kiss et al. [92] with fixed infectious period. The model is extended to clustered networks, and still shows a good agreement with numerical simulation.

In Chapter 4, the MP method is introduced for the spread of disease with arbitrary independent transmission and recovery processes, after which I introduce a novel non-Markovian EBCM that has the same degree of generality. I explain how this model is constructed and rigorously prove that under the same initial conditions the MP method

and our model produce identical solutions, and, therefore, the models are equivalent. Since the MP method is exact on the ensemble of CM networks, this implies that our model is also exact under the same conditions. I then present a proof for the final epidemic size derived directly from the EBCM. By assuming a Markovian transmission process it is shown that a pairwise-like model (PLM) can be derived, which generalises the work of Wilkinson et al. [169] to heterogeneous networks. The PLM is then used to build a model hierarchy; being the most general pairwise model I show how it reduces to many well-known pairwise models under appropriate assumptions, such as, homogeneous degree distribution or Markovian recovery. Many pairwise models are defined heuristically [44, 64, 70]. Placing them within the hierarchy validates the conditions under which they become exact. Once again, the output from the model is compared to numerical simulation with excellent agreement for various choices of infectious period distribution.

Chapter 5 is devoted to adaptive networks. I consider an SIS epidemic on a random graph with delayed adaptive rewiring of edges. Susceptible nodes disconnect from infected neighbours at a given rate, but then they must wait for a delay of fixed length before they can draw a connection to a random susceptible node. I discuss why it is important to consider a delay in the rewiring process and discuss the complexities it adds when constructing the model. In particular, I discuss in detail how to model the fact that susceptible nodes can become infected while waiting to draw a new edge. A threshold parameter is found using linear stability analysis of the disease-free equilibrium, but an analytical solution for the long-term behaviour is not possible. Numerical solution shows that increasing the delay can cause a Hopf bifurcation and the emergence of stable oscillatory solutions. These oscillations are found in a much larger region of the parameter space than when rewiring is instantaneous [64]. Continuing to increase the duration of the delay causes the amplitude of oscillations to grow. Altering ω, the rate at which nodes disconnect edges reveals an enclosed 'endemic bubble' in the parameter space within which stable oscillations are observed. We explain the likely cause of this phenomenon by showing how the network topology changes as a result of the adaptive behaviour. When the response is swift enough and the delay significant, the pathogen is effectively starved of transmission routes, and prevalence begins to decay, until the edges are redrawn, and the disease is able to spread once more.

The thesis concludes in Chapter 6, with a discussion of results and open problems.

Chapter 2

Paper 1: Dynamics of multi-stage infections on networks

N. Sherborne[1], K. B. Blyuss[1] and I. Z. Kiss[1]

[1]Department of Mathematics, School of Mathematical and Physical Sciences, University of Sussex, Brighton, BN1 9QH, UK

2.1 Abstract

This Chapter investigates the dynamics of infectious diseases with a non-exponentially distributed infectious period. This is achieved by considering a multi-stage infection model on networks. Using pairwise approximation with a standard closure, a number of important characteristics of disease dynamics are derived analytically, including the final size of an epidemic and a threshold for epidemic outbreaks, and it is shown how these quantities depend on disease characteristics, as well as the number of disease stages. Stochastic simulations of dynamics on networks are performed and compared to the results of pairwise models for several realistic examples of infectious diseases to illustrate the role played by the number of stages in the disease dynamics. These results show that a higher number of disease stages results in faster epidemic outbreaks with a higher peak prevalence and a larger final size of the epidemic. The agreement between the pairwise and simulation methods is excellent in the cases we consider.

2.2 Introduction

Mathematical models of infectious diseases are known to provide an invaluable insight into the mechanisms driving disease invasion and spread. In many cases, to obtain the first approximation of the spread of a disease it is sufficient to use a version of the classical SIR model [89]. However, major outbreaks of avian and swine influenza [48], SARS [41], and more recently, Ebola [33], have highlighted the need for a more accurate description of the disease dynamics that would provide predictive power to be used for developing measures for disease control and prevention [83].

One of the major simplifying assumptions often used in mathematical models of disease dynamics is the exponential distribution of infectious periods. Effectively, this means that the chance of an individual recovering during any given time period does not depend on the duration of time that individual has already been infected. Whilst such an assumption may provide significant mathematical convenience and be reasonably realistic in some situations, most often it is violated, and this requires the inclusion of the precise distribution of infectious periods in the model [8, 152]. There are several methods that can be employed to explicitly include a non-exponential distribution, including a multi-stage approach [4, 34], an integro-differential formulation [68, 89, 86], and a PDE-based formulation akin to that for age-structured models [6]. In the multi-stage framework, it is assumed that the infectious stage of a disease is characterised by

a number K of distinct stages [34, 102, 103], with the duration of each stage being an independent exponentially distributed random number. Due to the fact that the sum of independent exponentially distributed random variables obeys a gamma distribution [42], one can replace an exponential distribution with the mean infectious period $1/\gamma$ by a gamma distribution $\Gamma(K, 1/(K\gamma))$ that has the same mean infectious period $1/\gamma$. The so-called *linear chain trick* [34, 106] then consists in replacing a single infectious stage with K identical exponentially distributed sub-stages, each having a mean period $1/(K\gamma)$. These multiple stages of infection can be used to represent periods of increased or decreased risk of transmitting the disease [105]. The same approach can be extended to models with multiple classes [87, 129], as well as non-exponentially distributed latency and temporary immunity periods [17, 168]. Following the methodology of introducing multi-stage of infection to better represent the distribution of infectious periods, we proceed with dividing the infected population into K identical stages $I_1, I_2, \ldots, I_K$ to create the so-called SI^{K}R model [103], and we denote the total infected population by $I = \sum_{i=1}^{K} I_i$. One should note that $K\gamma$ is now used as the transition rate between successive infectious stages in order to keep the average duration of infection as $1/\gamma$. With these notations, the SI^{K}R model takes the form

$$\begin{aligned} dS/dt &= -\beta SI, \\ dI_1/dt &= \beta SI - K\gamma I_1, \\ dI_2/dt &= K\gamma I_1 - K\gamma I_2, \\ &\vdots \\ dI_K/dt &= K\gamma I_{K-1} - K\gamma I_K, \\ dR/dt &= K\gamma I_K, \end{aligned} \tag{2.1}$$

where S denotes the proportion of susceptible individuals, R is the proportion of recovered or removed individuals, β is the disease transmission rate taken to be the same for all stages of infection, and the disease is assumed to confer a life-long immunity. The importance of including not just the mean infectious period, but the actual distribution of infectious periods, as achieved by the system (2.1) is further highlighted by the inspection of actual values of epidemiological parameters for several real diseases as presented in Table 2.1. This table illustrates that whilst the transmission rate and the average infectious period may vary between different diseases, in all of these cases the number of stages that has to be included in order to correctly represent the disease dynamics may also be quite high, this reinforces an earlier observation about the

non-exponential nature of infectious period distribution.

Whilst this method of introducing multiple stages of infection is clearly more realistic, the assumption of a homogeneous fully mixed population remains very important, having significant effects on the disease dynamics [83]. Although this assumption often provides a good approximation that helps reduce complexity of the model, in many cases it is just not realistic and results in erroneous conclusions about the onset and development of epidemic outbreaks [9, 25]. To address this issue, networks have been and are being used successfully to model the contact structure of the population to a high degree of detail [35, 85]. Typically, network models are parameterised with empirical data or synthetic models that can be either purely theoretical, e.g. regular random networks or Erdős-Rényi random graphs, or obey some widely observed network characteristics, such as a particular degree distribution or clustering. However, with added model realism comes complexity, which in the case of epidemic network models can be handled via mean-field models, such as pairwise models [70, 84] that are able to better account for the explicit nature of network links. As long as such mean-field models provide a good approximation to the explicit stochastic network models, they open up the possibility to analyticaly compute important quantities such as epidemic threshold, final epidemic size and so on. Thus, the explicit stochastic network simulation model and the pairwise model combine favourably to provide a more accurate model with some degree of analytical tractability.

In this Chapter we are concurrently relaxing the assumptions of homogeneous random mixing and exponentially distributed infectious periods to generate a multi-stage pairwise model for the spread of epidemics on networks. The Chapter is organised as follows. The next Section contains a brief summary and discussion of earlier results on the properties of the $\mathrm{SI}^K\mathrm{R}$ model (2.1). In Section 2.4 we employ the framework of pairwise approximations to derive a multi-stage infection pairwise model and use this to derive analytical expressions for the probability of transmission of infection along an infected edge in a network, a threshold parameter controlling the onset of epidemic outbreaks, and the final size of an epidemic. In Section 2.5 numerical simulations of the pairwise and the full network models are performed using realistic parameter values from Table 2.1 to investigate the accuracy of pairwise approximation and to illustrate the role played by the number of stages in the multi-stage distribution in the disease dynamics. The Chapter concludes in Section 2.6 with discussion of results and future outlook.

Table 2.1: Estimates of epidemiological parameters for different infectious diseases.

Disease	β	γ^{-1} (days)	Stages K	Source(s)
Measles	Seasonal	5	20	[152]
SARS	0.545	5-6	3	[14, 138]
Influenza	1.66	2.2	3	[30, 83]
Smallpox	0.49	8.6	4	[49, 93]

2.3 Dynamics of the well-mixed model

As a first step, we consider the $\mathrm{SI}^K\mathrm{R}$ model (2.1), which has an implicit assumption that every member of the population has a sufficient level of contact so that the infection can be passed from any individual to any other. This is a natural extension of the basic SIR model [89], and as such it has been well-studied in a number of papers [103, 105, 159].

Perhaps, one of the most important and commonly used parameters characterising the severity of epidemics and stability of the disease-free equilibrium is the *basic reproduction number* $\mathcal{R}_0$ defined as the expected number of secondary infections caused by a single typical infectious individual in a wholly susceptible population. The value of $\mathcal{R}_0$ is related to the stability of the disease-free equilibrium, and it is an important threshold parameter signifying that an epidemic will spread when $\mathcal{R}_0 > 1$ and die out otherwise.

The basic reproduction number for the system (2.1) can be found as follows [73, 105, 159]:

$$\mathcal{R}_0 = \frac{\beta}{\gamma}, \tag{2.2}$$

which depends on the average duration of infection $1/\gamma$ but is independent of the number of stages in the model. A practically important characteristic of an epidemic outbreak is the *final epidemic size* [83]. Since the total population size is closed with no inflow or outflow of individuals, i.e. $S(t) + I_1(t) + I_2(t) + ... + I_K(t) + R(t) = 1$, at the end of an outbreak we have a burn-out of the epidemic, i.e. $I_1 = I_2 = \ldots = I_K = 0$, and hence $S(\infty) + R(\infty) = 1$ and $R(\infty) = 1 - S(\infty)$. This results in the following implicit equation for the final size of an epidemic that determines the proportion of individuals not affected by the disease [6, 39]

$$R(\infty) = 1 - e^{-\mathcal{R}_0 R(\infty)}, \tag{2.3}$$

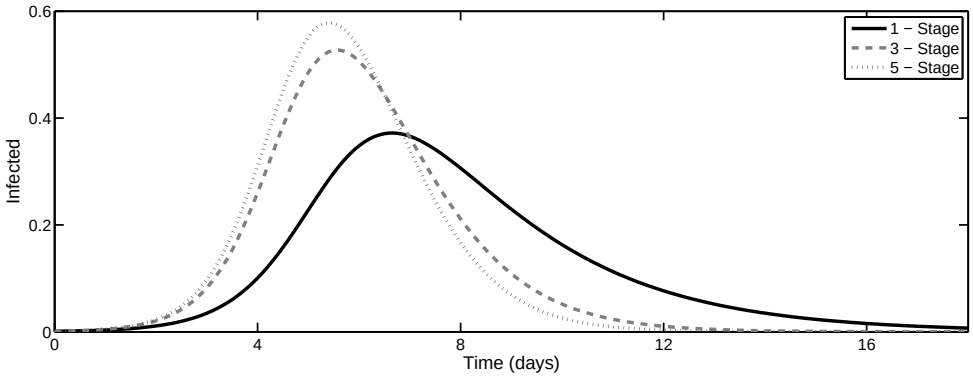

Figure 2.1: A comparison of infection dynamics for a one-, three- and five-stage SI^KR models with data from Keeling and Rojani [83]. Each curve represents the sum of all I_i in the model. Adding extra stages causes epidemics to occur earlier and result in a higher peak of epidemic, although $\mathcal{R}_0$ and the final size are identical for each curve. The parameter values are $N = 1000$, $\beta = 1.66$/day, $\gamma = 0.4545$/day.

which coincides with the final epidemic size in the original SIR model [89]. Ma and Earn [105] have recently discussed various aspects related to the derivation and validity of formula (2.3), and Andreasen [7] has studied the effects of population heterogeneity on the size of epidemic. A major implication of the above results is the fact that inclusion of possibly more realistic gamma distribution of infectious periods does not alter the threshold of an epidemic outbreak, nor does it affect the final epidemic size. One should note, however, that when a stochastic version of the SI^KR model is considered, the number of stages influences the distribution of final epidemic sizes, while the average final size remains the same [16, 71]. We see that in Fig. 2.1 the three curves show that considering multi-stage infectious periods has a significant effect of the dynamics of the epidemic. In order to get a better understanding of the distinction in the dynamics of SIR and SI^KR models, it is therefore instructive to look at the development of epidemics. In the standard SIR model, an outbreak can only take place if $\mathcal{R}_0 > 1$, and at the initial stage, the number of infected individuals can be approximated as $I(t) \approx I(0)\exp(\lambda t)$, where the growth rate is $\lambda = \gamma(\mathcal{R}_0 - 1)$. In the case of a multi-stage SI^KR model, however, the basic reproduction number $\mathcal{R}_0$ does not depend on the number of stages, hence, it cannot by itself be used to determine the exponential growth rate during an early stage of an outbreak. For this model Wearing et al. [168] have derived the following relation between the basic reproduction number $\mathcal{R}_0$ and the initial growth

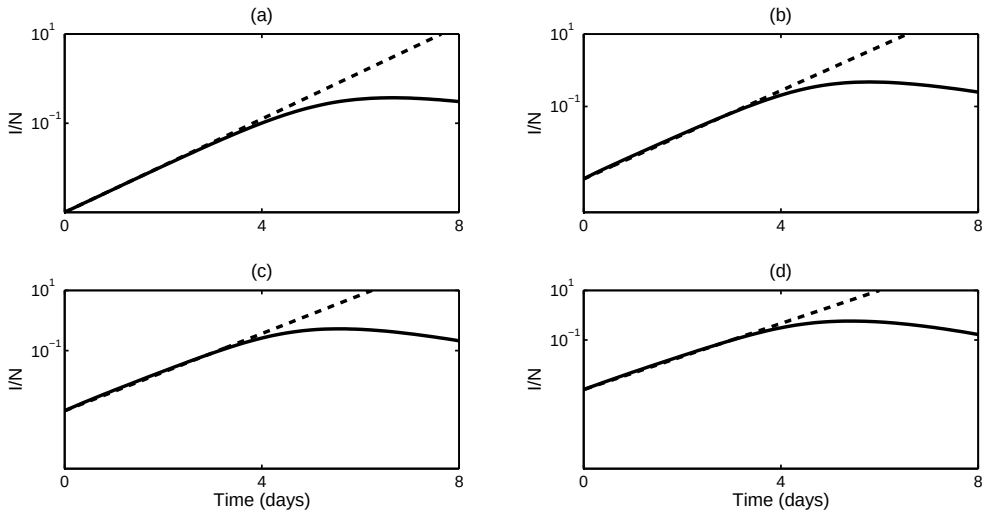

Figure 2.2: Proportion of infected individuals during a boarding school influenza outbreak with $\beta = 1.66$/day and $\gamma = 0.4545$/day [83]. In each plot the solid black line is the numerical solution of the model (2.1) with an appropriate number of stages, and the dashed line is the exponential growth curve with the rate determined by equation (2.4) shown on a logarithmic scale. (a) One-stage model with $\lambda \approx 1.2055$, (b) Two-stage model with $\lambda \approx 1.4035$, (c) Three-stage model with $\lambda \approx 1.4762$, (d) Five-stage model with $\lambda \approx 1.534$. In each case note that in the earliest stages the exponential approximation is virtually identical to the infection curve.

rate λ

$$\mathcal{R}_0 = \frac{\lambda}{\gamma\left(1 - \left(\frac{\lambda}{K\gamma} + 1\right)^{-K}\right)}. \tag{2.4}$$

Figure 2.2 illustrates early dynamics of epidemic outbreaks for different numbers of stages; in each case an exponential curve was fitted, which provides an accurate approximation for the initial growth rate of the infection as determined by equation (2.4). This figure shows the effects of the gamma distribution on the early growth rate, peak prevalence and overall time frame of the disease, and it also suggests that the largest effect of the gamma distribution on the disease dynamics occurs during intermediate stages of disease progression.

Besides the basic reproduction number, final epidemic size and the initial growth rate of an epidemic, another practically important characteristic of epidemic outbreaks is the peak prevalence defined as the maximum number or proportion of infected individuals

that can be achieved during an outbreak. In the case of an SIR model, the peak prevalence can be found as follows [47, 69]:

$$I_{max} = 1 - \frac{1}{\mathcal{R}_0}[1 + \ln(\mathcal{R}_0)].$$

Feng [47] has recently considered an SEIR model with gamma distributed infectious period and derived an expression for the peak of a weighted average of infectious compartments. This result gives some intuition into how the number of stages affects peak prevalence, but it does not provide a closed form expression for the actual peak prevalence in an $\mathrm{SI}^K\mathrm{R}$ model. Numerical results in Fig. 2.2 suggest that for the same average infectious period, the overall peak prevalence increases with the number of stages included in the model.

2.4 Network dynamics with multiple stages

Inclusion of multiple stages of infection in the $\mathrm{SI}^K\mathrm{R}$ model gives a more realistic representation of the infectious period, but the model still has certain limitations due to its underlying assumptions. In the model (2.1) it is assumed that the disease is not fatal, and that transitions between different infected classes, or stages of infection, take place at exactly the same rate $K\gamma$. Another major assumption behind model (2.1) is that the population is well-mixed, i.e. each individual has equal chances of encountering and transmitting a disease to any other individual in a population. Whilst this may be appropriate in the case of outbreaks in small closed communities, for a large number of communicable diseases, such as SARS, influenza and most sexually transmitted infections, this assumption is a gross simplification of the actual dynamics as it overlooks spatial variability, as well as the complexities of a network structure for infections that are transmitted through direct close contact between individuals [70, 85].

Modelling complex contact patterns explicitly via networks has had a profound effect on mathematical epidemiology. This new modelling framework has led to a myriad of models ranging from exact to mean-field and simulation models [18, 35, 85, 127, 131]. The many degrees of freedom in modelling offered by networks however, often comes at the price of increasing levels of complexity, where models can be challenging to evaluate analytically and sometimes even numerically. Nevertheless, many valuable paradigm models have been developed which have furthered our understanding of the impact of contact heterogeneity, preferential mixing and clustering on the outbreak threshold and

other epidemic descriptors. A particularly useful way of capturing epidemic dynamics on networks is by using the pairwise model [84]. This model is based around deriving in a hierarchical way evolution equations for the expected number of nodes, edges, triples and so on. A closure is then employed that curtails the dependence on ever higher order moments. Its premise is simple and quite intuitive, although it can be also shown rigorously [154] that pairwise models before closure are exact. The basic idea of the model is to recognise that changes at node level depend on the status of the neighbours and thus involves edges, e.g. the rate of change in the number of infectious nodes is proportional to the number of $S-I$ links in the network. Similarly, the number of edges can change due to pair interactions and transitions but also due to interactions induced from outside the edge, e.g. the number of $S-S$ links decrease proportionally to the number of $S-S-I$ triples, where infection from the I node destroys the fully susceptible pair. This framework has been used and extended extensively, to asymmetric [148] and weighted networks [136] for example, and has proved to be a valuable framework.

2.4.1 Pairwise model

As a first step in the analysis of dynamics of multi-stage epidemics on networks, we re-formulate the SI^{K}R model using the framework of *pairwise equations*, which allows one to analyse the expected values for the number of nodes and links of each type as a function of time [70, 84, 154]. The particular strength of pairwise models lies in their analytical tractability and the fact that they provide a more accurate description than well-mixed ODE models but do not go to the level of full individual-based stochastic simulations [70]. In this formalism of pairwise models, notations $[X]$, $[XY]$ and $[XYZ]$ are used to denote the expected numbers of individuals in state X, the expected number of links between nodes of type X and Y and the expected number of triples of the form $X-Y-Z$, respectively. More precisely, given a 'frozen' network with nodes labels X, Y or Z and subscripts indicating nodes i, j and k then

$$[X] = \sum_{i=1}^{N} X_i, \quad [XY] = \sum_{i,j=1}^{N} X_i Y_j a_{ij}, \quad [XYZ] = \sum_{i,j,k=1}^{N} X_i Y_j Z_k a_{ij} a_{jk},$$

where $X, Y, Z \in \{S, I_1, I_2, \ldots, I_K, R\}$, and $A = (a_{ij})_{i,j=1,2,\ldots,N}$ is the adjacency matrix of the network such that $a_{ii} = 0$, $a_{ij} = a_{ji}$ and $a_{ij} = a_{ji} = 1$ if nodes i and j are connected and zero otherwise. Moreover, X_i returns one if node i is in state X and zero otherwise. The average degree of each node is denoted by n, and the number of

nodes in the network by N. The new pairwise SI^{K}R model with a gamma distributed infectious period can then be written as follows,

$$\begin{aligned}
&[\dot{S}] = -\tau \textstyle\sum_{i=1}^{K} [SI_i],\\
&[\dot{I}_1] = \tau \textstyle\sum_{i=1}^{K} [SI_i] - K\gamma[I_1],\\
&[\dot{I}_j] = K\gamma[I_{j-1}] - K\gamma[I_j], \quad \text{for} \quad j = 2, 3, \ldots, K,\\
&[\dot{SS}] = -2\tau \textstyle\sum_{i=1}^{K} [SSI_i],\\
&[\dot{SI}_1] = -(\tau + K\gamma)[SI_1] + \tau \left(\textstyle\sum_{i=1}^{K} [SSI_i] - \sum_{i=1}^{K} [I_i SI_1] \right),\\
&[\dot{SI}_j] = -(\tau + K\gamma)[SI_j] + K\gamma[SI_{j-1}] - \tau \textstyle\sum_{i=1}^{K} [I_i SI_j], \quad \text{for} \quad j = 2, 3, \ldots, K.
\end{aligned} \tag{2.5}$$

where $\tau = \beta/n$ is the transmission rate per link. Since we consider a closed population, this immediately implies $[S] + \sum_{i=1}^{K}[I_i] + [R] = N$. The system (2.5) is not closed as additional equations describing the dynamics of triples are needed. To eliminate this dependence on higher moments and close the system, we will use the classical moment closure approximation which assumes that short loops and clusters are excluded from the network and that there is no correlation between nodes with a common neighbour [84].

$$\begin{aligned}
[SSI_i] &\approx \frac{(n-1)}{n} \frac{[SS][SI_i]}{[S]}, \quad \text{for} \quad i = 1, \ldots, K,\\
[I_j SI_i] &\approx \frac{(n-1)}{n} \frac{[I_j S][SI_i]}{[S]}, \quad \text{for} \quad i, j = 1, \ldots, K.
\end{aligned} \tag{2.6}$$

Applying these closures to the system (2.5) makes it a self-consistent system of $(2K+2)$ equations.

2.4.2 The probability of transmission across an infected edge

When one considers a stochastic network-based simulation, an important quantity characterising the disease dynamics is the probability $\widetilde{\tau}$ of disease transmission across a given $S-I$ link. In a simple one-stage model, where both infection and recovery are assumed to be distributed exponentially, the probability of no infection event occurring during

time t is given by $p_0(t) = e^{-\tau t}$; hence $1 - p_0(t)$ is the probability that infection does take place over the same time period. Averaging this via integration for all possible recovery times yields the probability that the susceptible node becomes infected. In a standard SIR model with exponentially distributed infectious and recovery period, this probability is, therefore [35, 36]

$$\widetilde{\tau} = 1 - \frac{\gamma}{\tau + \gamma} = \frac{\tau}{\tau + \gamma}. \tag{2.7}$$

In the case of an $\mathrm{SI}^K\mathrm{R}$ model, the duration of infection is described by the density function of the appropriate gamma distribution

$$g(x; K, 1/(K\gamma)) = \frac{1}{(K-1)!}(K\gamma)^K x^{K-1} e^{-K\gamma x}. \tag{2.8}$$

The implication of this fact is the following result for the probability of transmission across an edge.

Lemma 1. *For the stochastic SI^KR model with the period of infection following the gamma distribution (2.8), the probability of disease transmission across a given $S - I$ link is given by*

$$\widetilde{\tau} = 1 - \left(\frac{K\gamma}{\tau + K\gamma}\right)^K. \tag{2.9}$$

The proof of this lemma is given in Appendix A.

By rewriting expression (2.9) in the form

$$\widetilde{\tau} = 1 - \left(\frac{K\gamma + \tau - \tau}{\tau + K\gamma}\right)^K = 1 - \left(1 - \frac{\tau}{\tau + K\gamma}\right)^K,$$

and using the fact that $e^x = \lim_{n\to\infty}(1 + x/n)^n$, it follows that

$$\lim_{K\to\infty} \widetilde{\tau}(K) = 1 - \exp\left(-\frac{\tau}{\gamma}\right). \tag{2.10}$$

Figure 2.3 illustrates the dependence of $\widetilde{\tau}$ on the number of stages K, as well as a limiting behaviour as $K \to \infty$. This figure illustrates that while $\widetilde{\tau}$ is growing with the increasing number of stages K, it eventually saturates at a level determined by Eq. (2.10). In fact, this saturation at higher K is observed not only in the probability of transmission, but also in the peak prevalence rate, as well as in the early growth rate. When compared to an exponential distribution, it is these substantial changes in $\widetilde{\tau}$

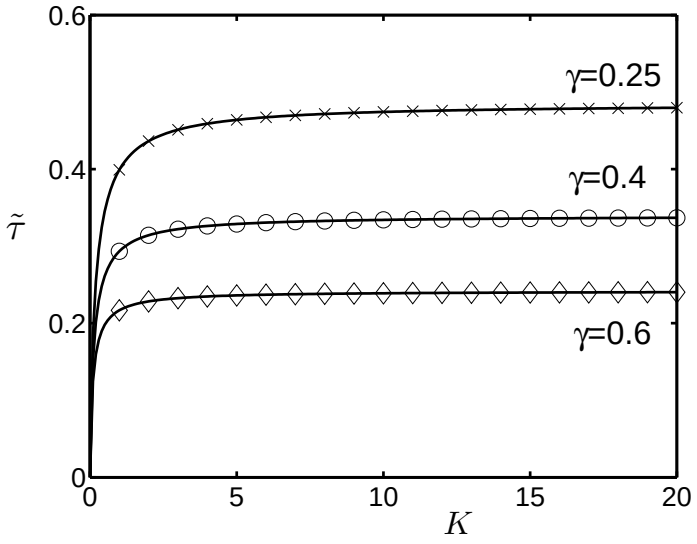

Figure 2.3: Dependence of the probability of transmission across an $S-I$ edge $\widetilde{\tau}$ on the number of stages K as given by Eq. (2.9) for different mean infectious periods with $\tau = 0.166$. Crosses, circles and diamonds correspond to integer values of K on each curve.

observed for smaller values of K that explain the changes in the profile of the infection curves. As will be shown later, $\widetilde{\tau}$ is a very important quantity that controls various properties of epidemic dynamics, such as the threshold for an outbreak and the final size of an epidemic.

2.4.3 $\mathcal{R}_0$-like threshold parameter

Unlike epidemic models in well-mixed populations, defining an appropriate $\mathcal{R}_0$ for pairwise models is more challenging. This is in part due to the difficulty of identifying the typical infectious individual. In order to derive a value for $\mathcal{R}_0$, one needs to consider and correctly account for the correlation between susceptible and infected nodes and measure $\mathcal{R}_0$ when this has stabilised, see Keeling [84] and Eames [43]. Intuitively, this means that the epidemic is allowed to spread in order to become established in the network. This allows for 'typical' infectious individuals to develop and for $\mathcal{R}_0$ to be measured. In large networks this regime can still be considered to be close to or only a small perturbation away from the disease-free steady state.

We now proceed to derive an $\mathcal{R}_0$-like threshold parameter $\mathcal{R}$ which can be used to predict when the epidemics occur, by allowing outbreaks only when $\mathcal{R} > 1$ [136]. To

this end, we linearise the model (2.5) with a classic closure (2.6) near the disease-free equilibrium which has the form $[S] = N$, $[SS] = nN$, and all other quantities being zero. As in the standard approach, the condition necessary for the initial growth of an epidemic is that the real part of the dominant eigenvalue λ_{max} of the resulting characteristic polynomial is positive, and a threshold parameter is obtained as a condition on system parameters that ensure the stability change, i.e. $\lambda_{max} = 0$. In the Appendix B it is shown that the characteristic equation for eigenvalues λ of the linearised system near the disease-free steady state for a K-stage model (2.5) is given by

$$\lambda^2(\lambda + K\gamma)^K \Bigg[(\tau + K\gamma + \lambda)^K - \tau(n-1) \Bigg[(\tau + K\gamma + \lambda)^{K-1} + \sum_{i=1}^{K-1} (K\gamma)^{K-i} (\tau + K\gamma + \lambda)^{i-1} \Bigg] \Bigg] = 0.$$

In Appendix B we prove that the largest eigenvalue λ satisfying this equation goes through zero, i.e. $\lambda_{max} = 0$, when

$$\mathcal{R} := (n-1)\widetilde{\tau} = 1. \tag{2.11}$$

This defines a new $\mathcal{R}_0$-like threshold parameter with $\widetilde{\tau}$ introduced in (2.9). A closer inspection shows that this parameter $\mathcal{R}$ describes the probability of spreading the disease across a given link multiplied by the likely number of susceptible contacts of the individual assuming that they are the earliest people being infected, which perfectly agrees with the standard definition of $\mathcal{R}_0$ as the average number of secondary cases produced in a fully susceptible population by a single typical infectious individual. Whilst $\mathcal{R}$ does not quantify the early growth rate of an epidemic, through its dependence on $\widetilde{\tau}$ and K it allows one to better predict epidemic outbreaks in the case of a more realistic gamma distribution of infectious period, where in the case of an exponential distribution with the same mean infectious period. We also note that whilst in the implementation of the classic $\mathrm{SI}^K\mathrm{R}$ model there was no effect of changing the number of stages on $\mathcal{R}_0$, this more sophisticated model results in a threshold which implicitly accounts for multi-stage infectious periods.

2.4.4 The final size of an epidemic

Since the pairwise model (2.5) is a network representation of an epidemic with life-long immunity and fixed population size, eventually an epidemic will burn out, leaving

some proportion of the population unaffected and still susceptible to the disease. Since $[I_1](\infty) = [I_2](\infty) = \ldots = [I_K](\infty) = 0$, the final size of an epidemic is given by the proportion of people in the removed class, i.e. $[R]_\infty = N - [S]_\infty$. As we saw earlier for the SI^{K}R model (2.1) in a well-mixed population, the final size of a single epidemic does not change with the number of stages. However, the same conclusion no longer holds for the pairwise model (2.5) with the closure (2.6), in which case we have the following result.

Theorem 1. *For a single epidemic outbreak in a closed population with a vanishingly small starting level of infection, the final size of an epidemic in the pairwise model (2.5) with the classical closure (2.6) is given by*

$$R_\infty = 1 - (1 - \widetilde{\tau} + \widetilde{\tau}\theta)^n \,, \tag{2.12}$$

where

$$\theta = (1 - \widetilde{\tau} + \theta\widetilde{\tau})^{n-1} \,, \tag{2.13}$$

and $\widetilde{\tau}$ is defined in (2.9).

Proof. To prove this statement we extend the methodology developed by Keeling [84] for one-stage epidemics. We first introduce some new variables and parameters

$$a = \frac{n-1}{n}, \quad F = \frac{\sum_{i=1}^K [SI_i]}{[S]^a}, \quad G = \frac{[SR]}{[S]^a}, \quad L = \frac{[SS]}{[S]^a}, \quad M = \frac{[SS]}{\exp(n[S]^{1/n})[S]^{2a}},$$

and

$$P_i = \frac{[SI_i]}{[S]^a} \quad \text{for } i = 1, 2, \ldots, K. \tag{2.14}$$

From (2.5) and the easily derived function

$$\dot{[SR]} = -\tau a \frac{[SR]\sum_{i=1}^K [SI_i]}{[S]} + K\gamma[SI_K],$$

it follows that these new variables satisfy the following system of equations

$$\begin{aligned}
\dot{F} &= -\tau F - K\gamma P_K + a\tau \frac{[SS]}{[S]} F, \\
\dot{G} &= K\gamma P_K, \\
\dot{L} &= -a\tau \frac{[SS]}{[S]} F, \\
\dot{M} &= \tau M F.
\end{aligned} \tag{2.15}$$

Since $[I_i](0) = [I_i](\infty) = 0$ for any $i = 1, 2, \ldots, K$, this implies $F(0) = F(\infty) = 0$. Integrating the first equation in (2.15) gives

$$\begin{aligned} F(\infty) - F(0) = 0 &= -\tau \int_0^\infty F dt - K\gamma \int_0^\infty P_K dt + a\tau \int_0^\infty \frac{[SS]}{[S]} F dt \\ &= -[\ln(M(\infty)) - \ln(M(0))] - [G(\infty) - G(0)] - [L(\infty) - L(0)] \\ &= -[\ln(M(\infty)) - \ln(M(0))] - \widetilde{\tau}\,[L(\infty) - L(0)]\,, \end{aligned} \tag{2.16}$$

where in the last step we have used the fact that $G(0) = 0$ and the relation

$$G(\infty) = \frac{[SR]_\infty}{[S]_\infty^a} = (\widetilde{\tau} - 1)[L(\infty) - L(0)], \tag{2.17}$$

derived in Appendix C together with another relation

$$[SS]_\infty = \frac{n[S]_\infty^{2a}}{N^{a-1/n}}. \tag{2.18}$$

Substituting these two relations into Eq. (2.16) and using the fact that $[S](0) = N$ yields

$$\begin{aligned} 0 &= -nN^{1/n} + n[S]_\infty^{1/n} - \widetilde{\tau}\left(\frac{n[S]_\infty^a}{N^{a-1/n}} - nN^{1/n}\right) \\ &= -1 + \left(\frac{[S]_\infty}{N}\right)^{1/n} - \widetilde{\tau}\left[\left(\frac{[S]_\infty}{N}\right)^a - 1\right]. \end{aligned}$$

Introducing the fraction of susceptible individuals as $S_\infty = [S]_\infty/N$, the above equation can be rewritten as follows,

$$1 - S_\infty^{1/n} = \widetilde{\tau}\,(S_\infty^a - 1)\,,$$

or alternatively, as another implicit equation for S_∞

$$S_\infty = (1 - \widetilde{\tau} + \widetilde{\tau}\theta)^n\,, \quad \text{where } \theta = S_\infty^a. \tag{2.19}$$

Since $[I]_i(\infty) = 0$, introducing $R_\infty = [R]_\infty/N$ yields the desired expression for the final size of an epidemic

$$R_\infty = 1 - S_\infty = 1 - (1 - \widetilde{\tau} + \widetilde{\tau}\theta)^n\,.$$

Using the fact that $\theta = S_\infty^a$, equation (2.19) can be rewritten in the form

$$\theta^{1/a} = (1 - \widetilde{\tau} + \widetilde{\tau}\theta)^n \quad \Longrightarrow \theta = (1 - \widetilde{\tau} + \widetilde{\tau}\theta)^{n-1}\,,$$

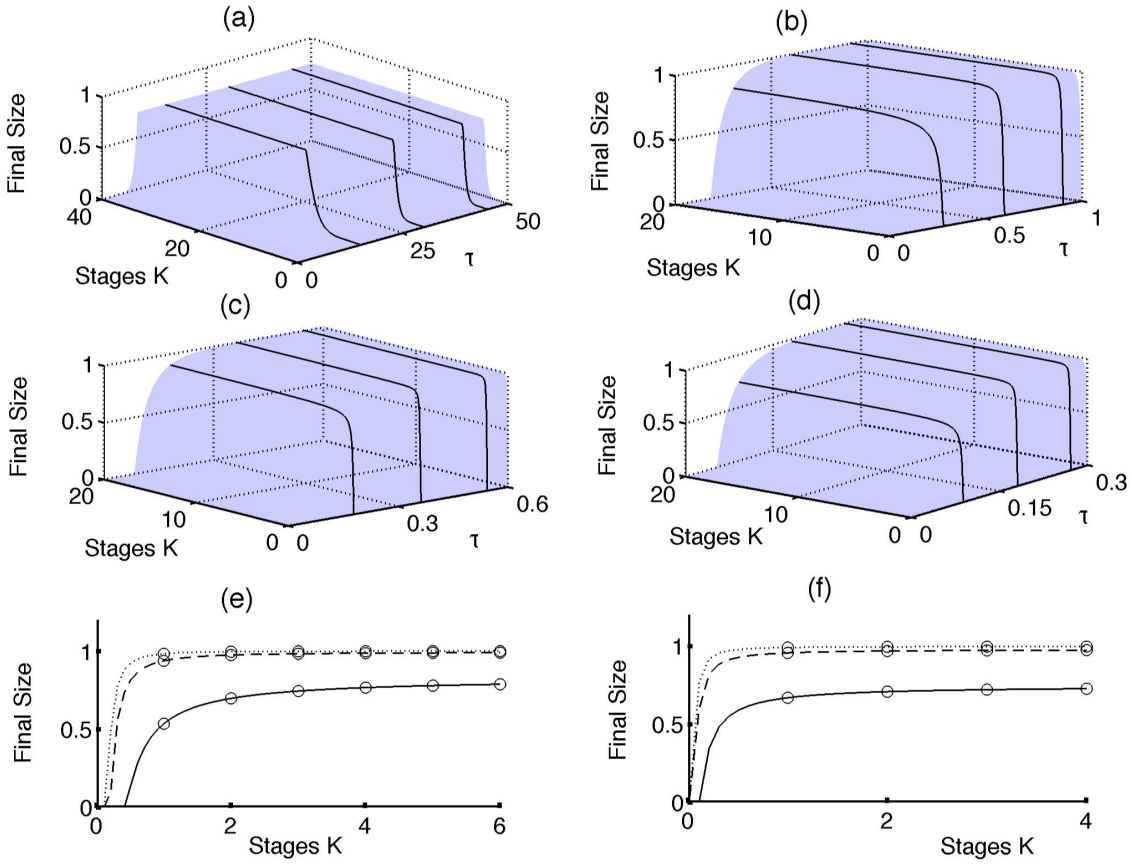

Figure 2.4: Dependence of the final size of an epidemic (2.12) on the per-link transmission rate τ and the number of stages K in the pairwise model (2.5) with $\gamma = 0.4545$ for different average node degrees. (a) $n = 2$. (b) $n = 4$. (c) $n = 7$. (d) $n = 10$. (e) $n = 4$, $\tau = 0.3$ (solid), $\tau = 0.6$ (dashed), $\tau = 0.9$ (dotted). (f) $n = 10$, $\tau = 0.09$ (solid), $\tau = 0.18$ (dashed), $\tau = 0.27$ (dotted). Circles correspond to integer values of K on each curve. The case $n = 2$ is used solely for illustrative purposes, as the resulting networks would be disconnected and thus inappropriate for direct comparison to results from the pairwise model.

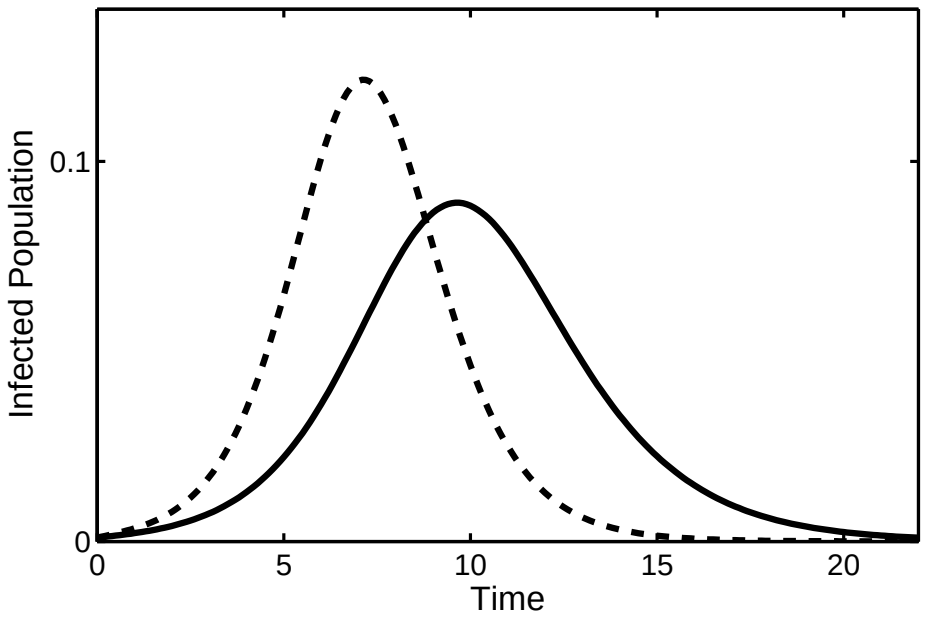

Figure 2.5: Numerical solution of the pairwise $\mathrm{SI}^K\mathrm{R}$ model (2.5) with different average infectious periods and a different number of stages, but the same final size due to identical transmissibility $\widetilde{\tau}$. Parameter values are $\tau = 0.2$, $n = 10$, $\gamma = 1$ and $K = 1$ (solid) and $\tau = 0.2$, $n = 10$, $\gamma \approx 1.06$ and $K = 3$ (dashed). The solution curves for the overall infected population show a radically different intermediate behaviour, but with $\widetilde{\tau} = 1/6$ in both cases, they have the same final epidemic size.

where in the last step we have used the relation $a = (n-1)/n$. This completes the proof. □

We note that our result in Theorem 1 is functionally identical to the result achieved by Keeling [84], and it generalises the final size equation by replacing $\tau/(\tau+\gamma)$ with the parameter $\widetilde{\tau}$. In the case $K = 1$ these two values are equivalent, thus we have perfect agreement with the existing theory. Equivalent relations have also been derived by Newman [126] using percolation theory. Those results were later corrected and shown to hold in all cases where the distribution of infectious periods is degenerative [88]. An equivalent relation has been derived for a static configuration network model with an arbitrary degree distribution [116]. Figure 2.4 illustrates Theorem 1 by showing how the final size of an epidemic on a network depends on the number of infectious stages and, hence, the shape of the distribution of infectious period, which makes it different from earlier analytical results for a well-mixed population [105]. This suggests that inclusion of a more realistic population structure has effect not only on the intermediate disease dynamics, but also on the final proportion of the population that will be affected by the disease. Furthermore, this Figure suggests that for the same mean infectious period, the final size of an epidemic is increasing with the increasing number of stages K. One should note that the number of stages K has the largest effect on the final size of an epidemic for sufficiently low values of K, and then this dependence saturates. As expected, the average node degree n plays an important role, with the minimum value of τ or K required for an epidemic outbreak decreasing with increasing n in perfect agreement with an earlier result in Eq. (2.11). Stochastic simulations (not shown) demonstrate excellent agreement with the results in Fig. 2.4, especially for denser networks. The conclusions of Theorem 1 highlight the importance of collecting accurate and reliable data about the infectivity profile of a disease for predicting the scale of an outbreak.

It is worth noting that whilst the final size depends on the distribution of the infectious period, this dependence is not necessarily unique. This means that two different distributions of infected periods can provide the same transmissibility $\widetilde{\tau}$, resulting in the same final epidemic size in accordance with Theorem 1 but having different intermediate dynamics of infection, as illustrated in Fig. 2.5. The consequence of this observation is that although the epidemic threshold and final epidemic size can both be accurately computed using an estimate for the transmissibility of the disease [126], it is not sufficient to correctly predict the dynamics of the infection spreading process

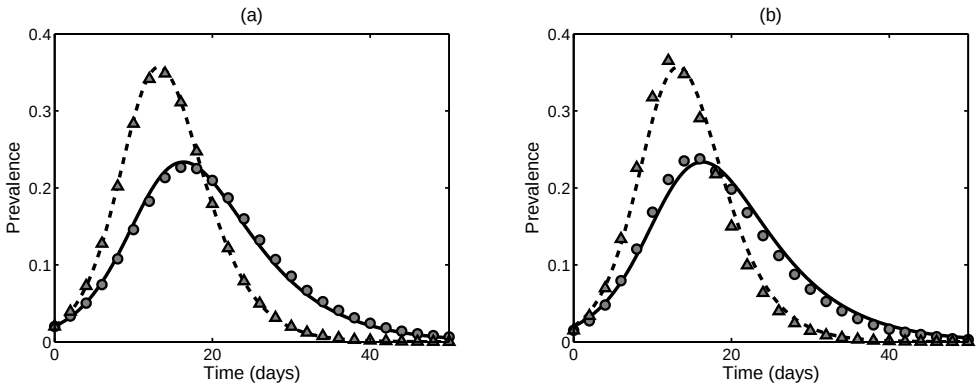

Figure 2.6: Simulation of a SARS outbreak using data from Table 2.1 with $n = 10$ and $N = 1000$. Lines correspond to a numerical solution of the pairwise model (2.5) ($K = 1$ solid line, $K = 3$ dashed line), while symbols represent the average of 250 serious outbreaks ($K = 1$ filled circles, $K = 3$ triangles). (a) Homogeneous network. (b) Erdős-Rényi random graph.

over time, which can be done with our model.

2.5 Impact of a realistic infectious period distribution: case studies

In order to test the accuracy of the pairwise model (2.5) and to illustrate the role played by the distribution of infectious period, we consider the examples of outbreaks of several diseases mentioned in Table 2.1 in a population that is initially fully susceptible. We concentrate on two common and fairly simple network structures, namely, random regular and Erdős-Rényi networks [124], with stochastic simulations being performed using a Gillespie algorithm [55, 32]. We restrict our attention to these network types as we have a pairwise model with closures for regular networks and we would not expect it to work well for other networks. Following the derivation of the pairwise model, the per-link transmission rate is taken to be $\tau = \beta/n$, and we now perform the comparison of an average of 250 stochastic outcomes of serious epidemics on regular and Erdős-Rényi networks against the results of a pairwise model with gamma distributed infectious period. To highlight the impact of including a realistic distribution for the infectious period, we compare the results of simulations with realistic values of parameters from Table 2.1 against those obtained using an exponentially distributed infectious period as assumed in many existing models.

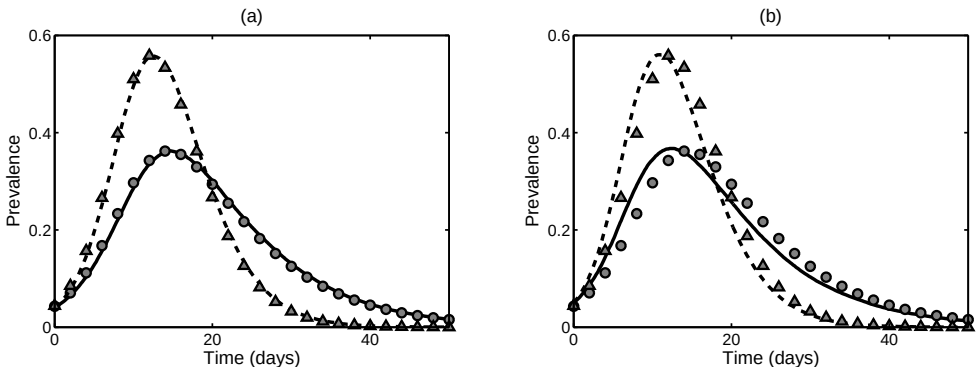

Figure 2.7: Simulation of a smallpox outbreak using data from Table 2.1 with $n = 10$ and $N = 1000$. Lines correspond to a numerical solution of the pairwise model (2.5) ($K = 1$ solid line, $K = 4$ dashed line), while symbols represent the average of 250 serious outbreaks ($K = 1$ filled circles, $K = 4$ triangles). (a) Homogeneous network. (b) Erdős-Rényi random graph.

Severe Acute Respiratory Syndrome (SARS) is a viral disease characterised by flu-like symptoms which is primarily spread through close contacts with infected individuals that makes it a perfect candidate for deducing some basic parameters from epidemiological observations. Figure 2.6 illustrates the comparison of SARS dynamics on regular and Erdős-Rényi networks with a pairwise approximation. One can observe that the effects of including more stages in the disease model on intermediate behaviour are similar to those seen earlier, namely, that gamma distribution of infectious period shortens the overall duration an epidemic and increases peak prevalence. It is also worth noting that, in accordance with Theorem 1, the final size of an epidemic also increases with K.

The second example we consider is smallpox, a viral disease that has been eradicated globally except for two stocks kept in the secure labs and being used for further research. Several papers have modelled the effectiveness of smallpox when used as a bio-weapon, as well strategies for its containment during possible outbreaks [49, 79, 112]. Due to a profound impact smallpox has had on a human population over several centuries, an extensive and quite accurate data has been collected about its transmission. Smallpox is spread through a contact with the mucus of an infected individual, which implies that a close contact is essential for a successful disease transmission. In Fig. 2.7 we show the simulations of smallpox outbreaks on regular and Erdős-Rényi networks using parameter values from Table 2.1 compared to results of the numerical solution of the corresponding pairwise model (2.5). The first important observation that the higher

severity of epidemics outbreaks as suggested by these data makes the pairwise model more accurate, as expected. The effect of including the realistic distribution of infectious period is more pronounced in this case as compared to the SARS simulations, which can be attributed to the fact that smallpox model includes four stages of infection, while the SARS model had only three stages. Despite changes in the intermediate behaviour for smallpox being more pronounced compared to SARS, the final size of an epidemic as given by the pairwise model only increases from 96.34% to 97.89%, which is consistent with an earlier observation that the effect of increasing the number of stages on the final epidemic size is less noticeable for higher K.

Figure 2.8 illustrates the comparison of a pairwise model (2.5) with the closure (2.6) and a stochastic simulation on the example of influenza data with different number of stages of infection. Comparison of figures (a) and (b) shows that the heterogeneity introduced by the degree distribution makes the pairwise model less accurate due to the fact that this model only takes into account the mean degree n. This suggests that whilst our model is very helpful for understanding general features of multi-stage disease dynamics on networks, it has to be extended further to deal effectively with wider and more realistic node degree distributions. One should note that the effects of increasing the number of stages on peak prevalence and the duration of epidemics reduce for higher values of K, as can be observed by comparing the minor changes between temporal profiles of the three- and five-stage influenza epidemics presented as shown in Fig. 2.8.

2.6 Discussion

In this Chapter we have analysed the behaviour of multi-stage infections with particular emphasis on contact networks. Unlike the well-mixed models, for which the number of stages modifies the temporary profile of an outbreak but does not affect the final epidemic size or the condition for disease outbreak, in the case of disease spread on a network, the number of stages, i.e. the precise distribution of infectious period, plays a much more prominent role.

In order to make analytical progress with the analysis of disease dynamics on networks, we have employed the framework of pairwise approximation. This has allowed us to determine the probability of disease transmission across a network edge and to find an $\mathcal{R}_0$-like threshold that controls the onset of epidemics. We have also derived an

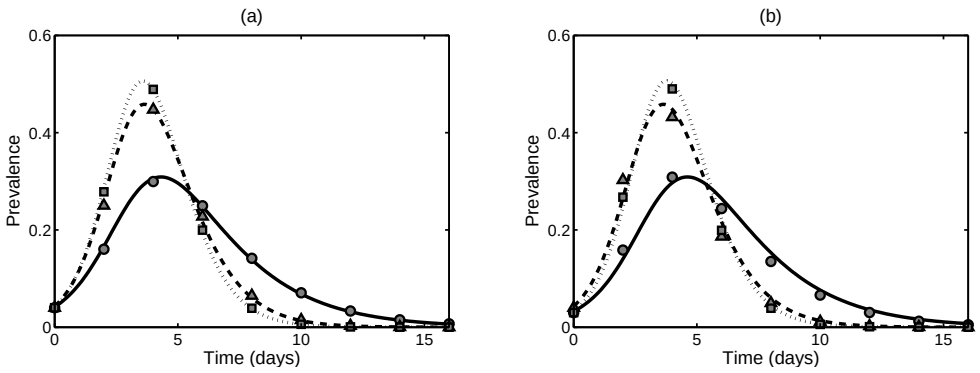

Figure 2.8: Simulation of an influenza outbreak using data from Table 2.1 with $n = 10$ and $N = 1000$. Lines correspond to a numerical solution of the pairwise model (2.5) ($K = 1$ solid line, $K = 3$ dashed line, $K = 5$ dotted line), while symbols represent the average of 250 serious outbreaks ($K = 1$ filled circles, $K = 3$ triangles, $K = 5$ squares). (a) Homogeneous network. (b) Erdős-Rényi random graph.

analytical expression for the final size of an epidemic, which is in perfect agreement with the final size computed using percolation theory [88, 126], and therefore, our findings can be considered exact in the limit of infinite population size. All of these quantities depend not only on the basic disease characteristics, such as, the transmission rate and the average infectious period, but also on the distribution of the infectious period as represented by the number of stages in the model. The importance of this result lies in the fact that unlike earlier studies of multi-stage models in well-mixed populations [4, 105], for the same average duration of the infection period, the final epidemic size is not constant but increasing with the number of stages. We also observe that the threshold at which point a major epidemic is expected depends on the number of infectious stages, with epidemics becoming more likely as the number of stages is increased. This dependence emerges due to the higher resolution of our model which allows us to identify new links between model ingredients and disease dynamics. Similar results have been noted in related studies, for example, in models concerned with contact tracing [45] and models of coupled disease and information transmission on networks [52].

Numerical simulations of epidemic outbreak for several different multi-stage infections demonstrate that while the pairwise model provides a reasonably good approximation of the network dynamics, the agreement with stochastic simulations is affected by clustering and local network structure that can induce correlations in the dynamics of different nodes, as well as the inhomogeneity in the node degree distribution, as should be expected from the fact that the pairwise closure only depends on the average

node degree.

There are several directions in which the approach presented in this Chapter could be extended. These include the analysis of SIS and SEIR models, as well as inclusion of multiple stages for both the latent and infected classes (Nguyen and Rojani 2008) [129]. Whilst inclusion of latent classes may have no effect on the basic reproduction number or the final size distribution in a fully well-mixed model (Black and Ross 2015; House et al. 2013) [16, 71], whether the same would be true in a network model remains to be seen. Another interesting and important problem would be the consideration of network dynamics for epidemic models with temporary immunity (Blyuss and Kyrychko 2010) [17]. Allowing the level of infectiousness of different nodes to vary depending on the stage of infection they belong to would result in even more realistic models of multi-stage diseases on networks.

It should also be possible to apply such a multi-stage approach to other elements of the model. For instance, a multi-stage progression for susceptibles, where each transmission event moves them into a latter stage and, ultimately, to becoming infected. This would represent a disease where multiple exposures were needed in order to become infected. It is known that repeated exposure can increase the risk of infection [98], but extra justification would be needed for repeated exposure to be required in order for the disease to spread. S-I edges could also go through some number of stages. This would lead to a gamma distributed transmission process by the same reasoning that altered the infectious period in the model presented in this paper. There is growing evidence that transmission may be distributed according to a power law [29, 31]. Imposing a gamma distribution may be able to replicate the heavy-tail of power law distributions but, crucially, it will not be able to also capture the tendency for multiple events to occur rapidly within a short window of time.

One of the challenging but practically important generalisations of the present framework would be an extension of a pairwise model that would account for heterogeneity in node degree distribution (House and Keeling 2011) [70]. This would provide deterministic models potentially amenable to analytical treatment that would more accurately represent stochastic disease dynamics.

Acknowledgements N. Sherborne acknowledges funding for his PhD studies from the Engineering and Physical Sciences Research Council (EPSRC). The authors would like to thank the anonymous referees for helpful comments and suggestions that have

helped to improve the presentation.

2.7 Appendices

2.7.1 Appendix A - Transmissibility

In this Appendix we prove an expression (2.9) for the probability of transmission across a given link. For an arbitrary number of stages and transition/recovery parameter $K\gamma$, the distribution of the infectious period is gamma distributed, and hence we consider here the density function originally stated in (2.8)

$$g(x; K, 1/(K\gamma)) = \frac{1}{(K-1)!}(K\gamma)^K x^{K-1} e^{-K\gamma x}.$$

Since the probability of infection taking place for a given $S-I$ link during time t is given by $1-e^{-\tau t}$, the probability of transmission across this link in a K-stage is given by

$$\begin{aligned}\widetilde{\tau} &= \int_0^\infty (1-e^{-\tau x}) \left(\frac{1}{(K-1)!}(K\gamma)^K x^{K-1} e^{-(K\gamma)x} \right) dx \\ &= \frac{(K\gamma)^K}{(K-1)!} \left[\int_0^\infty x^{K-1} e^{-(K\gamma)x} dx - \int_0^\infty x^{K-1} e^{-(\tau+K\gamma)x} dx \right] \qquad (2.20) \\ &= 1 - \frac{(K\gamma)^K}{(K-1)!} \int_0^\infty x^{K-1} e^{-(\tau+K\gamma)x} dx,\end{aligned}$$

where the final equality is obtained by noting that the first integral is simply the integral of the gamma distribution function over $\mathbb{R}^+$, and, hence, is equal to one. Integration by parts yields a recursive relation

$$\int_0^\infty x^{K-1} e^{-(\tau+K\gamma)x} dx = \frac{K-1}{\tau+K\gamma} \int_0^\infty x^{K-2} e^{-(\tau+K\gamma)x} dx,$$

which is valid for any integer $K > 1$, and this then implies

$$\int_0^\infty x^{K-1} e^{-(\tau+K\gamma)x} dx = \frac{(K-1)!}{(\tau+K\gamma)^K}.$$

Substituting this expression into Eq. (2.20) yields

$$\widetilde{\tau} = 1 - \frac{(K\gamma)^K}{(K-1)!} \frac{(K-1)!}{(\tau+K\gamma)^K} = 1 - \frac{(K\gamma)^K}{(\tau+K\gamma)^K}.$$

2.7.2 Appendix B - $\mathcal{R}_0$-like threshold parameter

Linearisation of the pairwise model (2.5) with the closure (2.6) at the disease-free equilibrium yields the stability condition for eigenvalues λ as a $(2K+2)\times(2K+2)$ matrix. It is useful to first consider it in a block form as follows,

$$\begin{pmatrix} A & B \\ C & D \end{pmatrix}$$

where C is a zero $(K+1)\times(K+1)$ matrix, and the matrix A is lower-diagonal, and therefore, its determinant is the product of the diagonal terms. Hence, the characteristic equation can be written as

$$\lambda^2(\lambda+K\gamma)^K \begin{vmatrix} \tau(n-1)-K\gamma-\tau-\lambda & \tau(n-1) & & \dots & \tau(n-1) \\ K\gamma & -K\gamma-\tau-\lambda & 0 & \dots & 0 \\ 0 & K\gamma & \ddots & \ddots & \vdots \\ \vdots & 0 & \ddots & \ddots & 0 \\ 0 & \dots & 0 & K\gamma & -K\gamma-\tau-\lambda \end{vmatrix} = 0$$

This matrix can now be reduced to a series of lower-diagonal matrices to give the following general form of the characteristic equation

$$\begin{aligned} 0 = \lambda^2(\lambda+K\gamma)^K \Bigg[& (\tau(n-1)-K\gamma-\tau-\lambda)(-K\gamma-\tau-\lambda)^{K-1} \\ & - \tau(n-1)\left(\sum_{i=1}^{K-1}(-1)^{K-i}(K\gamma)^{K-i}(-K\gamma-\tau-\lambda)^{i-1}\right)\Bigg] \\ = \lambda^2(\lambda+K\gamma)^K \Bigg\{ & (\tau+K\gamma+\lambda)^K \\ & - \tau(n-1)\left[(\tau+K\gamma+\lambda)^{K-1} + \sum_{i=1}^{K-1}(K\gamma)^{K-i}(\tau+K\gamma+\lambda)^{i-1}\right]\Bigg\}. \end{aligned}$$

It immediately follows that the above equation has roots of $\lambda=0$, $\lambda=-K\gamma$, the other K roots are determined by the roots of the expression in curly brackets. The two zero roots exist because the system has a line of equilibria. So long as $\sum_i[I_i]=0$ the system is in equilibrium, with $[S]+[R]=N$ and $[SS]+2[SR]+[RR]=nN$. We thus ascertain the stability of the DFE based on having zero recovered population, to mimic the early stage of the epidemic. If all of the remaining eigenvalues are negative, then there is no exponential growth phase and the DFE is stable.

Since an epidemic outbreak occurs when the disease-free equilibrium becomes unstable, one has to identify conditions on parameters when the stability of the disease-free steady state changes, i.e. where $\lambda = 0$. Substituting $\lambda = 0$ into the expression in curly brackets yields

$$0= (\tau + K\gamma)^K + \tau(n-1)\left[(\tau + K\gamma)^{K-1} - \sum_{i=1}^{K-1}(K\gamma)^{K-i}(\tau + K\gamma)^{i-1}\right]$$

$$= (\tau + K\gamma)^K - (n-1)\Big[(\tau + K\gamma)^K - (K\gamma)^K\Big].$$

This relation can be recast as

$$1 = (n-1)\left(1 - \frac{(K\gamma)^K}{(\tau + K\gamma)^K}\right) = (n-1)\widetilde{\tau},$$

which gives the desired expression of $\mathcal{R} = (n-1)\widetilde{\tau}$ in Eq. (2.11).

2.7.3 Appendix C - Final epidemic size

To prove relation (2.17), we consider the time derivatives of the functions $P_i = \frac{[SI_i]}{[S]^a}$ for $i = 1, 2, \ldots, K$, which can be found from the pairwise model (2.5):

$$\dot{P}_1 = -(\tau + K\gamma)P_1 + \tau a\frac{[SS]}{[S]}F,$$
$$\dot{P}_i = -(\tau + K\gamma)P_i + K\gamma P_{i-1}, \quad i = 2, 3, \ldots, K.$$

We also remind the reader of the functions G and L and equations for their dynamics

$$G = \frac{[SR]}{[S]^a} \implies \dot{G} = K\gamma P_K, \quad L = \frac{[SS]}{[S]^a} \implies \dot{L} = -a\tau\frac{[SS]}{[S]}F.$$

Integrating the equation for P_1 and using the fact that $[SI_1](0) = [SI_1](\infty) = 0$, gives

$$\begin{aligned} 0 = \int_0^\infty \dot{P}_1 dt &= -(\tau + K\gamma)\int_0^\infty P_1 dt + a\tau\int_0^\infty \frac{[SS]}{[S]}F dt \\ &= -(\tau + K\gamma)\int_0^\infty P_1 dt - [L(\infty) - L(0)]. \end{aligned} \tag{2.21}$$

In a similar way, integrating the equation for P_2 yields

$$0 = \int_0^\infty \dot{P}_2 dt = -(\tau + K\gamma)\int_0^\infty P_2 dt + K\gamma\int_0^\infty P_1 dt,$$

which can be rewritten as

$$\int_0^\infty P_1 dt = \frac{\tau + K\gamma}{K\gamma} \int_0^\infty P_2 dt.$$

Proceeding the the same way, one obtains

$$\int_0^\infty P_i dt = \frac{\tau + K\gamma}{K\gamma} \int_0^\infty P_{i+1} dt, \quad i = 2, 3, \ldots, K-1.$$

Going through all stages of infections, we find

$$\int_0^\infty P_1 dt = \frac{(\tau + K\gamma)^{K-1}}{(K\gamma)^{K-1}} \int_0^\infty P_K dt.$$

On the other hand, integrating equation for G and using $G(0) = 0$ gives

$$G(\infty) - G(0) = \frac{[SR]_\infty}{[S]_\infty^a} = K\gamma \int_0^\infty P_K dt \quad \Longrightarrow \quad \int_0^\infty P_K dt = \frac{1}{K\gamma} \frac{[SR]_\infty}{[S]_\infty^a}.$$

Combining the last two expressions, we obtain

$$\int_0^\infty P_1 dt = \frac{(\tau + K\gamma)^{K-1}}{(K\gamma)^K} \frac{[SR]_\infty}{[S]_\infty^a},$$

and substituting this result into Eq. (2.21) gives the final relation (2.17):

$$\frac{[SR]_\infty}{[S]_\infty^a} = (\widetilde{\tau} - 1)[L(\infty) - L(0)]. \tag{2.22}$$

In order to prove relation (2.18), we examine the ratio $[SS]/[S]$, whose dynamics is governed by the following equation

$$\frac{d}{dt}\frac{[SS]}{[S]} = -\tau \frac{(n-2)}{n} \frac{[SS]}{[S]} \frac{\sum_{i=1}^K [SI_i]}{[S]}.$$

Separating variables and integrating this equation gives

$$\left[\ln\left(\frac{[SS]}{[S]}\right)\right]_0^\infty = -\tau \frac{(n-2)}{n} \int_0^\infty \frac{\sum_{i=1}^K [SI_i]}{[S]} dt. \tag{2.23}$$

Rather than compute the integral in the right-hand side of the above equation, we use the first equation of the pairwise model (2.5), which can be written as

$$\frac{1}{[S]}\frac{d}{dt}[S] = -\tau \frac{\sum_{i=1}^K [SI_i]}{[S]}.$$

Integrating this equation gives

$$\int_0^\infty \frac{1}{[S]} d[S] = -\tau \int_0^\infty \frac{\sum_{i=1}^K [SI_i]}{[S]} dt \quad \Longrightarrow \quad (\ln[S])_0^\infty = -\tau \int_0^\infty \frac{\sum_{i=1}^K [SI_i]}{[S]} dt.$$

Using this expression to replace an integral in (2.23) gives

$$\ln\left(\frac{[SS]_\infty}{[S]_\infty}\right) - \ln\left(\frac{[SS]_0}{[S]_0}\right) = \frac{n-2}{n}\ln\left(\frac{[S]_\infty}{[S]_0}\right).$$

Substituting $[S]_0 = N$ and $[SS]_0 = nN$, this formula can be rewritten as

$$\ln\left(\frac{[SS]_\infty}{[S]_\infty}\right) = \ln\left(\frac{nN}{N}\right) + \ln\left(\frac{[S]_\infty}{N}\right)^{\frac{n-2}{n}},$$

or alternatively,

$$\frac{[SS]_\infty}{[S]_\infty} = n\left(\frac{[S]_\infty}{N}\right)^{\frac{n-2}{n}}.$$

Multiplying both sides by $[S]_\infty$ and using the definition $a = (n-1)/n$, we obtain

$$[SS]_\infty = n\frac{[S]_\infty^{2(n-1)/n}}{N^{(n-2)/n}} = n\frac{[S]_\infty^{2a}}{N^{a-1/n}},$$

which gives the desired relation (2.18).

Chapter 3

Paper 2: Compact pairwise models for epidemics with multiple infectious stages on degree heterogeneous and clustered networks

N. Sherborne[1], K. B. Blyuss[1] and I. Z. Kiss[1]

[1]Department of Mathematics, School of Mathematical and Physical Sciences, University of Sussex, Brighton, BN1 9QH, UK

3.1 Abstract

This Chapter presents a compact pairwise model that describes the spread of multi-stage epidemics on networks. The multi-stage model corresponds to a gamma-distributed infectious period which interpolates between the classical Markovian models with exponentially distributed infectious period and epidemics with a constant infectious period. We show how the compact approach leads to a system of equations whose size is independent of the range of node degrees, thus significantly reducing the complexity of the model. Network clustering is incorporated into the model to provide a more accurate representation of realistic contact networks, and the accuracy of proposed closures is analysed for different levels of clustering and number of infection stages. Our results support recent findings that standard closure techniques are likely to perform better when the infectious period is constant.

3.2 Introduction

Mathematical models of infectious diseases have proven to be an invaluable tool in understanding how diseases invade and spread within a population, and how best to control them [6, 37, 131].

Given a good understanding of the biology of the disease and of the behaviour and interaction of hosts, it is possible to develop accurate models with good predictive power, which provide the means to develop, test and deploy control measures to mitigate the negative impacts of infectious diseases, a good example being influenza [48]. However, as has been highlighted by the recent Ebola outbreak in West Africa [33], models can be very situation-specific and can become highly sophisticated or complex depending on intricacies of the structure of the population and the characteristics of the disease.

In the last few decades the use of networks to describe interactions between individuals has been an important step change in modelling and studying disease transmission [35, 84, 85, 131]. There is now overwhelming empirical evidence that in many practical instances individuals interact in a structured and selective way, e.g. in the case of sexually transmitted diseases [99]. Thus, the well-mixed assumption of early compartmental models [89] has to be relaxed or models need to be refined by including multiple classes and mixing between classes. However, in some cases a network representation could be more realistic than a description based on compartmental models. Conventionally, nodes in network-based models represent individuals, and the edges describe connec-

tions between people who have sufficient contact to be able to transmit the disease [35, 85, 131]. The total number of edges a node has is known as its degree, and the frequency of nodes with different degrees is determined by a specific *degree distribution* p_k which can either be empirically measured or given theoretically. In either case p_k is the probability of a randomly chosen node having degree k. Early network models often assumed regular networks where all nodes have the same degree, or well-studied networks from graph theory, such as the Erdős-Rényi random graphs [46]. However, empirical research showed that real biological, social or technological networks do not conform to such idealised models. In fact, many studies on human interactions ranging from sexual contact networks [99] to using the travel of banknotes as an indicator of human activity [24], or even internet connectivity [26] have observed *wide-tail distributions*, with the majority of nodes having a low number of contacts, and a few nodes in the network having a much higher degree. This structure is most closely approximated by scale-free networks described by a power-law degree distribution $p_k \sim k^{-\alpha}$ with some positive exponent α, which for most accurately described human contact patterns lies in the range $\alpha \in [2, 3]$ (see, for example, [132]). The impact of contact heterogeneity on the spread of epidemics is significant, and studies have highlighted the disproportionate role which may be played by a few highly-connected nodes [75].

Another striking feature of real social contact patterns is the presence of small and highly-interconnected groups which occur much more frequently than if edges were to be distributed at random. This is known as *clustering*, and its presence in empirical data [51, 128] has driven the need to consider network models that include this feature. Perhaps, one of the most well-known and parsimonious theoretical models with tuneable clustering is the small-world network [167], where nodes are placed on a ring, and the network is dominated by local links to nearest neighbours with a few links rewired at random, which means that the average path length is not too large and comparable to that found in equivalent random networks. For a summary of numerous alternative algorithms that can be used to generate clustered networks see, for example, [61] or [140]. It is well known that modelling epidemic spread on such networks is more challenging, although some models have successfully incorporated clusterings [81, 115, 141, 163, and references therein]. However, it is often the case that such models only work for networks where clustering is introduced in a very specific way, e.g. by considering non-overlapping triangles or other subgraphs of more than three nodes.

Besides the details of the network structure, another major assumption that sig-

nificantly reduces the mathematical complexity of models and makes them amenable to analysis with mean-field models of ordinary differential equations and tools from Markov chain theory is the assumption that the spreading/transmission of infection and recovery processes are Markovian. However, it has long been recognised that this is often not the case, and, for example, the infectious periods are typically far from exponential, and, perhaps, are better described by a normal-like or peaked distribution [58, 103, 168]. Modelling non-Markovian processes can be challenging and often leads to delay differential or integro-differential equations that are much more difficult to analyse. Recently, Kiss et al. [92] have put forward a generalisation of a pairwise model for Markovian transmission with a constant infectious period for a susceptible-infected-recovered (SIR) dynamics. The resulting model is a system of delay differential equations with discrete and distributed delays which makes it possible to gain insight into how the non-Markovian nature of the recovery process affects the epidemic threshold and the final epidemic size. Other important recent research in this direction includes the message passing formalism [80, 170] and an approach based on renewal theory [28].

In light of the importance of the above-mentioned network properties (i.e. degree heterogeneity and clustering) and the non-Markovian nature of the spreading and/or recovery processes driving the epidemics, in this Chapter we generalise our recent research on a multi-stage SIR epidemic model [149] and focus on modelling a Markovian spreading process with gamma-distributed infectious period on networks that account for heterogeneous degree distribution and clustering. This is achieved within the framework of pairwise models [84], and we show that the additional model complexity induced by degree heterogeneity and non-Markovian recovery can be effectively controlled via a reduction procedure proposed by Simon and Kiss [151]. This allows one to derive an approximate deterministic model that helps numerically determine the time evolution of the epidemic and the final epidemic size. Moreover, the model allows us to gain insights into the interactions of the three main model ingredients, namely, degree heterogeneity, clustering and non-exponential recovery and the agreement between the model and the stochastic network simulation. The Chapter is organised as follows. In the next section we derive a compact pairwise model for unclustered networks whose size is independent of the range of degrees and derive and discuss some analytical results for this model. All results are validated by comparing the numerical solution of the pairwise model to results from direct stochastic network simulation. In Section 3.4, we investigate the case when the same epidemic unfolds on clustered networks. The corresponding pairwise

model is derived, and we discuss the extra complexities necessary to more accurately approximate the spread of the disease. More importantly, we investigate how clustering and the non-Markovian recovery affect the agreement between the pairwise model and simulations. Finally, in Section 3.5 we conclude with a discussion of our results and future work.

3.3 Disease dynamics in the absence of clustering

As a first step in the analysis of the spread of epidemics on unclustered networks, we introduce the necessary concepts from multi-stage infections and pairwise models [149]. In the SI^{K}R model, once a susceptible individual S becomes infected, they progress through K equally infectious stages denoted as $I^{(i)}$, $1 \leq i \leq K$. The transition rates between successive stages are given by $K\gamma$. Thus, in simulation the times spent in each of the K stages are independent exponentially distributed random numbers. The total time of infection is, therefore, the sum of K exponential distributions, which is a gamma distribution with the mean time of γ^{-1} [42]. In order to describe the dynamics of an epidemic we consider the state of the nodes in the network and the edges connecting them. Since a susceptible individual can only become infected upon a transmission across an $S - I^{(i)}$ link we need to consider the expected number of edges connecting susceptible and infected individuals (in any of the K stages) at time t over the whole network, to be denoted as $[SI^{(i)}](t)$. Here we have taken $[SI^{(i)}]$ independently of the degrees of the nodes in state S and $I^{(i)}$, i.e. $[SI^{(i)}] = \sum_{a,b}[S_a I_b^{(i)}]$ where a and b denote the degrees in the range between the minimum and maximum degrees in the network, denoted as k_{min} and k_{max}, respectively. This definition applies to all pairs, i.e. $[AB]$ stands for the population level count of all $A - B$ edges taken across all possible connections between nodes of different degrees;

$$[AB] = \sum_{a,b}[A_a B_b], \quad \text{and} \quad A, B \in \{S, I_1, I_2, \ldots, I_K, R\} := \mathbb{S}.$$

Here and henceforth $\mathbb{S}$ will denote the set of all possible states for a node. The expected number of $S - S$ edges depends on the expected number of $S - S - I^i$ triples, with this being the case for other edge types as well. To break the dependency on higher order moments, closure relations must be introduced which allow us to approximate the number of triples using the number of pairs and nodes in different states [84].

We begin our analysis by considering the simpler case where the contact network has a locally tree-like structure characterised by zero clustering. The Markovian, or

single stage, pairwise model has been proven to be exact prior to closure [154], and the approach can be extended to a $\mathrm{SI}^K\mathrm{R}$ multi-stage model. In order to obtain a pairwise model for the $\mathrm{SI}^K\mathrm{R}$ dynamics for unclustered and degree heterogeneous networks, we start with the unclosed model for a general K-stage disease and describe an *a priori* method to derive a new set of closures at the level of triples. It should be noted that our approach resembles that used in recent works of Simon and Kiss [151] and House and Keeling [70]. The system describing the dynamics of a K-stage disease has the following form [149]

$$
\begin{aligned}
&[\dot{S}] = -\tau[SI],\\
&[\dot{I^{(1)}}] = \tau[SI] - K\gamma[I^{(1)}],\\
&[\dot{I^{(j)}}] = K\gamma[I^{(j-1)}] - K\gamma[I^{(j)}], \quad \text{for} \quad j = 2, 3, \ldots, K,\\
&[\dot{SS}] = -2\tau[SSI],\\
&[\dot{SI^{(1)}}] = -(\tau + K\gamma)[SI^{(1)}] + \tau\left([SSI] - [ISI^{(1)}]\right),\\
&[\dot{SI^{(j)}}] = -(\tau + K\gamma)[SI^{(j)}] + K\gamma[SI^{(j-1)}] - \tau[ISI^{(j)}], \quad \text{for} \quad j = 2, 3, \ldots, K,\\
&[\dot{SR}] = -\tau[ISR] + K\gamma[SI^{(K)}],
\end{aligned}
\tag{3.1}
$$

where τ is the per-link disease transmission rate, and the terms without superscripts represent summation over all infected compartments, i.e. $[SI] = \sum_{i=1}^{K}[SI^{(i)}]$, $[SSI] = \sum_{i=1}^{K}[SSI^{(i)}]$ and $[ISI^{(j)}] = \sum_{i=1}^{K}[I^{(i)}SI^{(j)}]$. While the above equations do not seem to account separately for the degrees of the nodes, we will show that it is possible to keep such a system and include all the information about the degree distribution in a new closure relation at the level of pairs. The closure for this model can be obtained by first considering the classical triple closure for a regular network proposed by Keeling et al. [82]

$$
[XSI^{(i)}] \approx \frac{n-1}{n}\frac{[XS][SI^{(i)}]}{[S]}, \tag{3.2}
$$

where n is the degree of every node in the network (and thus also the mean degree), and $X \in \mathbb{S}$. The derivation of a new closure for heterogeneous networks starts from noting that closure (3.2) depends on the degree of the middle node, which allows us to write

$$
[XS_jY] \approx \frac{j-1}{j}\frac{[XS_j][S_jY]}{[S_j]}, \quad X, Y \in \mathbb{S}, \tag{3.3}
$$

for a susceptible node of degree j, with $j \in [k_{min}, k_{max}]$. To make further progress, one can use the approximation used by Eames and Keeling [44],

$$[S_j Y] \approx [SY] \frac{j[S_j]}{\sum_{m=k_{min}}^{k_{max}} m[S_m]}. \tag{3.4}$$

This assumes that the number of $S_j - Y$ pairs is approximately equal to the number of $S - Y$ pairs (regardless of node degree) multiplied by the fraction of S nodes with degree j. Substituting this approximation into (3.3) yields

$$[XS_jY] \approx [XS][SY] \frac{j(j-1)[S_j]}{T_1^2}, \tag{3.5}$$

where

$$T_1 := \sum_{m=k_{min}}^{k_{max}} m[S_m] = [SS] + \sum_{i=1}^{K} [SI^{(i)}] + [SR]$$

denotes the total number of edges emanating from susceptible nodes. The second expression for T_1 above follows directly from the pairwise model (3.1) and explains the need for explicitly including an equation for $[SR]$. Taking the sum of all triples in (3.5) over all degrees j gives

$$[XSY] = \sum_{j=k_{min}}^{k_{max}} [XS_jY] \approx [XS][SY] \frac{T_2 - T_1}{T_1^2}, \tag{3.6}$$

with

$$T_2 = \sum_{m=k_{min}}^{k_{max}} m^2[S_m].$$

Unfortunately, T_2 cannot be expressed in a closed form from the solution of system (3.1). However, it should be possible to estimate the degree distribution of susceptible nodes [150, 151]. This distribution is given by

$$s_k := [S_k]/[S],$$

and has the mean

$$n_S = T_1/[S].$$

Simon and Kiss [151] have shown by means of numerical simulations that the (dynamic) degree distribution of susceptible nodes is proportional to the degree distribution p_k. Numerical simulations shown in Fig. 3.1 demonstrate that despite being entirely heuristic, this relation between the two distributions holds for all the different networks it

was tested on. We use this linear relationship between s_k and p_k in order to derive a compact model. A brief explanation is given below, for the full method one can refer to [151]. As they will be needed later, we first introduce the moments of the degree distribution p_k, namely,

$$n_i = \frac{\sum_{m=k_{min}}^{k_{max}} m^i N_m}{N} = \sum_{m=k_{min}}^{k_{max}} m^i P(m),$$

where N is the total population size. It is easy to see that

$$T_2 = [S] \sum_{m=k_{min}}^{k_{max}} m^2 s_m,$$

and so our goal is to find an estimate for s_k. Introducing a new variable $q_k = s_k/p_k$ linearity enforces the following relation for all $k \in [k_{min}, k_{max}]$

$$\frac{q_k - q_{k_{min}}}{k - k_{min}} = \frac{q_{k_{max}} - q_{k_{min}}}{k_{max} - k_{min}}.$$

By manipulating this equation one can identify a relation between s_k and p_k; namely

$$s_k = \frac{(k - k_{min})\, q_{k_{max}} + (k_{max} - k)\, q_{k_{min}}}{k_{max} - k_{min}} p_k. \tag{3.7}$$

Since the sum of all s_k's is one, and the distribution has the mean n_S, it is then possible to recast $q_{k_{min}}$ and $q_{k_{max}}$ in terms of the known quantities n_1, n_2, n_3 and n_S. Feeding these back into (3.7) gives an estimate for s_k, and thus T_2. Using this estimate we arrive at the following relation

$$\frac{T_2 - T_1}{T_1^2} \approx \frac{1}{n_S^2 [S]} \left(\frac{n_2(n_2 - n_1 n_S) + n_3(n_S - n_1)}{n_2 - n_1^2} - n_S \right).$$

This gives the closure for the heterogeneous compact pairwise SI^{K}R model (3.1) in the form

$$[XSY] \approx \zeta(t) \frac{[XS][SY]}{[S]}, \tag{3.8}$$

where

$$\zeta(t) = \frac{n_2(n_2 - n_1 n_S) + n_3(n_S - n_1)}{n_S^2\,(n_2 - n_1^2)} - \frac{1}{n_S}. \tag{3.9}$$

It is evident that the range of degrees and the degree distribution have been implicitly accounted for in the closure relation, thus allowing us to work with a set of equations whose size is independent of the range of degrees. In other words, regardless of the

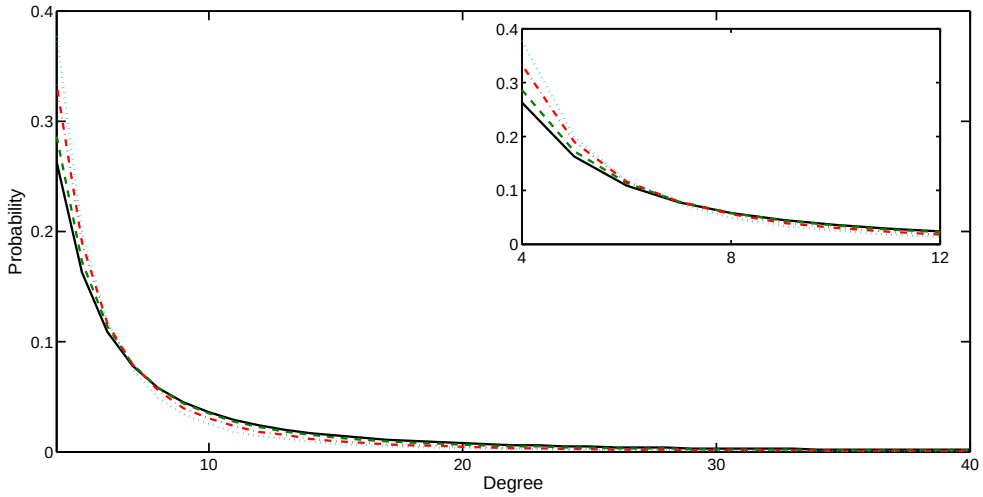

Figure 3.1: The results of testing the relation between the degree distribution p_k and the distribution of susceptible nodes s_k over time for a truncated scale-free network. The black line represents the degree distribution p_k that coincides with s_k at $t = 0$, and the green, red and light blue lines represent s_k at times 10, 15 and 20, respectively from 100 simulations of the epidemic. Note that all lines show the same qualitative behaviour.

exact nature of the contact network we will only ever need $2K+3$ equations in (3.1) to model the epidemic. This is due to all of the information about the degree distribution being included in $\zeta(t)$. In the special case of regular contact networks, where every node has the same degree n, one has that $n_S = n_1 = n$, $n_2 = n^2$ and $n_3 = n^3$, hence $\zeta(t)$ reduces to

$$\zeta = \frac{n-1}{n},$$

and the closure reverts back to the simpler version given in (3.2).

3.3.1 Numerical simulation results

In order to test the effectiveness of model (3.1) with closure (3.8), we compare its output to numerical simulation of epidemics spreading on networks with bimodal and truncated scale-free degree distributions, with both types of networks being constructed using the configuration model [15]. For bimodal networks, all nodes have degree k_1 or k_2, and the proportion of nodes with degrees k_1 and k_2 in the network; each node is then given either k_1 or k_2 half-edges which are connected to other half-edges at ran-

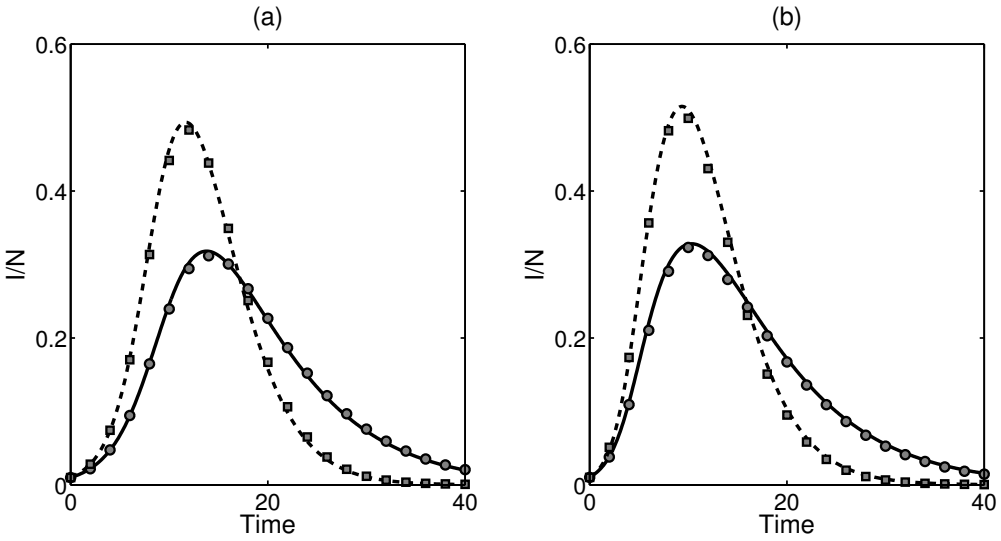

Figure 3.2: Dynamics of epidemics spreading on unclustered networks of 1000 nodes with (a) bimodal degree distribution with an even split of nodes having degrees 4 or 12, and (b) truncated scale-free degree distribution $p_k \sim k^{-\alpha}$ bounded by $k_{min} = 4$, $k_{max} = 60$, and with $\alpha = 2.5$, and the mean degree of around 8. For both topologies, the simulations are performed for $K = 1$ (black line, circles) and $K = 4$ (dashed line, squares). Lines show the solution of the pairwise model (3.1) with the closures given in (3.8), and symbols correspond to stochastic network simulation. Other parameter values are $\tau = 0.07$, $\gamma = 0.15$.

dom to create the edges. The generation of truncated scale-free networks begins by choosing bounds of minimum and maximum degree k_{min} and k_{max}. One then generates a power law distribution with a chosen exponent α and samples the normalized probability of a node having degree $k \in [k_{min}, k_{max}]$, after which half-edges are drawn and connected at random. If the total number of half-edges is odd, one is removed at random, the effect of which is small and diminishes rapidly as the total number of nodes N grows. Each simulation begins with a single infected individual, and the time is rescaled to zero after the number of infected individuals reaches ten, when counted across all compartments. The results of these tests are presented in Fig. 3.2, which show the comparison of an average of 100 simulations (consisting of 20 simulations for five different random networks with the same topology) and the output from the pairwise model (3.1). Figure 3.2 shows that increasing the number of infectious stages leads to a more rapid spread of the disease with higher peak prevalence, despite the mean duration of infection remaining unchanged. This suggests that the lead time to imple-

ment any control measures is much shorter than estimates based on standard models where recovery is Poisson would suggest. This behaviour was also observed in the case of homogeneous populations [149]. We further note that for the same parameters of the disease dynamics, the trend of faster growth is even more profound for scale-free networks. This effect can be attributed to the influence of a small number of highly connected nodes; these individuals are at greater risk of receiving infection, and also have a much greater capacity to spread the disease, thereby causing a rapid increase in the number of new infections. This also has a significant impact on the threshold parameter which describes the point at which an epidemic occurs, as will be discussed later.

3.3.2 Characteristics of the multi-stage compact model

Now that the system of pairwise equations (3.1) with closures given in (3.8) has been shown to accurately match simulations for a range of networks, we focus on deriving analytical results from this model. The first quantity we consider is the *transmissibility* of the disease, defined as the probability of the disease being successfully transmitted across a given $S-I$ link, when considered in isolation. To compute this quantity, we recall that the recovery times are now gamma-distributed. For a successful infection attempt to occur across an $S-I$ link, the infection must be transmitted before the infected node recovers, hence, it can be computed as follows [149],

$$\widetilde{\tau} := \int_0^\infty \left(1-e^{-\tau x}\right) \frac{1}{(K-1)!}(K\gamma)^K x^{K-1} e^{-(K\gamma)x} dx = 1 - \left(\frac{K\gamma}{\tau + K\gamma}\right)^K. \qquad (3.10)$$

Although this estimate for the probability of transmission provides some indication of how likely a major epidemic is, it does not, however, take into account the heterogeneity in the network structure. To identify a threshold parameter that can indicate whether an epidemic will occur, we perform a linear stability analysis of the disease-free equilibrium (DFE) with $[S] = N$, $[SS] = n_1 N$, $[I^{(j)}] = [SI^{(j)}] = [SR] = 0$, $j = 1, 2 \ldots, K$ of system (3.1) with the closure given in (3.8). If the DFE is stable, then any small outbreak will die out. The stability of the DFE is determined by eigenvalues of the Jacobian matrix $\mathcal{J} \in \mathbb{R}^{(2K+2)\times(2K+2)}$ ($[SR]$ can be safely excluded as it only introduces a further row and column of zeros). Due to the nature of the system, $\mathcal{J}$ can be recast in the block form $\mathcal{J} = \begin{pmatrix} A & B \\ C & D \end{pmatrix}$, where A is a lower-diagonal $(K+2)\times(K+2)$ matrix, B is a $(K+2)\times K$ matrix, C is a zero $K\times(K+2)$ matrix, and D is a $K\times K$

matrix. This simplifies the calculations, since the characteristic equation can be rewritten as the product of diagonal elements of the matrix A multiplied by the determinant of the matrix D, i.e.

$$\lambda^2(\lambda+K\gamma)^K \begin{vmatrix} \tau n_1\zeta(0)-K\gamma-\tau-\lambda & \tau\zeta(0) & & \dots & \tau\zeta(0) \\ K\gamma & -K\gamma-\tau-\lambda & 0 & \dots & 0 \\ 0 & K\gamma & \ddots & \ddots & \vdots \\ \vdots & 0 & \ddots & \ddots & 0 \\ 0 & \dots & 0 & K\gamma & -K\gamma-\tau-\lambda \end{vmatrix} = 0.$$

This equation is similar to the one analysed by Sherborne et al. [149]. At time $t = 0$ note that $n_S = n_1$, thus from (3.9) $\zeta(0) = (n_2-n_1)/(n_1^2)$. By considering the conditions under which the maximum eigenvalue changes its sign, it is possible to identify a threshold parameter

$$\mathcal{R} := n_1\frac{n_2-n_1}{n_1^2}\widetilde{\tau} = \frac{n_2-n_1}{n_1}\widetilde{\tau}, \tag{3.11}$$

such that for $\mathcal{R} < 1$ the epidemic will die out, and for $\mathcal{R} > 1$ the epidemic will develop in the deterministic model (3.1). This threshold translates to stochastic simulations, however, there is still a small possibility that an early disease die-out can occur even when $\mathcal{R} > 1$. Similarly, small epidemics may occur in some cases where $\mathcal{R} < 1$. It is important to note that although $\widetilde{\tau}$ emerges directly from the linear stability analysis, identifying it as the transmissibility restores the conventional interpretation of the threshold for epidemic spread as the expected number of secondary infections caused by a single infected individual in a fully susceptible population. In this way, our findings agree with the literature (see, for example, [36]).

An interesting result can be reached by considering $\mathcal{R}$ in the case of a scale-free distribution with $p_k \sim k^{-\alpha}$ where $\alpha \leq 3$. In this case, unless p_k is truncated, higher moments n_2, n_3 of the degree distribution are not defined as the population size tends to infinity, and, hence, as the population size grows, the threshold parameter $\mathcal{R}$ will diverge for any non-trivial choice of the disease parameters τ, γ and K. Under these circumstances, the network topology dominates the dynamics of disease, and unless the contact structure can be altered or influenced, the disease will always spread through the population. This conclusion has been reached before in other models [132].

Since we are studying the spread of epidemics in a closed population, every epidemic will reach an end when there are no more infected individuals, at which point every member of the population is either still susceptible or in the removed class. To quantify

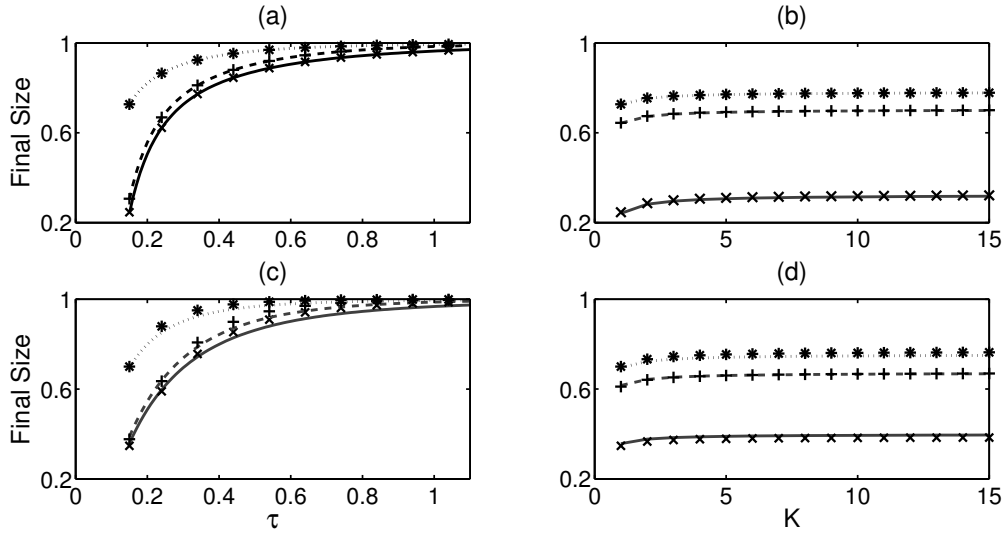

Figure 3.3: Comparison of the final epidemic size as determined by equations (3.12) and (3.13) (lines) and solutions of the pairwise model (3.1) (markers) for bimodal (a)-(b) and truncated scale-free networks (c)-(d), respectively. The parameter values are: (a), (c) $K = 1$, $\gamma = 1$ (solid line, crosses), $K = 4$, $\gamma = 1$ (dashed line, pluses), $K = 1$, $\gamma = 0.5$ (dotted line, stars); (b), (d) $\tau = 0.15$, $\gamma = 1$ (solid line, crosses), $\tau = 0.25$, $\gamma = 1$ (dashed line, pluses), $\tau = 0.15$, $\gamma = 0.5$ (dotted line, stars).

the severity of an epidemic, it is instructive to look at the proportion of the population who will become infected over the entire lifetime of the epidemic; this quantity is known as the *final epidemic size*. In principle, it may be possible to manipulate the equations in (3.1) with the newly derived closure approximation (3.8) to find first-integral-like relations and thus find an expression for the final epidemic size [84, 149]. However, by considering the final epidemic size problem using a bond percolation model, Newman [126] showed that it is possible to obtain an exact result for the mean final epidemic size. Based on the generating function for the degree distribution $G_0(x) := \sum_k p_k x^k$, the generating function for the excess degree distribution $G_1(x) = \frac{1}{n_1} G_0'(x) = \frac{1}{n_1} \sum_k k p_k x^{k-1}$, and the transmissibility, which for our model is given by $\widetilde{\tau}$ in (3.10), the final epidemic size is given by [126]:

$$\mathcal{R}_\infty = 1 - G_0(1 + (\theta - 1)\widetilde{\tau}) = 1 - \sum_k p_k (1 + (\theta - 1)\widetilde{\tau})^k, \tag{3.12}$$

where θ is the unique solution in $(0, 1)$ of the following equation

$$\theta = G_1(1 + (\theta - 1)\widetilde{\tau}) = \frac{1}{n_1} \sum_k p_k (1 + (\theta - 1)\widetilde{\tau})^{k-1}. \tag{3.13}$$

Newman's work has been revisited by Kenah and Robins [88], and whilst they showed that the distribution of final sizes suggested by Newman's original work was incorrect for non-constant infectious periods the mean final epidemic size given by (3.12) and (3.13) is correct.

Figure 3.3 shows the comparison of the final epidemic size results based on equations (3.12) and (3.13) to results from the numerical solution of the new pairwise model (3.1), and the agreement is excellent. It is noteworthy that in all cases the final epidemic size behaves as expected with respect to the disease parameters, i.e. a higher (lower) transmission rate τ results in a larger (smaller) final epidemic size, the mean duration of infection (γ^{-1}) has a similar effect, and a tighter distribution of the infectious periods (higher K) increases the predicted final epidemic size. Furthermore, a careful comparison of bimodal and truncated scale-free networks shows that having a broader degree distribution leads to certain differences in the dynamics. Namely, for relatively low transmission rates, epidemics of measurable size are predicted in truncated scale-free networks but not necessarily for the bimodal distribution. However, as the transmissibility grows (either through increasing τ or K) there comes a point where the final epidemic size becomes larger for the bimodal network. This is likely due to the large number of low-degree nodes in truncated scale-free networks, it is difficult for any epidemic to reach these nodes, even once highly-connected nodes have been infected.

3.3.3 Limiting cases

It is instructive to look at the behaviour of model (3.1) in two particular limits of the number of infectious stages. When $K = 1$, model (3.1) reverts to the classical Markovian pairwise model which has been thoroughly studied [44, 69]. As the number of stages increases, the shape of the distribution for the infectious period changes, as shown in Fig. 3.4. For larger K one can see that the distribution grows tighter around the mean, which is kept constant at γ^{-1} due to the particular formulation of the model, and there is also much less variation in the duration of infection. The limiting case of $K \to \infty$ results in the infected period having a Dirac delta distribution $\delta\left(t - \gamma^{-1}\right)$ around the mean infectious period. It has been recently shown that this case can be accurately described by a system of pairwise delay differential equations (DDEs) for homogeneous populations [92], in which case the above-mentioned concept of transmissibility is also applicable. In this case, the transmission process is still Markovian (thus the spreading process is characterised by the probability density function $\tau e^{-\tau t}$),

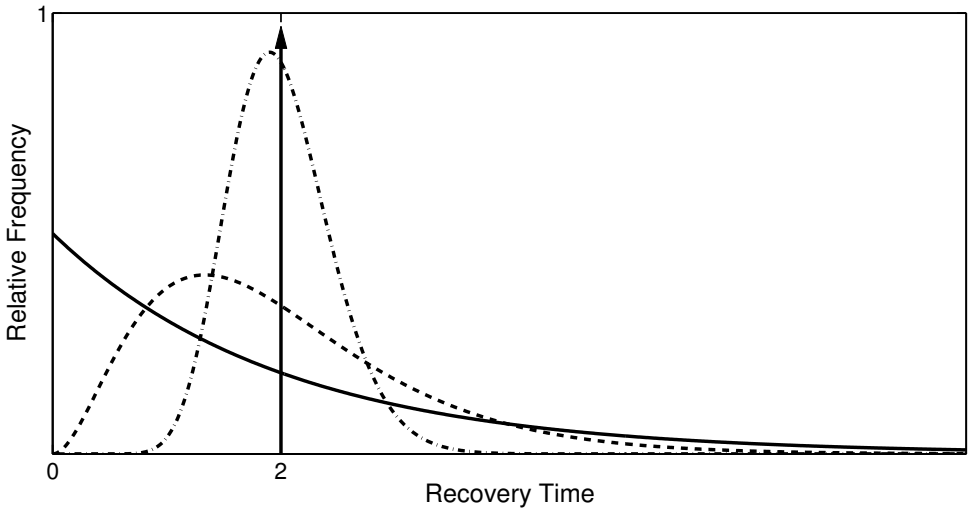

Figure 3.4: The distribution of infectious periods in the Markovian case of $K = 1$ (solid), for $K = 3$ (dashed), $K = 20$ (dash-dotted), and, the Dirac delta distribution corresponding to $K = \infty$. The mean infectious period is equal to 2 for all four distributions.

however, the infectious period is now constant, hence the probability of the infected node recovering is given by $\xi(t)$, where

$$\xi(t) = \begin{cases} 0 & \text{if} \quad 0 \leq t < \gamma^{-1}, \\ 1 & \text{if} \quad t \geq \gamma^{-1}. \end{cases}$$

Under these circumstances the transmissibility for a disease with a constant infectious period is given by

$$\widetilde{\tau}_{\text{const.}} = \int_0^\infty \tau e^{-\tau x} \xi(x) dx = 1 - e^{-\tau/\gamma}.$$

It is easy to show that taking the limit $K \to \infty$ in (3.10) yields the same result, i.e.

$$\lim_{K \to \infty} \widetilde{\tau} = 1 - e^{-\tau/\gamma}.$$

This suggests that results for the final epidemic size and the threshold parameter $\mathcal{R}$ for the case of a constant infectious period can be derived independently from the DDE system [92], and they coincide with the result of taking the limit as $K \to \infty$ for the multi-stage model (3.1). This model, therefore, bridges the gap between the traditional Markovian and delay-based scenarios, and accurately represents the spread of a disease with a distribution of infectious period which cannot be modelled by either.

3.4 The pairwise model on clustered networks

As has already been mentioned, clustering is known to play an important role in the spread of epidemics on networks. A convenient way to quantitatively characterise the level of clustering in a given network is through the clustering coefficient φ, most commonly defined as the proportion of closed triangles of nodes out of the total number of triples (open and closed together) in the network. This coefficient can be computed as follows [84]

$$\varphi = \frac{\text{trace}(A^3)}{||A^2|| - \text{trace}(A^2)}, \tag{3.14}$$

where $A = (a_{ij})_{i,j=1,2,\ldots,N}$ is the adjacency matrix of the network, with $a_{ij} = a_{ji}$, $a_{ii} = 0$ for all i, j, $a_{ij} = 1$ if nodes i and j are connected and zero otherwise, and $||\cdot||$ stands for the sum of all the elements of the matrix. In the previous section it was assumed that $\varphi = 0$. The challenge presented by clustered networks is that one can no longer assume that all triples are open, and, therefore, the closures of pairwise models have to be reconsidered and appropriately modified to effectively approximate the dynamics. In the most general formulation, one can start from a triple $[X_a S_b Y_c]$ where the degree of nodes is considered explicitly. Based on House and Keeling [69], we can write

$$[X_a S_b Y_c] \approx \frac{b-1}{b} \frac{[X_a S_b][S_b Y_c]}{[S_b]} \left(1 - \varphi + \varphi \frac{n_1 N}{ac} \frac{[X_a Y_c]}{[X_a][Y_c]}\right), \tag{3.15}$$

where again $X, Y \in \mathbb{S}$. In order to remove the dependency on node degree, we employ two *a priori* approximations first introduced by Eames and Keeling [44]. The first of these approximations has already featured earlier in (3.4), namely,

$$[X_a Y] \approx \frac{a[X_a]}{\sum_j j[X_j]}[XY],$$

and the second has the form

$$[X_a Y_b] \approx \frac{[X_a Y][XY_b]}{[XY]} \frac{[ab] n_1 N}{a[a]b[b]} \approx \frac{[X_a Y][XY_b]}{[XY]}, \tag{3.16}$$

where n_1 is the mean degree, and $[a]$ is the expected number of individuals with degree a in the network. The new approximation assumes that the joint probability of a pair can be accurately estimated by removing dependence on the degree of the other node and multiplying by a second term that captures the specifics of the network structure. This term is known as the *assortativity* of nodes with degrees a and b, and it measures whether nodes with similar degrees are more likely or less likely to connect to each

other [127]. The simplification shown in (3.16) assumes null assortativity (i.e. random connection between nodes) and will be used throughout this section.

We are now in a position to derive closures for the multi-stage model on clustered networks. In (3.15) the terms outside the bracket are similar to the closure in (3.8) and (3.9) for unclustered networks. In fact, the sum over all degrees a and c will result in the same expression but with the subscripts dropped, as can be checked using (3.4) and (3.16). Thus, the first part of the derivation follows exactly the same methodology as for the unclustered network case discussed in Section 3.3. Focusing on the final term in (3.15), which is responsible for clustering, we use the above approximations to obtain

$$\begin{aligned}\frac{n_1 N}{ac}\frac{[X_a Y_c]}{[X_a][Y_c]} &\approx \frac{n_1 N}{ac}\frac{[X_a Y]}{[XY][X_a]}\frac{[XY_c]}{[Y_c]} \approx \frac{n_1 N}{ac}\frac{a[X_a][XY]}{[XY][X_a]\sum_i i[X_i]}\frac{[XY_c]}{[Y_c]},\\ &\approx \frac{n_1 N}{c}\frac{1}{\sum_i i[X_i]}\frac{c[Y_c][XY]}{[Y_c]\sum_j j[Y_j]} \approx n_1 N\frac{[XY]}{\sum_i i[X_i]\sum_j j[Y_j]}.\end{aligned}$$

In a similar way as it was done for T_1, it is possible to define $J_1^{(i)}$ and P_1 as the sums of all edges emanating from infected nodes in the i-th stage and from removed nodes, respectively. Then $J_1 = \sum_{j=1}^{K} J_1^{(j)}$ is the number of edges pointing outwards from *all* infected nodes, regardless of their degree and the stage of the disease which they are in. The full closures necessary for the model with clustering can now be stated as follows,

$$\begin{aligned}[SSI] &= \zeta(t)\frac{[SS][SI]}{[S]}\left(1-\varphi+\varphi n_1 N\frac{[SI]}{T_1 J_1}\right),\\ [ISI^{(i)}] &= \zeta(t)\frac{[IS][SI^{(i)}]}{[S]}\left(1-\varphi+\varphi n_1 N\frac{[II^{(i)}]}{J_1 J_1^{(i)}}\right), \quad \text{for} \quad i=1,2,\ldots,K,\\ [ISR] &= \zeta(t)\frac{[SI][SR]}{[S]}\left(1-\varphi+\varphi n_1 N\frac{[IR]}{J_1 P_1}\right),\end{aligned} \tag{3.17}$$

where $\zeta(t)$ is still given by (3.9), and we have defined the time dependent quantities

$$\begin{aligned}T_1 &= [SS] + \sum_{i=1}^{K}[SI^{(i)}] + [SR],\\ J_1^{(j)} &= [SI^{(j)}] + \sum_{i=1}^{K}[I^{(i)}I^{(j)}] + [I^{(j)}R], \qquad J_1 = \sum_{j=1}^{K} J_1^{(j)},\\ P_1 &= [SR] + \sum_{i=1}^{K}[I^{(i)}R] + [RR].\end{aligned}$$

The model now has to explicitly consider every possible combination of pairs, which, for a disease with a K-stage gamma distributed infectious period, yields the following system of (K^2+3K+4) equations

$$
\begin{aligned}
&[\dot{S}] = -\tau[SI],\\
&[\dot{I^{(1)}}] = \tau[SI] - K\gamma[I^{(1)}],\\
&[\dot{I^{(j)}}] = K\gamma[I^{(j-1)}] - K\gamma[I^{(j)}], \quad \text{for} \quad j = 2,3,\ldots,K,\\
&[\dot{SS}] = -2\tau[SSI],\\
&[\dot{SI^{(1)}}] = -(\tau+K\gamma)[SI^{(1)}] + \tau\left([SSI] - [ISI^{(1)}]\right),\\
&[\dot{SI^{(j)}}] = -(\tau+K\gamma)[SI^{(j)}] + K\gamma[SI^{(j-1)}] - \tau[ISI^{(j)}], \quad \text{for} \quad j = 2,3,\ldots,K,\\
&[\dot{SR}] = -\tau[ISR] + K\gamma[SI^{K}],\\
&[\dot{I^{(1)}I^{(1)}}] = 2\tau[SI^{(1)}] + 2\tau[ISI^{(1)}] - 2K\gamma[I^{(1)}I^{(1)}],\\
&[\dot{I^{(1)}I^{(j)}}] = \tau[SI^{(j)}] + \tau[ISI^{(j)}] + K\gamma\left([I^{(1)}I^{(j-1)}] - 2[I^{(1)}I^{(j)}]\right), \quad \text{for} \quad j = 2,3,\ldots,K,\\
&[\dot{I^{(j)}I^{(k)}}] = K\gamma\left([I^{(j-1)}I^{(k)}] + [I^{(j)}I^{(k-1)}] - 2[I^{(j)}I^{(k)}]\right), \quad \text{for} \quad j,k = 2,3,\ldots,K,\\
&[\dot{I^{(1)}R}] = \tau[ISR] + K\gamma\left([I^{(1)}I^{(K)}] - [I^{(1)}R]\right),\\
&[\dot{I^{(j)}R}] = K\gamma\left([I^{(j)}I^{(K)}] + [I^{(j-1)}R] - [I^{(j)}R]\right), \quad \text{for} \quad j = 2,3,\ldots,K,\\
&[\dot{RR}] = 2K\gamma[I^{(K)}R],
\end{aligned}
\tag{3.18}
$$

with the closures for $[SSI]$, $[ISI^{(j)}]$ and $[ISR]$ given in (3.17). Note that, as one would expect, setting $\varphi = 0$ reduces this model back to the simpler compact model introduced and discussed in Section 3.3.

3.4.1 Numerical Simulations

To investigate the accuracy of model (3.18), we compare its output to stochastic network simulation. First, it is necessary to explain how one can construct clustered networks, which is achieved using the *big-V rewiring* method [10]. This algorithm takes as an input a random unclustered network constructed with the configuration model, and at each iteration it looks for a chain of five nodes $u - v - x - y - z$, such that newly created links after the rewiring process do not yet exist. Once such a chain is found, the

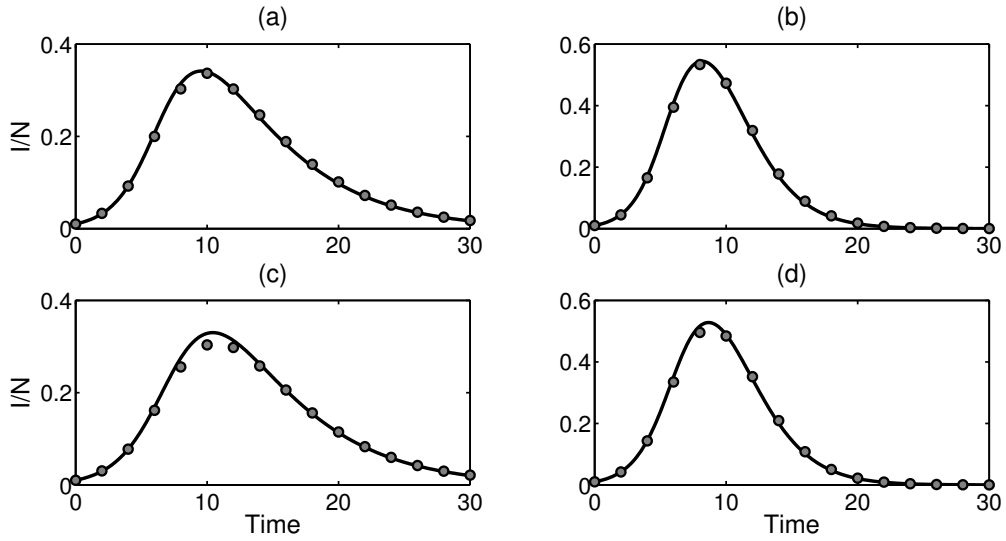

Figure 3.5: Comparisons of numerical results (circles) and the compact pairwise model on a bimodal network with an even split of nodes having degrees 4 and 12. (a) $K = 1$, $\varphi = 0$, (b) $K = 5$, $\varphi = 0$, (c) $K = 1$, $\varphi = 0.2$, (d) $K = 5$, $\varphi = 0.2$. Other parameter values are τ=0.1, $\gamma = 0.2$.

algorithm deletes $u-v$ and $y-z$ edges, and connects $v-y$ and $u-z$ in order to replace the five-node chain with a triangle and a separately connected edge. If this procedure increases local clustering, then the rewiring is accepted, and the algorithm continues until the target clustering coefficient φ is reached. The benefit of this approach is that while the level of clustering can be varied, the degree distribution remains the same.

Figure 3.5 illustrates the results of simulations on bimodal networks both for unclustered networks and for rewired networks with the clustering coefficient $\varphi = 0.2$. Whilst the agreement is good in all cases, the clustering introduces some inaccuracy. This is to be expected since the number of susceptible neighbours of a node is now harder to predict due to the presence of short cycles. Furthermore, the inclusion of triangles appears to slow down the spread of the epidemic. The grouping of nodes into small communities decreases the number of individuals at risk of infection at any time, because the disease has fewer routes to spread away from an infectious seed. One should also note that with the introduction of a gamma-distributed infectious period, the trend of faster epidemic growth and higher peak prevalence with increasing values of K is preserved. This reinforces the earlier conclusion that the inclusion of a more realistic distribution of infectious periods can lead to more rapid severe epidemics than what would be predicted by the traditional models with an exponentially distributed

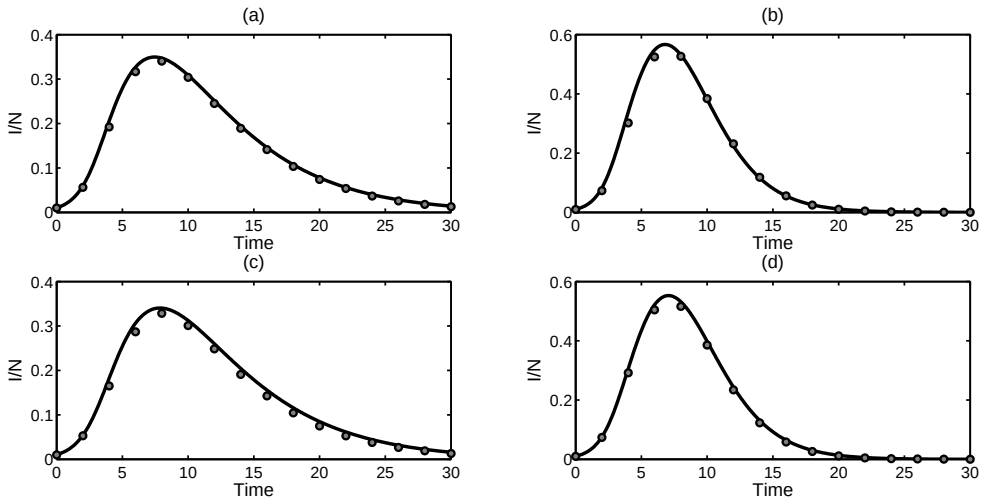

Figure 3.6: Numerical simulations (circles) compared to the pairwise model (black line) for truncated scale-free networks with exponent $\alpha = 2.5$, τ=0.1, $\gamma = 0.2$. (a) $K = 1$, $\varphi = 0$; (b) $K = 5$, $\varphi = 0$; (c) $K = 1$, $\varphi = 0.2$; (d) $K = 5$, $\varphi = 0.2$.

infectious period.

Similar changes in the dynamics are observed in the case of truncated scale-free networks, as shown in Fig. 3.6. However, unlike the bimodal case, the impact of higher clustering has a less pronounced effect on the timescale of the epidemic. This is likely due to the fact that highly connected nodes cannot be effectively restricted to a single small community, and, therefore, their ability to spread the disease is not significantly

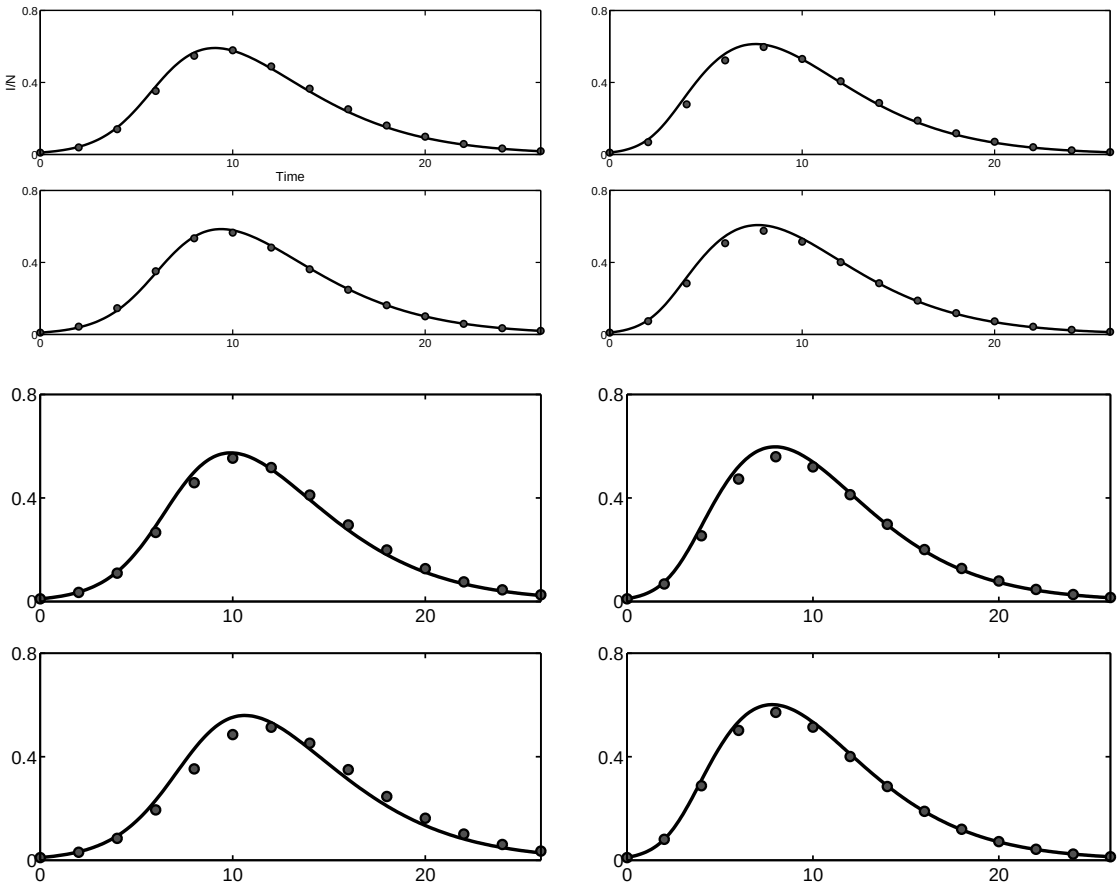

Figure 3.7: Comparison between the clustered pairwise model (3.18) (solid lines) and network simulation (circles) for different values of the clustering coefficient φ. The left column shows results for bimodal networks with an even split of nodes having degrees 4 or 12, the right column shows the results for truncated scale-free networks with the exponent $\alpha = 2.5$ and node degrees bounded between $k_{min} = 4$ and $k_{max} = 60$. Parameter values are $\tau = 0.1$, $\gamma = 0.15$, $K = 3$, with φ increasing through 0.1, 0.2, 0.3, 0.4 from top to bottom. As the clustering φ increases beyond 0.2, the inaccuracy of the clustered pairwise model becomes more pronounced.

affected. It can also be seen that a larger value of K appears to improve the accuracy of the pairwise model (3.18).

Despite its successes, the pairwise model (3.18) becomes less accurate as clustering in the network increases. To investigate this in more detail, we have performed numerous comparisons between simulations and the numerical solution to the pairwise model (3.18) for networks with bimodal and truncated scale-free degree distributions, with increasing levels of clustering. The results of these tests are presented in Fig. 3.7

which shows that system (3.18) is reasonably accurate for low levels of φ, however, this accuracy reduces as φ increases. The most likely explanation for this reduction in model accuracy is the assumption of null assortativity explicitly made in (3.16) when deriving closures for the clustered model, since it is known that clustering in networks increases assortativity [51]. Furthermore, it has also been shown in a number of earlier studies that high levels of assortativity are the norm in real social networks (see, for example, [125]). Since the null assortativity assumption is violated in such networks, it is not surprising that the pairwise model (3.18) does not provide an accurate representation of dynamics for high levels of clustering. Figure 3.8 shows the comparison in terms of the final epidemic size recorded from simulation and the pairwise model. Again, it is clear to see that the pairwise model performs less well for higher levels of clustering. However, what can be seen from the results is that when clustering is present in the network the threshold appears to increase and thus measurable epidemics are less likely to occur. This can be seen in Fig. 3.8, as a higher transmission rate is required in order for the final epidemic size to diverge away from zero when the epidemic takes place in a clustered network. Similarly, for clustered networks, simulation results show that the final epidemic size will be reduced when compared to equivalent networks with the same degree distribution, no clustering and the same parameters of the disease dynamics. This makes sense intuitively, since rewiring a network makes the population more segregated and thus less at risk of widespread epidemics.

Figure 3.8 further suggests that the difference between the pairwise model and simulations is less marked for the non-Markovian case (i.e. $K > 1$). In an extensive recent study of small/toy networks, Pellis et al. [133] proved that for an SIR epidemic on a single open triple or closed triangle the classical closures, such as those given in (3.3) and (3.15), are exact for constant infectious periods (see Proposition 3 in [133]). As has been previously discussed in Section 3.3.3, as the number of stages, K, increases in the pairwise model, we approach the limit of a constant infectious period. Therefore, if the results of Pellis et al. [133] extend to larger networks, one would expect that the accuracy of our pairwise model for clustered networks (3.18) should improve as K increases. To test the validity of this hypothesis, in Fig. 3.9 we plot the value of the error between the final epidemic size computed from the pairwise model (3.18) and the results of 100 simulations under the same parameters, for bimodal and truncated scale-free networks. Figure 3.9 indicates that the error does indeed decrease for any φ as the infectious period becomes tighter around the mean (as characterised by an increasing

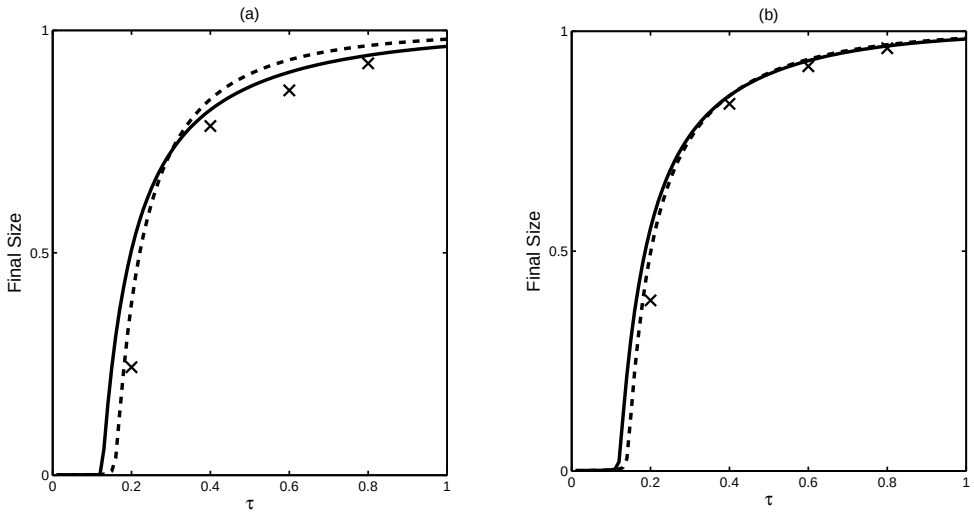

Figure 3.8: Dependence of the final epidemic size on the per-link transmission rate for bimodal networks with degree 4 or 12, split equally. The parameter γ is fixed at 1, and in (a) $K = 1$, (b) $K = 3$. Solid lines correspond to epidemics on unclustered networks, dashed lines illustrate equivalent epidemics on a network with $\varphi = 0.4$, and the crosses represent results from 100 numerical simulations on the same clustered networks.

K), thus providing evidence that Pellis et al.'s results are relevant for large networks where both open and closed triples are present. Furthermore, one should note that in all but two cases the pairwise model (3.18) over-estimates the final epidemic size when compared to simulations. This suggests that in most cases the model can be expected to give an upper bound on the size of an epidemic. Even though our newly derived compact closures (3.17) are not exact, their performance improves greatly when the infectious period approaches the limit of a fixed infectious period. This is an important result that justifies the continued use of pairwise-like methods for non-Markovian epidemics on networks.

3.5 Discussion

In this Chapter we have derived and studied a new pairwise model for the spread of infectious diseases which includes three major characteristics that are not consistently studied concurrently, despite being essential for understanding disease dynamics in many realistic scenarios. Our pairwise model can account for degree heterogeneity, clustering and gamma-distributed infectious periods, and the number of equations in

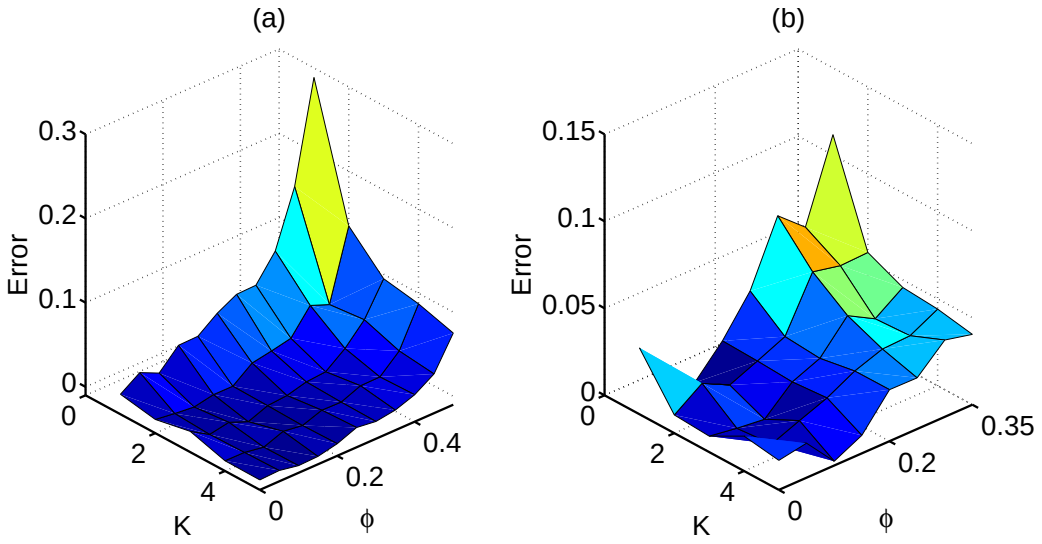

Figure 3.9: The error between the final epidemic sizes obtained from the solution of the pairwise model (3.18) and from the average of 100 numerical simulations plotted against the clustering coefficient φ and the number of stages of infection K. (Plotted as pairwise subtract simulation). Parameter values are $\tau = 0.3$, $\gamma = 1$. (a) A bimodal network with an even split of nodes having degrees $k_1 = 4$ and $k_2 = 12$. (b) A scale-free network of 1000 nodes with $k_{min} = 4$, $k_{max} = 60$, and $p_k \sim k^{-2.5}$. Note that as predicted, even in the presence of clustering, as K grows the error becomes smaller, and hence the pairwise model becomes more accurate.

the pairwise model does not depend on the range of different node degrees. This approach follows the methodology of the so-called *compact pairwise models* [70, 151], and the output from the resulting pairwise model shows excellent agreement with results of numerical simulation for networks with either no or low levels of clustering, and for all the different degree distributions that have been considered.

In the absence of clustering we have used linear stability analysis to determine a threshold parameter from the pairwise model, and we have shown that existing methods for finding the final epidemic size [126] can be applied. Equivalent results have not been found in the case of clustered networks. However, extensive numerical simulations have shown that introducing multiple stages of infection increases the speed of epidemic spread, as well as the peak prevalence and the final epidemic size. The interactions of degree heterogeneity, clustering and the distribution of infectious period all have significant yet contrasting impacts on an outbreak. For example, we have seen that both degree heterogeneity and a larger number of infectious stages (corresponding to

a tighter distribution for the duration of infection) increase the growth rate of the epidemic in the early stages, however, this is countered when one includes clustering that is likely to be present in real contact networks. These findings are consistent with earlier results on the effects of clustering on the spread of epidemics [43]. Serrano and Boguñá [147] have shown that whilst clustering makes epidemics less likely, for scale-free topologies, and in the limit of infinite networks, an epidemic threshold does not exist, and a significant outbreak will always occur. The complexity of the pairwise model for clustered networks has meant that analytical expressions for the epidemic threshold and the final epidemic size have not been found. In fact, analytical results have so far only been obtained for clustered networks with a specific construction, e.g. non-overlapping triangles [115]. Random rewiring enforces fewer restrictions on the network and thus allows for more complex topologies to emerge; it is likely to provide more realistic but also more challenging scenarios for modelling than networks with a prescribed nature of clusters.

A strength of the final pairwise model which we have presented is that it can be tuned based on the characteristics of the disease and population being studied. There are several ways to include more features into this model. For example, assortativity could be made an explicit consideration in the closures, and by allowing the transmission rate to vary depending on the stage of infection, one could model diseases with varying infectivity. Setting $\tau = 0$ in any number of initial stages also opens the possibility for multi-stage $SEIR$ models to be studied, again without altering the basic framework of the model.

Models, such as the one presented in this paper, could also be used for a more thorough study of the performance of closures and for mapping out how different approximations behave under different regimes, such as stochastic models for the transmission and recovery processes. Furthermore, one could consider whether non-Markovian transmission processes can be incorporated into pairwise or pairwise-like models. Additional motivation for research into this area comes from studies which have suggested that human contact patterns are typically very 'bursty' [29, 31]. This means that there are many short periods with high levels of interaction and longer periods of little or no action, and this may have a significant impact on how an epidemic may spread. Incorporating this into some future development would be a radical departure as, to our knowledge, no published pairwise model has ever featured a non-Markovian transmission process. However, it may be possible to use partial or integro-differential equations

to achieve this, since they have been successfully applied to model non-Markovian distributions of the infectious period, as described further in Chapter 4. The message passing method [80], and the novel EBCM introduced in Chapter 4 are both formulated for general transmission and recovery processes, so these models are better suited to exploring the effect that a bursty transmission process has on the dynamics of an epidemic.

There have been many recent developments in the area of dynamic or adaptive networks [64, 90, 139, 146] where pairwise models have been used successfully to couple the dynamics of an epidemic on the network with the dynamics of the network. These models have shown that using pairwise approximation techniques it is possible to capture non-trivial properties of both network and epidemic dynamics in a single model. There is a wide scope for further research focussed on modelling the rewiring process, as well as for analysis of a reaction of networks to a spreading epidemic when considered as a non-Markovian process.

The pairwise model presented in this Chapter does well at accounting for non-Markovian infectious periods, indeed, it becomes more accurate in this case, yet it is limited in capturing epidemics on realistic clustered networks. This highlights that complexities in the structure of social networks are difficult to model even with a large number of equations. The above suggests that when studying epidemics on networks and designing disease control strategies or interventions, it is essential to use accurate and reliable data about the population being studied, as well as about epidemiological characteristics of the disease.

Acknowledgements

Neil Sherborne acknowledges funding for his PhD studies from EPSRC (Engineering and Physical Sciences Research Council), EP/M506667/1, and the University of Sussex.

Chapter 4

Paper 3: Mean-field models for non-Markovian epidemics on networks

N. Sherborne[1], J. C. Miller[2], K. B. Blyuss[1] and I. Z. Kiss[1]

[1]Department of Mathematics, School of Mathematical and Physical Sciences, University of Sussex, Brighton, BN1 9QH, UK

[2] Institute for Disease Modeling, Bellevue, WA, United States of America

4.1 Abstract

This paper introduces a novel extension of the edge-based compartmental model to epidemics where the transmission and recovery processes are driven by general independent probability distributions. Edge-based compartmental modelling is just one of many different approaches used to model the spread of an infectious disease on a network; the major result of this Chapter is the rigorous proof that the edge-based compartmental model and the message passing models are equivalent for general independent transmission and recovery processes. This implies that the new model is exact on the ensemble of configuration model networks of infinite size. For the case of Markovian transmission the message passing model is re-parametrised into a pairwise-like model which is then used to derive many well-known pairwise models for regular networks, or when the infectious period is exponentially distributed or is of a fixed length.

4.2 Introduction

The use of mathematical tools to study and understand the spread of infectious diseases is a mature and fruitful area of research. In their 1927 paper Kermack and McKendrick [89] established the susceptible-infected-recovered (SIR) framework which forms the basis of many models to this day. However, their model assumes that any individual can interact with any other. In reality, in large populations each individual only interacts with a few others, and these connections determine the possible routes of disease transmission. Moreover, studies have found significant heterogeneity in the number of contacts a single individual may have [132]. The use of graphs or networks to describe these contact patterns represented a major advance in our ability to model more realistic social behaviour. In network-based models individuals are represented by nodes in the network, with edges (or links) encoding the interactions between nodes.

Since the direct analysis of stochastic epidemics on networks is far from trivial, one often relies on deterministic mean-field models that are aimed at approximating some average quantities taken from the stochastic models. Deriving mean-field models can be done in several different ways depending on what one chooses to focus on. For example, considering all nodes and edges in all possible states leads to pairwise models [70, 84], while considering separately each individual and all possible ways in which it can become infected by its neighbours leads to the message passing (MP) formalism [80]. Focussing on all possible star-like structures, typically defined by a node and all

its neighbours, and also taking into account their disease status, yields the so-called effective-degree models [100]. Edge-based compartmental models (EBCM) are based on considering a randomly chosen test node and working out the probability of it staying susceptible, with this probability being then equivalent to the proportion of susceptible nodes in the entire population [119]. See Danon et al. [35], Pastor-Satorras et al. [131] and Kiss et al. [91] for reviews. All of these models start from the same stochastic model, thus, it is not surprising that some of these models [70, 91, 118, 155] are, in fact, equivalent, as we will demonstrate later.

While network models capture contact more accurately, the assumption that the underlying stochastic transmission and recovery processes are memoryless [70, 85, 162] remains restrictive. Of course, memoryless processes are mathematically more tractable and relatively simple to analyse when compared to models where the inter-event times are chosen from distributions other than the exponential. However, when compared to data, these assumptions are often violated. For example, diseases can exhibit unique and non-Markovian behaviour in terms of the strength and duration of infection. In this respect, the distribution of the infectious period is usually better approximated by some peaked distribution with a well defined mean, see e.g. [8, 58, 168] and references therein.

The MP method does not rely on these assumptions and is able to predict the average behaviour of an epidemic outbreak with general distributions for the transmission times and the duration of infection, although we still require these be independent. Throughout the Chapter we will denote these distributions as $\tau(a)$ and $q(a)$, where a is the time since the node became infected, known as the age of infection. Once a susceptible node has been exposed to a transmission event, it becomes infected immediately, while the recovery from the disease grants a lifetime immunity. Using these distributions assumes a homogeneous response to disease; whilst this restriction is not always necessary (see e.g. [170]), it is a common simplification in order to obtain a concise model. However, the main focus of this Chapter is to explore the flexibility of the EBCM in being able to capture epidemics where the infection and recovery processes are described by general independent distributions.

The rest of the Chapter is organised as follows. In the following Section we introduce the MP method [80] and show how the epidemic model is constructed. We then go on to present the extension of the edge-based compartmental model [119] to SIR epidemics with general but independent distributions for time to transmission and duration of the

infectious period. This Section also contains the main result of the Chapter, namely, a full rigorous proof that MP model and the EBCM are equivalent, and hence, that the EBCM provides an exact representation of the average stochastic behaviour on the ensemble of infinite Configuration Model (CM) networks [15, 122, 123]. Section 4.4 contains a re-parametrisation of the MP model in the special case of Markovian transmission. This proves to be a useful tool in showing how several well-known models can be derived from the MP model or the EBCM when additional assumptions about the network or recovery process are made. In Section 4.5, we compare numerical solutions of the mean-field models to averaged results from explicit stochastic network simulations. The Chapter concludes with a discussion of main results and possible directions for future research.

4.3 Model summary

4.3.1 The message passing (MP) method

In their 2010 paper, Karrer and Newman [80] introduced the message passing approach to model SIR dynamics on networks. Here, we briefly present the ideas behind their model and its assumptions. Recalling $\tau(a)$ and $q(a)$ as the densities for transmission and duration of the infectious period one can introduce a new function $f(a)$

$$f(a) = \tau(a) \int_a^\infty q(x)\, dx, \tag{4.1}$$

such that the probability that a node infected at time 0 attempts to transmit the disease to a given neighbour before time t is $\int_0^t f(a)da$, since a neighbour can only transmit the disease if it has not yet recovered. Note that the integration of (4.1) over all time is the overall probability of an attempted transmission of the disease across a given network edge, commonly known as the *transmissibility* of the disease. This is a quantity which is important in percolation models to determine the epidemic threshold and expected final epidemic size of a major outbreak [88, 126].

In order to model the dynamics of disease spread, consider a test node u. This node is placed into a cavity state where it can become infected but is not able to transmit the disease to any of its neighbours. This has no effect on the probability of the node being in any given state [119]. Now consider a node v which is a neighbour of u; the *message* is the probability that v has *not* attempted to transmit the disease to u by calendar time t, denoted $H^{u \leftarrow v}(t)$. This probability is comprised of two distinct possibilities; the

first possibility is that v will make no attempt to transmit the disease before age t, this is given by $1 - \int_0^t f(a)\,da$. This means that even if v is one of the initially infected nodes, it would not attempt to transmit to u. Alternatively, it could be that v will transmit to u at some age $a < t$, but v itself was infected at some time $t_1 > t - a$ and has, therefore, not yet attempted to transmit the disease to its neighbour u. This requires v to have initially been susceptible (with probability z) and to have escaped transmission from each of its neighbours until at least time $(t - a)$. On a tree network with no loops, this is exactly $z \int_0^t f(a) \prod_{w \in \mathcal{N}(v)\setminus u} H^{v \leftarrow w}(t - a)\,da$, where $\mathcal{N}(v)$ denotes the set of neighbours of v. Hence, combining these two gives

$$H^{u \leftarrow v}(t) = 1 - \int_0^t f(a) \left[1 - z \prod_{w \in \mathcal{N}(v)\setminus u} H^{v \leftarrow w}(t - a) \right] da. \tag{4.2}$$

In principle, one could calculate (4.2) for all edges (in both directions) to find a full solution for the proportion of the population that is susceptible, infected or removed at any time t. For example, the probability that u is susceptible is the product of $H^{u \leftarrow w}(t)$ across all neighbours $w \in \mathcal{N}(u)$ multiplied by the probability that it was initially susceptible, z. On a single fixed finite tree network, solving (4.2) for all edges will, in fact, yield the exact solution of the stochastic epidemic [80]. The size of such a system of equations would be twice the number of all edges in the network (since both $H^{u \leftarrow v}(t)$ and $H^{v \leftarrow u}(t)$ would need to be calculated).

Throughout this Chapter we consider unweighted, bi-directional and static networks constructed according to the configuration model (CM). Every node is assigned a number of neighbours, known as its degree, according to a probability distribution p_k, known as the *degree distribution*, that describes the probability that a randomly chosen node has degree k. Let us now focus on an ensemble of CM networks and consider an average message, H_1, instead of considering distinct messages across every edge [80]. For CM networks, as the size of the network tends to infinity, so does the length of the shortest loops, and, therefore, the network becomes locally tree-like. This means that the messages that a node receives from each of its neighbours are independent, and the average message received by the test node u is equal to the product of the average message for each neighbour.

The product in (4.2) is then this H_1 raised to the power of the *excess degree* of the node, its degree excluding the edge which connects it to the test node. The following

moment generating functions average this product over the degree distribution

$$\begin{aligned} G_0(x) &:= \sum_k p_k x^k, \quad G_1(x) := \frac{1}{\langle k \rangle} \sum_k p_k k x^{k-1}, \\ G_2(x) &:= G_1'(x) = \frac{1}{\langle k \rangle} \sum_k p_k k(k-1) x^{k-2}, \end{aligned} \tag{4.3}$$

where $\langle k \rangle = G_0'(1)$ is the mean degree. $G_1(x)$ is the generating function for the *excess degree distribution*, since $kp_k/\langle k \rangle$ describes the probability that a node reached by traversing a randomly selected edge has $(k-1)$ other contacts [126]; the mean excess degree is given by $G_2'(1)$. The moment generating function $G_2(x)$ will be used to trace the route of infection in later models. Using G_1 to replace the product in (4.2), the equation for the average message $H_1(t)$ is

$$H_1(t) = 1 - \int_0^t f(a) \left[1 - z G_1(H_1(t-a))\right] \, da, \tag{4.4}$$

with $H_1(0) = 1$.

In practice, the trajectory of $H_1(t)$ is found by identifying and then solving a differential or integro-differential equation. For example, the purely Markovian case (i.e. $\tau(a)$ and $q(a)$ are both exponential distributions), with transmission and recovery parameters β and γ, leads to

$$\frac{dH_1}{dt} = \gamma - (\beta + \gamma) H_1(t) + \beta z G_1(H_1(t)),$$

where, again, z is the fraction of the population which was initially susceptible at time $t = 0$ [80]. However, the precise form of this equation is not universal, it depends on the particular choice of $\tau(a)$ and $q(a)$. The proportions of susceptible, infected and recovered individuals at any time t are then given, in terms of the message $H_1(t)$, as

$$\begin{aligned} \langle S \rangle(t) &= z G_0(H_1(t)), \\ \langle R \rangle(t) &= \int_0^t q(a) \left[1 - \langle S \rangle(t-a)\right] \, da, \\ \langle I \rangle(t) &= 1 - \langle S \rangle(t) - \langle R \rangle(t). \end{aligned} \tag{4.5}$$

The MP model (4.5) with the average message H_1 is exact when the stochastic epidemic is considered on the ensemble of infinite CM networks [80]. This approach is able to model dynamics for general choices of independent transmission and recovery processes, see Karrer and Newman [80], or Wilkinson and Sharkey [170], for several examples where output from the MP model is compared to results based on simulations.

4.3.2 EBCM for general transmission and recovery processes

The edge-based compartmental model is an established tool for Markovian dynamics [119]. We introduce a new extended EBCM which generalises the method to general transmission and recovery processes $\tau(a)$ and $q(a)$. Again, the EBCM uses the fact that the probability that the test node u remains susceptible is the probability that u escapes transmission from all of its neighbours. This concept is similar to the notion and use of H_1 in MP models. What separates the two models, conceptually at least, is in the construction of the models. Whereas MP rigorously derives equations for all quantities, the EBCM is constructed by directly and heuristically defining a system of differential equations which describe the trajectory of an epidemic.

Recovery is modelled using age-structured differential equations. However, the EBCM uses the instantaneous rates of transmission and recovery given by the *hazard functions* rather than the raw densities $\tau(a)$ and $q(a)$. These are defined as

$$\zeta(a) := \frac{\tau(a)}{\xi_\tau(a)}, \quad \text{and} \quad \rho(a) := \frac{q(a)}{\xi_q(a)}, \tag{4.6}$$

where $\xi_\tau(a)$ and $\xi_q(a)$ are the respective *survival functions* (see, e.g., [121]).

$$\begin{aligned} \xi_\tau(a) &= \int_a^\infty \tau(\hat{a})\, d\hat{a} = e^{-\int_0^a \zeta(\hat{a})\, d\hat{a}}, \\ \xi_q(a) &= \int_a^\infty q(\hat{a})\, d\hat{a} = e^{-\int_0^a \rho(\hat{a})\, d\hat{a}}. \end{aligned} \tag{4.7}$$

All of these disease variables and related functions are summarised in Table 4.1. As before, the contact network is a CM network with degree distribution and generating functions as defined in (4.3). The basis of the EBCM revolves around finding the probability that a random test node (in a cavity state) is in a susceptible, infected or recovered state at time t. As this test node is chosen at random, these probabilities are equal to the proportions of the population in each state at time t, denoted $S(t)$, $I(t)$ and $R(t)$, respectively.

The first important quantity is $\Theta(t)$, defined in a manner similar to $H_1(t)$ in (4.4) as the probability that the representative test node has not received transmission from a given neighbour by time t. This approach then differs from MP by directly expressing a differential equation for the dynamics of Θ. The model is known as "edge-based" because it considers the state of the neighbours of the test node; the densities $\Phi_S(t)$,

$\Phi_I(t)$ and $\Phi_R(t)$ describe the probability that at time t a random neighbour of the test node is (i) still susceptible, (ii) infected but has not attempted to transmit the disease to the test node, (iii) recovered, and did not transmit to the test node whilst it was infected. The age of infection is, in general, crucial in determining the hazard rates, and so we introduce $i(t,a)$ as the density of infected nodes with the age of infection a. Similarly, $\phi_I(t,a)$ is the density of infected neighbours who have not transmitted to the test node and have age a. Thus, it is clear that $I(t) = \int_0^t i(t,a)da$ and $\Phi_I(t) = \int_0^t \phi_I(t,a)da$. These variables are summarised in Table 4.2. We also introduce the Dirac delta distribution as follows [54]:

$$\delta(x) = \begin{cases} +\infty, & x = 0 \\ 0, & x \neq 0 \end{cases}, \qquad \int_{-\infty}^{\infty} \delta(x)dx = 1.$$

Before writing down the new edge-based compartmental model it is worth introducing and explaining the structure of its equations. The message Θ is monotonically decreasing, and it depends on the density and age of infected neighbours, $\phi_I(t,a)$, and the hazard rate $\zeta(a)$. We must consider the possibility of an infected neighbour of any age up to time t transmitting the disease, hence, we have

$$\frac{d\Theta(t)}{dt} = -\int_0^t \zeta(a)\phi_I(t,a)\,da.$$

Given $\Theta(t)$ it follows that $\Phi_S(t) = zG_1(\Theta(t))$. Since the test node is in a cavity state, the probability of a neighbour being susceptible is the probability of it escaping infection from its other contacts averaged over the excess degree distribution.

The rate at which susceptible neighbours are infected is the boundary condition for infected neighbours, i.e.

$$\phi_I(t,0) = -\dot{\Phi}_S(t) = (1-z)\delta(t) + zG_2(\Theta(t))\int_0^t \zeta(a)\phi_I(t,a)\,da,$$

where the first term represents the introduction of the disease at time $t = 0$, and is zero everywhere else. As these neighbours age, they may attempt to transmit the disease, and will eventually recover from it. These events depend on the calendar time and the age of infection, and so we have a von Foerster-type equation

$$\left(\frac{\partial}{\partial t} + \frac{\partial}{\partial a}\right)\phi_I(t,a) = -\left[\zeta(a) + \rho(a)\right]\phi_I(t,a), \qquad 0 < a \leq t.$$

The density of nodes in each state depends on Θ and ϕ_I. By the same logic seen in the MP model, the density of susceptible nodes is $S(t) = zG_0(\Theta(t))$. The rate at

Variable	**Definition**
$\tau(a)$	The density of the transmission process.
$q(a)$	The density of the duration of the infectious period.
$\xi_\tau(a)$	The *survival function* of the transmission process. The probability that an infected node of age a has not yet attempted to transmit the disease along a given edge: $\int_a^\infty \tau(x)\,dx$.
$\xi_q(a)$	The *survival function* of the recovery process. The probability that an infected node reaches at least age a before recovering: $\int_a^\infty q(x)\,dx$.
$\zeta(a)$	The *hazard function* of the transmission process. The probability of an edge of age a transmitting in a small interval of time $(a, a+\Delta a)$: $\frac{\tau(a)}{\xi_\tau(a)}$.
$\rho(a)$	The *hazard function* of the recovery process. The probability of an infected node of age a recovering in a small interval of time $(a, a+\Delta a)$: $\frac{q(a)}{\xi_q(a)}$.
$f(a)$	The probability that, in a small interval, an infectious contact is made by an infected node of age a :$\tau(a)\int_a^\infty q(x)\,dx$.
$g(a)$	The probability that, in a small interval, an infectious node of age a recovers, without attempting to transmit the disease to a given neighbour: $q(a)\int_a^\infty \tau(x)\,dx$.

Table 4.1: The variables and functions describing the transmission and recovery processes.

Variable	**Definition**
$\Theta(t)$	The probability that the initially susceptible test node has not received a transmission from a random neighbour by time t.
$\Phi_S(t)$	The probability that a random neighbour of the test node u is still susceptible.
$\Phi_I(t)$	The probability that a random neighbour of the test node u is infected, but has not transmitted to u.
$\phi_I(t,a)$	The probability a random neighbour of the test node u to be infected, have not transmitted to u by time t and have age of infection a, $\Phi_I(t) = \int_0^t \phi_I(t,a)\,\mathrm{d}a$.
$\Phi_R(t)$	The probability a random neighbour of the test node u has been infected and recovered without transmitting to u.
$S(t)$	The density of susceptible nodes.
$I(t)$	The density of infected nodes.
$i(t,a)$	The density of infected nodes with age of infection a.
$R(t)$	The density of recovered nodes.
$G_1(x)$	The generating function of the excess degree distribution: $\frac{1}{\langle k\rangle}\sum_{k=0}^{\infty} p_k k x^{(k-1)}$.
$G_2(x)$	The derivative of the generating function of the excess degree distribution: $\frac{1}{\langle k\rangle}\sum_{k=0}^{\infty} p_k k(k-1) x^{(k-2)}$.

Table 4.2: The list of variables in the EBCM.

which susceptible nodes become infected gives the boundary condition of newly infected nodes. Therefore, infected nodes are replenished according to

$$i(t,0) = -\dot{S}(t) = (1-z)\delta(t) + \langle k\rangle z G_1(\Theta(t)) \int_0^t \zeta(a)\phi_I(t,a)\,da,$$

where the first term represents the introduction of the disease. As infected nodes age, they recover according to $\rho(a)$; these dynamics depend on t and a, and we have a second

partial differential equation in the model

$$\left(\frac{\partial}{\partial t}+\frac{\partial}{\partial a}\right) i(t,a) = -\rho(a) i(t,a), \qquad 0 < a \leq t.$$

These equations together form the EBCM for general but independent transmission and recovery processes,

$$\frac{d\Theta(t)}{dt} = -\int_0^t \zeta(a)\phi_I(t,a)\,da, \tag{4.8a}$$

$$\Phi_S(t) = zG_1(\Theta(t)), \tag{4.8b}$$

$$\begin{aligned}\phi_I(t,0) &= -\dot{\Phi}_S(t)\\ &= (1-z)\delta(t) + zG_2(\Theta(t))\int_0^t \zeta(a)\phi_I(t,a)\,da,\end{aligned} \tag{4.8c}$$

$$\left(\frac{\partial}{\partial t}+\frac{\partial}{\partial a}\right)\phi_I(t,a) = -\left[\zeta(a)+\rho(a)\right]\phi_I(t,a), \qquad 0 < a \leq t, \tag{4.8d}$$

$$\Phi_I(t) = \int_0^t \phi_I(t,a)\,da, \tag{4.8e}$$

$$\Phi_R(t) = \Theta - \Phi_S - \Phi_I, \tag{4.8f}$$

$$S(t) = zG_0(\Theta(t)), \tag{4.8g}$$

$$\begin{aligned}i(t,0) &= -\dot{S}(t)\\ &= (1-z)\delta(t) + \langle k\rangle zG_1(\Theta(t))\int_0^t \zeta(a)\phi_I(t,a)\,da,\end{aligned} \tag{4.8h}$$

$$\left(\frac{\partial}{\partial t}+\frac{\partial}{\partial a}\right) i(t,a) = -\rho(a) i(t,a), \qquad 0 < a \leq t, \tag{4.8i}$$

$$I(t) = \int_0^t i(t,a)\,da, \tag{4.8j}$$

$$R(t) = 1 - S(t) - I(t). \tag{4.8k}$$

The new edge-based compartmental model (4.8) offers an alternative way to derive a system of equations that are able to characterise the dynamics of an epidemic outbreak. Although it seems more complex than the MP model, the EBCM is perhaps more intuitive, as many of the variables it involves relate directly to densities of nodes in

different states and to the transitions between different states. The EBCM has also proven to be quite versatile and easily extendable to account for different scenarios. For instance, Miller et al [119] extended the original EBCM for static networks to dynamic networks where edges are deleted, created or rewired. It may be possible to use similar techniques to extend (4.8) to model diseases spreading through dynamic networks. To our knowledge, the MP model has so far not been extended beyond static networks, although it may be possible.

As the MP model (4.5) and the non-Markovian edge-based compartmental model (4.8) are based on the same underlying stochastic epidemic, it is natural to question how accurate and how similar they are. Karrer and Newman [80] showed that the MP model (4.5) is exact on the ensemble of CM networks. Therefore, proving that the EBCM and MP model are equivalent will imply that the EBCM is exact under the same circumstances.

4.3.3 Model Equivalence

We now present and prove the main result of this Chapter, that the edge-based compartmental and MP model are equivalent for any suitable choices of $\tau(a)$ and $q(a)$.

Theorem 1. *If $\tau(a)$ and $q(a)$ are independent, integrable probability density functions, then the MP model* (4.5) *and the EBCM* (4.8) *are equivalent, and will produce identical trajectories for any shared initial conditions.*

Proof. The proof consists of showing equivalence for two main elements: the messages for the respective models $H_1(t)$ and $\Theta(t)$, and the densities of nodes in each state.

We first show that H_1 and Θ satisfy the same evolution equation. To do this, $H_1(t)$ (4.4) is differentiated using Leibniz's rule, which yields

$$\begin{aligned}\frac{dH_1}{dt} &= -f(t)[1 - zG_1(H_1(0))] - \int_0^t f(a)\left[-zG_2(H_1(t-a))\frac{dH_1(t-a)}{dt}\right] da \\ &= -f(t)[1 - zG_1(1)] + \int_0^t f(a)\left[zG_2(H_1(t-a))\frac{dH_1(t-a)}{dt}\right] da \\ &= -f(t)(1-z) + \int_0^t f(a)\left[zG_2(H_1(t-a))\frac{dH_1(t-a)}{dt}\right] da. \end{aligned} \tag{4.9}$$

The dynamics of Θ are governed by the following equation

$$\frac{d\Theta}{dt} = -\int_0^t \zeta(a)\phi_I(t,a)\, da.$$

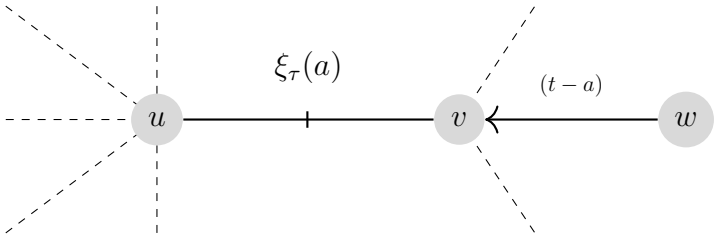

Figure 4.1: Consider the node labelled u as the test node and thus in a cavity state. For its link with node v to contribute to $\phi_I(t,a)$, it must be the case that v received transmission from some neighbour w at time $(t-a)$. If $t-a=0$, then this is equal to the initial proportion of infected nodes. Otherwise, we take the probability of a transmission event a time ago, which is $\frac{d\Theta(t-a)}{dt}$. For v to have been successfully infected at this time, it must have been susceptible until that point, since two of its neighbours will not have transmitted before this time (u is in a cavity state and w will transmit at $(t-a)$). The probability of this is $zG_2(H_1(t-a))$ for $t>a$, illustrated by the dashed lines. The probability of v not transmitting to u before time t is $\xi_\tau(a)$. Finally, the neighbour v must still be infected at age a, which is given by the survival function $\xi_q(a)$.

From (4.8d), one can use the integrating factor $\exp\left(\int_0^a [\zeta(\hat{a})+\rho(\hat{a})]\,d\hat{a}\right)$ to find

$$\phi_I(t,a) = \phi_I(t-a,0)e^{-\int_0^a [\zeta(\hat{a})+\rho(\hat{a})]\,d\hat{a}} \tag{4.10}$$

where

$$\phi_I(t-a,0) = (1-z)\delta(t-a) - zG_2(\Theta(t-a))\frac{d\Theta(t-a)}{dt}.$$

As an alternative, we offer a graphical explanation of (4.10) in Fig. 4.1.

Introducing $\hat{f}(a) := \zeta(a)e^{-\int_0^a [\zeta(\hat{a})+\rho(\hat{a})]\,d\hat{a}}$, we have

$$\begin{aligned}\frac{d\Theta}{dt} &= -\int_0^t \hat{f}(a)\left[(1-z)\delta(t-a) - zG_2(\Theta(t-a))\frac{d\Theta(t-a)}{dt}\right]da \\ &= -\hat{f}(t)(1-z) + z\int_0^t \hat{f}(a)G_2(\Theta(t-a))\frac{d\Theta(t-a)}{dt}\,da. \end{aligned}\tag{4.11}$$

Thus, H_1 and Θ have the same dynamics if one can show that $f(a)=\hat{f}(a)$. From the definition of $f(a)$ in (4.1) and using (4.7), we obtain

$$f(a) = \zeta(a)\xi_\tau(a)\xi_q(a) = \zeta(a)e^{-\int_0^a [\zeta(\hat{a})+\rho(\hat{a})]\,d\hat{a}} = \hat{f}(a).$$

Since H_1 and Θ have the same initial condition, this implies that $H_1(t)$ and $\Theta(t)$ will exhibit identical dynamics for general but independent transmission and recovery processes. As a direct consequence, this means that the dynamics of susceptibles are the same in both models, since $S(t)$ in (4.8g) and $\langle S\rangle(t)$ in (4.5) differ only in that Θ is replaced by H_1, which are identical and thus interchangeable.

All that remains is to show that the evolution equations for $\langle I\rangle(t)$ in (4.5) and $I(t)$ in (4.8j) are identical. From the EBCM we have that

$$I(t) = \int_0^t i(t,a)\,da,$$

which can be differentiated with respect to t

$$\begin{aligned}\frac{dI}{dt} &= \int_0^t \frac{\partial i(t,a)}{\partial t}\,da + i(t,t)\\ &= -\int_0^t \frac{\partial i(t,a)}{\partial a}\,da - \int_0^t \rho(a)i(t,a)\,da + i(t,t)\\ &= i(t,0) - \int_0^t \rho(a)i(t,a)\,da,\end{aligned}$$

making use of (4.8i). The density of infected individuals of age a is the same as the density of infected individuals created at time $t-a$ multiplied by the survival probability for the duration of infection, $\xi_q(a)$, i.e.

$$i(t,a) = \xi_q(a)i(t-a,0) = \xi_q(a)\dot{S}(t-a).$$

Utilising this substitution and the second identity in (4.6) gives

$$\frac{dI}{dt} = -\frac{dS}{dt} - \int_0^t q(a)\frac{dS(t-a)}{dt}\,da. \tag{4.12}$$

From the MP model (4.5) we can see that

$$\begin{aligned}\frac{d\langle I\rangle}{dt} &= -\frac{d\langle S\rangle}{dt} - \frac{d\langle R\rangle}{dt}\\ &= -\frac{d\langle S\rangle}{dt} - \int_0^t q(a)\frac{d\langle S\rangle(t-a)}{dt}\,da - q(t)(1-z).\end{aligned} \tag{4.13}$$

This final term describes the rate at which the initially infected individuals recover; this term is implicitly considered in the EBCM in (4.8h) and so $dI/dt \equiv d\langle I\rangle/dt$. This completes the proof. □

An implicit analytical relation for the final epidemic size can be found directly from (4.8). This result corresponds to well-known results based on tools from percolation theory [88, 114, 126], and to the final epidemic size obtained for MP models [80]. It is given in the following corollary.

Theorem 1. *The final size of the epidemic $r_\infty = R(\infty)$ in the EBCM (4.8) with a vanishingly small proportion of infected nodes at time $t = 0$ is given by*

$$r_\infty = 1 - G_0(\Theta_\infty),$$

where Θ_∞ solves the equation

$$\Theta_\infty = 1 - \widetilde{T} + \widetilde{T} G_1(\Theta_\infty),$$

and $\widetilde{T} = \int_0^\infty f(a)\, da = \int_0^\infty \zeta(a) \exp(-\int_0^a [\zeta(\hat{a}) + \rho(\hat{a})]\, d\hat{a})\, da$ is the transmissibility of the disease, i.e. the probability that the disease is transmitted along an edge (in isolation) before recovery.

Proof. From (4.8g), for $z \to 1$ and $t \to \infty$, it immediately follows that

$$r_\infty = 1 - S(\infty) = 1 - G_0(\Theta(\infty)).$$

Furthermore, we have

$$\Theta(\infty) = 1 - \int_0^\infty \int_0^t \zeta(a) \phi_I(t, a)\, da\, dt.$$

Interchanging the order of integration yields

$$\Theta(\infty) = 1 - \int_0^\infty \int_a^\infty \zeta(a) \phi_I(t, a)\, dt\, da.$$

Setting $u = t - a$ and noting from (4.10) that $\phi_I(t, a) = \phi_I(u, 0) \exp\left(-\int_0^a [\zeta(\hat{a}) + \rho(\hat{a})]\, d\hat{a}\right)$ yields

$$\begin{aligned}
\Theta(\infty) &= 1 - \int_0^\infty \int_0^\infty \phi_I(u, 0) \zeta(a) e^{-\int_0^a [\zeta(\hat{a}) + \rho(\hat{a})]\, d\hat{a}}\, du\, da \\
&= 1 - \left[\int_0^\infty \phi_I(u, 0) du\right] \int_0^\infty \zeta(a) e^{-\int_0^a [\zeta(\hat{a}) + \rho(\hat{a})]\, d\hat{a}}\, da \\
&= 1 + \left[\int_0^\infty \dot{\Phi}_S(u)\, du\right] \int_0^\infty \zeta(a) e^{-\int_0^a [\zeta(\hat{a}) + \rho(\hat{a})]\, d\hat{a}}\, da \\
&= 1 + (\Phi_S(\infty) - \Phi_S(0)) \widetilde{T} \\
&= 1 + \widetilde{T} G_1(\Theta(\infty)) - \widetilde{T}.
\end{aligned}$$

□

Now that the equivalence between the edge-based compartmental and MP models has been established, we consider the special cases resulting from making extra assumptions about the network (e.g. fully connected and regular) and the infection (e.g. Markovian) and recovery processes (e.g. Markovian or infectious periods of fixed length). This is motivated by the observation that many earlier epidemic models are based on $\tau(a)$, $q(a)$ and/or p_k having the specific forms listed above.

In the following section we aim to produce a model hierarchy by recasting/reducing the EBCM or MP models to earlier models. However, it is not straightforward to see how such earlier models can be derived directly from the EBCM or MP model. This problem can be solved by a re-parametrisation of the MP model in the spirit of pairwise models, and, as a result, one can begin to build a hierarchy of models starting from the most general formulation.

4.4 Model Hierarchy

Different model families (pairwise, effective degree, MP, EBCM etc.) emerge from different considerations of the same underlying stochastic process. In this section we aim to produce a model hierarchy on CM networks by showing that for specific choices of network topology or recovery process, many well-known models can be derived from the more general MP model. In particular, we will focus on deriving pairwise models [86, 92, 162, 169]. In order to do this, we first present a general re-parametrisation of the MP model (4.5), and this will act as stepping stone or interpolation between the EBCM/MP and the well-known earlier models. Since all earlier models use a Markovian infection process, the re-parametrisation also uses this assumption.

Pairwise models are based on differential equations for the expected number of nodes in each state. These depend on the number of edges connecting susceptible and infected nodes, and so differential equations are constructed for the expected number of such edges, which themselves depend on the numbers of triples in certain states (e.g. susceptible-susceptible-infected). To break this dependence, a moment closure approximation is commonly used to express the number of triples in terms of pairs and individuals [84].

Recently, Wilkinson and Sharkey [170] and Wilkinson et al. [169] have shown that for regular tree networks exact pairwise models can be derived from the MP model when the transmission process is assumed to be Markovian. Here we use similar methods and

the notation from Section 4.3.1 to extend this result to the class of CM networks.

Firstly, we define the new variable $\langle SI\rangle(t)$ as the proportion of edges in the network which connect a susceptible node to an infected one at time t. This can be defined in terms of existing quantities from the MP model. The susceptible node must have been initially susceptible and escaped infection from all other neighbours until time t, given by $zG_1(H_1(t))$. This must be multiplied by the probability that the remaining neighbour of the susceptible node is infected and has not yet transmitted the disease to this neighbour. To find this probability it is easier to calculate all other possibilities and subtract them from one. These possibilities are: (i) the neighbour is still susceptible, (ii) the neighbour has already transmitted the disease, (iii) the neighbour was infected but has recovered without transmitting the disease. Combining these gives

$$\begin{aligned}\langle SI\rangle(t) &= zG_1(H_1(t))\left[1 - zG_1(H_1(t))\right.\\ &\qquad\left. - \int_0^t \{f(a)+g(a)\}\left[1 - zG_1(H_1(t-a))\right]\,da\right], \qquad (4.14a)\\ &= zG_1(H_1(t))\left[H_1(t) - zG_1(H_1(t))\right.\\ &\qquad\left. - \int_0^t g(a)\left[1 - zG_1(H_1(t-a))\right]\,da\right], \qquad (4.14b)\end{aligned}$$

where

$$g(a) := q(a)\int_a^\infty \tau(x)\,dx, \qquad (4.15)$$

is the probability of an infected node recovering in the interval $(a, a+\Delta a)$ without transmitting to a given neighbour. The corresponding population-level quantity is given by

$$[SI](t) = \langle k\rangle N\langle SI\rangle(t), \qquad (4.16)$$

where N denotes the total size of the population.

The transmission process is $\tau(a) = \beta e^{-\beta a}$ which can be substituted into (4.4). Introducing the change of variable $t' = t - a$, and using the Leibniz rule gives

$$\begin{aligned}\frac{dH_1}{dt} &= -\beta\left[1 - zG_1(H_1(t)) - \int_0^t q(t-t')e^{-\beta(t-t')}\left[1 - zG_1(H_1(t'))\right]\,da\right.\\ &\qquad\left. - \int_0^t \beta e^{-\beta(t-t')}\left(\int_{t-t'}^\infty q(x)dx\right)\left[1 - zG_1(H_1(t'))\right]\,dt'\right]\\ &= -\beta\left[1 - zG_1(H_1(t)) - \int_0^t \{f(a)+g(a)\}\left[1 - zG_1(H_1(t-a))\right]\,da\right]\end{aligned}$$

$$= -\beta \frac{\langle SI \rangle(t)}{zG_1(H_1(t))} \tag{4.17}$$

$$= -\beta \frac{[SI]}{z\langle k \rangle N G_1(H_1(t))}. \tag{4.18}$$

For the infected population, using (4.5) and identities, such as $[S](t) = N\langle S \rangle(t)$, leads to

$$[\dot{I}] = -[\dot{S}] - [\dot{R}] \tag{4.19}$$

$$= \beta[SI] - \beta \int_0^t q(a)[SI](t-a)da - q(t)N(1-z). \tag{4.20}$$

The majority of pairwise epidemic models retain an explicit differential equation for the infected population [70, 169]. However, we choose to integrate (4.20) to reduce the number of differential equations that have to be integrated numerically. By noting that $[SI] = \beta \int_0^t [\dot{SI}](t-a)\xi_q(a)\,da$ and $q(a) = -\xi_q'(a)$, we have

$$[\dot{I}] = \beta \int_0^t \left([\dot{SI}](t-a)\xi_q(a) + \xi_q'(a)[SI](t-a) \right) da - q(t)N(1-z),$$

which is the result of differentiating

$$[I] = \beta \int_0^t [SI](t-a)\xi_q(a)\,da + N(1-z)\xi_q(t). \tag{4.21}$$

Whilst (4.20) facilitates easier comparison to existing models, its equivalent representation (4.21) offers greater computational efficiency.

For the variable $\langle SI \rangle$ the calculation is more laborious; working term-by-term from (4.14b) and using the new relation (4.18) one obtains

$$\begin{aligned}
\langle \dot{SI} \rangle = &-zG_2(H_1) \left(\beta \frac{[SI]}{z\langle k \rangle N G_1(H_1(t))} \right) \left[\cdot \right] \\
&- \beta \frac{[SI]}{\langle k \rangle N} + z\beta[SI] \frac{G_2(H_1(t))}{\langle k \rangle N} - q(t)e^{-\beta t}(1-z)zG_1(H_1(t)) \\
&- z\beta \int_0^t q(a)e^{-\beta a}[SI](t-a)G_2(H_1(t-a)) \frac{G_1(H_1(t))}{N\langle k \rangle G_1(H_1(t-a))}\,da,
\end{aligned}$$

where $[\cdot]$ denotes the large bracket in (4.14b), and the Leibniz rule has been used again to resolve the integral term. Finally, based on (4.14), $[\cdot] = \frac{\langle SI \rangle}{zG_1(H_1)}$, which allows us to eliminate $[\cdot]$ and replace it with a term involving $\langle SI \rangle$. Then, multiplying through by $\langle k \rangle N$ one obtains $[\dot{SI}]$ in (4.22) below.

$$\dot{H}_1 = -\beta \frac{[SI]}{z\langle k \rangle N G_1(H_1)}, \tag{4.22a}$$

$$\begin{aligned}[\dot{SI}] = &-\beta[SI]^2 \frac{G_2(H_1)}{z\langle k \rangle N [G_1(H_1)]^2} - \beta[SI] \\ &+ z\beta[SI]G_2(H_1) - q(t)e^{-\beta t}(1-z)zG_1(H_1)\langle k \rangle N \\ &- z\beta \int_0^t q(a)e^{-\beta a}[SI](t-a)G_2(H_1(t-a)) \frac{G_1(H_1(t))}{G_1(H_1(t-a))}\, da,\end{aligned} \tag{4.22b}$$

$$[I] = \beta \int_0^t [SI](t-a)\xi_q(a)\, da + N(1-z)\xi_q(t). \tag{4.22c}$$

At any time t the expected number of susceptibles is $[S](t) = zNG_0(H_1(t))$. System (4.22) has been derived directly from the MP model, and thus it becomes exact under the same conditions - on the ensemble of CM networks as the network size tends to infinity. Moreover, retaining the concept of the message, H_1, has meant that system (4.22) does not depend on higher order arrangements of nodes (e.g. triples). Therefore, unlike most pairwise models, no further approximations are required to close the model. Similar results have been achieved in the past using heuristic arguments [70]. Whilst we chose to begin from the MP model, it should be possible to achieve the same result using the variables in the EBCM (4.8) to derive the differential equations in (4.22).

This re-parametrised system (4.22) is the first crucial step in being able to move from general to specific models on CM networks, with special focus on unifying various approaches by considering different models from the same perspective.

As one would expect, earlier population-level models were constructed based on some more restrictive assumptions on network and epidemic dynamics. We will show that when these are applied to system/model (4.22), earlier models can be easily recovered. The simplifying assumptions refer either to the network (e.g. fully connected or regular [169]), or the distribution of the infectious period (e.g. Markovian [162], fixed length [92]). The remainder of this section is devoted to the explicit derivation of the relationships between models as illustrated in Fig. 4.2.

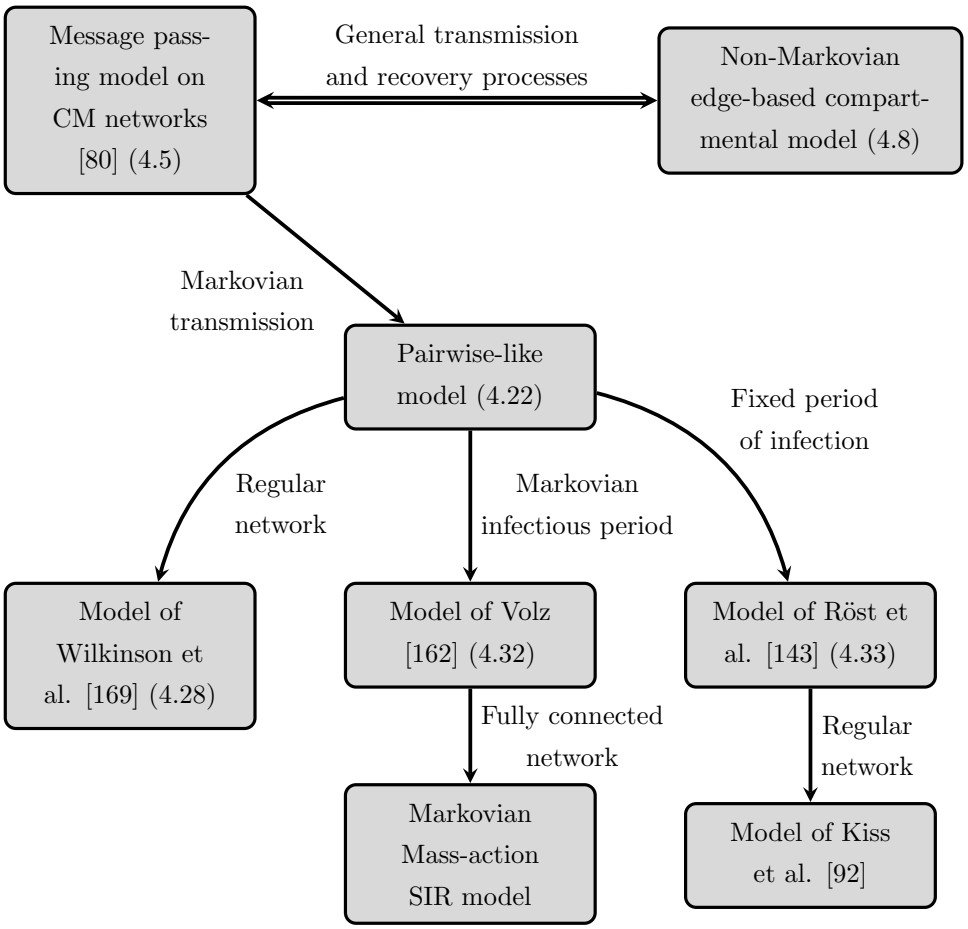

Figure 4.2: Diagram showing the relationship between the various models discussed in the Chapter. Labels on each branch state the necessary assumptions in order to reach the model at the end of the arrow.

4.4.1 Degree-regular networks

The first of these reductions concerns the special case of regular networks. For a k-regular (homogeneous) network, all nodes have the same degree, i.e. $k_u = \langle k \rangle = k$, and so the generating functions from (4.3) simplify to

$$G_0(x) = x^k, \quad G_1(x) = x^{k-1}, \quad \text{and} \quad G_2(x) = (k-1)x^{k-2}.$$

We also introduce two new variables

$$\begin{aligned} [S](t) &= zNG_0(H_1(t)) = zN[H_1(t)]^k, \\ [SS](t) &= \langle k \rangle N \left(zG_1(H_1(t))\right)^2 = kN \left(z[H_1(t)]^{k-1}\right)^2, \end{aligned} \tag{4.23}$$

that represent the expected number of susceptible individuals and the expected number of edges connecting two susceptible nodes, respectively. $[S](t)$ follows directly from (4.5), and $[SS](t)$ is defined as the number of edges connecting two nodes who were both initially susceptible at time $t = 0$ and have escaped infection from their $(k-1)$ other neighbours.

Now we return to the system (4.22) and the differential equation for $[I]$ (4.20). Substituting the simpler generating functions yields

$$\begin{aligned}
\dot{H}_1 &= -\beta \frac{[SI]}{zkNH_1^{k-1}}, \\
[\dot{I}] &= \beta[SI] - \beta \int_0^t q(a)[SI](t-a)da - q(t)N(1-z), \\
[\dot{SI}] &= -\beta[SI]^2 \frac{(k-1)H_1^{k-2}}{zkN[H_1^{k-1}]^2} - \beta[SI] \\
&\quad + z\beta[SI](k-1)H_1^{k-2} - q(t)e^{-\beta t}(1-z)zH_1^{k-1}kN \\
&\quad - z\beta \int_0^t q(a)e^{-\beta a}[SI](t-a)(k-1)[H_1(t-a))]^{k-2} \frac{[H_1(t)]^{k-1}}{[H_1(t-a)]^{k-1}} da.
\end{aligned} \tag{4.24}$$

This can be simplified further using (4.23), firstly noting that

$$\frac{[SS]}{[S]} = \frac{Nkz^2H_1^{2(k-1)}}{NzH_1^k} = kzH_1^{k-2}, \tag{4.25}$$

and, from $\dot{H}_1$ we see that

$$\frac{d(H_1^{k-1})}{dt} = -\beta(k-1)\frac{[SI]}{zkNH_1^{k-1}}H_1^{k-2} = -\beta\frac{(k-1)}{k}\frac{[SI]}{[S]}H_1^{k-1}. \tag{4.26}$$

Solving for H_1^{k-1} using separation of variables gives

$$H_1^{k-1}(t) = \exp\left(-\beta \int_0^t \frac{(k-1)}{k}\frac{[SI](u)}{[S](u)}\,du\right). \tag{4.27}$$

The result of this is that the system no longer requires the message H_1, as one can calculate the time derivatives of $[S]$ and $[SS]$ directly from (4.23). Using the new

relations (4.25) and (4.27), system (4.24) can be rewritten to give

$$\begin{aligned}
[\dot{S}] &= -\beta[SI], \\
[\dot{I}] &= \beta[SI] - \beta\int_0^t q(a)[SI](t-a)da - q(t)N(1-z), \\
[\dot{SS}] &= -2\beta\frac{(k-1)}{k}\frac{[SS][SI]}{[S]}, \\
[\dot{SI}] &= -\beta\frac{(k-1)}{k}\frac{[SI][SI]}{[S]} - \beta[SI] + \beta\frac{(k-1)}{k}\frac{[SS][SI]}{[S]} \\
&\quad - kNq(t)e^{-\beta t}(1-z)z\exp\left(-\beta\int_0^t \frac{(k-1)}{k}\frac{[SI](a)}{[S](a)}da\right) \\
&\quad - \beta\int_0^t q(a)e^{-\beta a}\frac{(k-1)}{k}\frac{[SS](t-a)[SI](t-a)}{[S](t-a)}\mathcal{F}(t)da,
\end{aligned} \tag{4.28}$$

where

$$\mathcal{F}(t) = \exp\left(-\beta\int_{t-a}^t \frac{(k-1)}{k}\frac{[SI](u)}{[S](u)}du\right). \tag{4.29}$$

This is identical to the system proposed by Wilkinson et al [169]. Recently, Röst et al. [143] have considered the same problem, namely, an SIR epidemic with Poisson transmission and an arbitrary distribution of the infectious period on a regular network. By constructing an age-structured system of PDEs they were able to reach a more compact model which is can also handle arbitrary initial conditions. We have, therefore, shown that (4.22) extends these recent models by allowing general degree distributions to be modelled.

4.4.2 Special distributions of the infectious period

As mentioned previously, a popular choice for the duration of infection is to assume an exponential distribution, i.e. $q(a) = \gamma e^{-\gamma a}$ for $\gamma > 0$, where $1/\gamma$ is the mean duration of infection. We briefly explain how this assumption simplifies the model and leads to familiar or well-known models. When this choice for $q(a)$ is substituted into (4.20), we have

$$[\dot{I}] = \beta[SI] - \gamma\left[\int_0^t e^{-\gamma a}\beta[SI](t-a)da + e^{-\gamma t}N(1-z)\right]. \tag{4.30}$$

Note that $e^{-\gamma a}$ is the probability of an infected node not recovering before age a, and since the number of infected nodes created a time ago is $\beta[SI](t-a)$ for $a < t$ and

$N(1-z)$ for $a=t$, (4.30) can be rewritten as

$$[\dot{I}] = \beta[SI] - \gamma[I]. \tag{4.31}$$

A similar result is reached in (4.22b). In this case the extra terms in the integral describe the probability for the susceptible node of an $[SI]$ edge to have survived until age a without receiving transmission, either along this edge or from another infected neighbour. Therefore, by the same logic one can replace the final two terms in (4.22b) with $\gamma[SI]$. This leads to a model, which, although formulated differently, is dynamically equivalent to models of Volz [162] and House and Keeling [70], namely,

$$\begin{aligned}
\dot{H}_1 &= -\beta\frac{[SI]}{z\langle k\rangle N G_1(H_1)},\\
[\dot{I}] &= \beta[SI] - \gamma[I],\\
[\dot{SI}] &= -\beta[SI]^2\frac{G_2(H_1)}{z\langle k\rangle N[G_1(H_1)]^2} - (\beta+\gamma)[SI] + z\beta[SI]G_2(H_1).
\end{aligned} \tag{4.32}$$

If one further assumes that the degree is regular, repeating the steps used to derive system (4.28) recovers the early pairwise model [86].

We examine one final special case, when the duration of infection is a fixed period of time, σ, so that $q(a) = \delta(a-\sigma)$. This means that as soon as a node is infected at time t_1, it is known that this node will recover at exactly $t_2 = t_1 + \sigma$. Therefore, the integral terms are non-zero only at the point $a = \sigma$. In this case the system of integro-differential equations (4.22) simplifies to a delay differential equation model, as stated below

$$\begin{aligned}
\dot{H}_1 &= -\beta\frac{[SI]}{z\langle k\rangle N G_1(H_1)},\\
[\dot{I}] &= \beta[SI] - \beta[SI](t-\sigma) - \delta(t-\sigma)N(1-z),\\
[\dot{SI}] &= -\beta[SI]^2\frac{G_2(H_1)}{z\langle k\rangle N[G_1(H_1)]^2} - \beta[SI]\\
&\quad + z\beta[SI]G_2(H_1) - \delta(t-\sigma)e^{-\beta t}(1-z)zG_1(H_1)\langle k\rangle N\\
&\quad - z\beta e^{-\beta\sigma}[SI](t-\sigma)G_2(H_1(t-\sigma))\frac{G_1(H_1(t))}{G_1(H_1(t-\sigma))}.
\end{aligned} \tag{4.33}$$

This model generalises the recent work of Kiss et al. [92] to heterogeneous networks, and once again the original model in that paper can be retrieved when $q(a)$ is chosen to

be a delta distribution in (4.28) (although that original model did not explicitly account for the recovery of initially infected nodes).

Finally, it is worth briefly noting that in the case of a fully connected network, corresponding to a homogeneously well-mixed population we have that $[SI] = [S][I]$, and thus, the Markovian mass-action SIR model, which assumes that the population is unstructured, is recovered. Moreover, with the proper conditions, Wilkinson et al. [169] proved that the message passing model is equivalent to the mass action model of Kermack and McKendrick [89] for general transmission and recovery processes.

4.5 Numerical simulation results

In order to illustrate the accuracy of (4.22), we compare the numerical solution of this model to results of direct stochastic network simulation. A common approach for simulating traditional Markovian models has been to use the Gillespie algorithm [55]. However, as modelling started to move away from the purely Markovian models, novel stochastic simulation methods have been derived [5, 19] which provide efficient simulation algorithms that are able to generate true sample paths of the stochastic process.

In this section we take advantage of the fact that in the system (4.22) transmission is a Poisson process in order to use an algorithm similar to those described by Barrio et al. [13]. This approach is sometimes known as the rejection method and was proven to be stochastically exact by Anderson [5]. The transmission process is run as in the standard Gillespie algorithm; whenever a node becomes infected, a duration of infection is drawn from the distribution $q(a)$; at each time step the time of next transmission is randomly generated, but if an infected node is scheduled to recover sooner, then the transmission event is rejected, and time is updated to the next recovery time (for full details see [5]).

In the very early stages of an outbreak stochastic effects dominate the dynamics of the epidemic spread, which means that numerical simulations can often produce results that significantly differ from deterministic predictions. In this situation, methods such as branching process approximations [38] are more appropriate. To ensure that this does not affect our results, we allow every iteration of the algorithm to reach a point where the stochastic effects are no longer a concern, and the infected population behaves deterministically. In practice this is achieved by running each individual realisation of

the epidemic from a single initial seed until a specified level of infectivity is reached, at which point time is reset to zero in both the simulation and the mean-field model.

A sufficient number of individual simulations are averaged to ensure that the mean behaviour of the stochastic model is correctly captured and is suitable for comparison with results derived from the deterministic models.

In Fig. 4.3 the results of numerical simulations are shown for three different distributions of the infectious period all having the same mean: a normal distribution, an exponential distribution, and a fixed infectious period, σ. Two important observations can be made. Firstly, the excellent agreement between the average of simulations (markers) and the mean-field model (lines) provides empirical validation of the mean-field model. Secondly, Figure 4.3 shows marked differences between the epidemics despite the mean of the infectious periods being the same. In particular, the exponential distribution leads to the slowest epidemic growth (and smallest epidemic peak) with the infectious periods of fixed length leading to the fastest growing epidemics (and largest epidemic peak). These results highlight the potential risks of using inaccurate modelling assumptions. The results also suggest that the variance in the duration of the infectious period has a significant effect on the time evolution of the epidemic: a decrease in variance leads to an increase in the initial growth rate [92].

Changes to the degree distribution, transmission and infectious processes will all have an impact on the final epidemic size, as determined by Corollary 1. In the tests shown in Fig. 4.3 only the distribution of the infectious period changes. Whilst this will affect the final epidemic size, it is not possible to tell which of the epidemics is going to produce the largest final epidemic size purely from examining the time evolution of the epidemic in Fig. 4.3. Indeed, it is possible for two epidemics with different time evolutions to have the same final epidemic size. For example, if the degree distribution remains the same, different choices for the distributions of the time to infection and infectious periods can produce identical values for the transmissibility, and the same final epidemic size.

4.6 Discussion

In this Chapter we have reviewed the message passing formalism for SIR epidemics on networks, and introduced a novel extension of the edge-based compartmental model to the case of general but independent transmission and recovery processes. Both

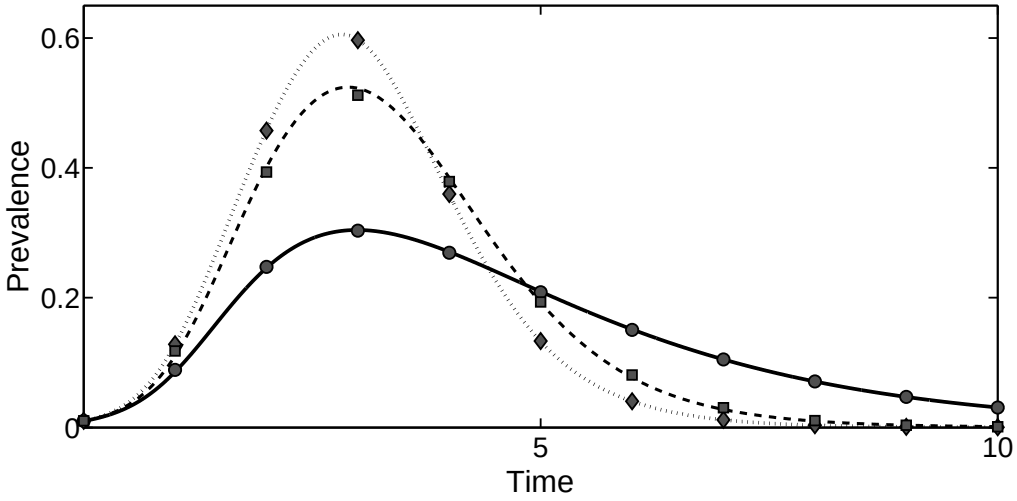

Figure 4.3: Comparison between system (4.22) and the average of numerical simulations. All tests are carried out on randomly generated, truncated scale-free networks of 1000 nodes with exponent 2.5, and the degree bounded between 3 and 60. The transmission rate is set to $\beta = 0.3$ in all cases. Results are plotted where the infectious period is exponentially distributed with parameter $\gamma = 0.5$ (solid line, circles), normally distributed with mean 2 and standard deviation 0.75 (dashed line, squares), and a fixed duration $\sigma = 2$ (doted line, diamonds). The mean duration of the infectious period is equal to 2 for all cases. The differences between the epidemics show that the shape of the distribution of the infectious period can have a significant effect on the dynamics of the epidemic.

of these models are capable of accurately describing the expected dynamics of non-Markovian epidemics on tree networks. The main result of the Chapter is the complete and rigorous proof of equivalence between these models, and, as a result, the non-Markovian EBCM (4.8) is exact on the ensemble of infinite-size CM networks.

Adapting recent methods [169, 170] enabled us to re-parametrise the MP model for the special case of a Markovian transmission process but arbitrary CM networks. The compact model (4.22) remains exact and is, in fact, a hybrid between MP and classical pairwise models.

Many pairwise models are defined heuristically [44, 64, 70], but by deriving the model (4.22) as a re-parametrisation of the MP model we have developed a general model from which existing pairwise models can be extracted. By demonstrating this we hope to provide some intuition for how these newer models work and to illustrate that

they build on existing models whilst providing a modern twist. It is encouraging that such mean-field models remain compact, consisting of only a few differential equations, highlighting that the SIR epidemic can be modelled quite effectively, as long as a small number of key characteristics of the network and the epidemic process are known.

The results from our numerical simulations illustrate the dangers of using inaccurate or overly simplistic data to make predictions, in particular, the common assumption of fully Markovian dynamics. The MP and non-Markovian edge-based compartmental models are, therefore, crucial if we are to develop accurate epidemic models on networks.

Numerous extensions of the present work are possible. For example, the implementation of an efficient solver of the novel EBCM is still outstanding. Efficient numerical methods to solve such age-structured models exist, but this was outside the scope of our study. In some sense the novel EBCM is the most complete mean-field model when one considers SIR epidemics on CM networks. This is due to the model being able to handle arbitrary degree distributions, as well as general independent transmission and recovery processes.

The restriction to CM networks implies zero clustering, i.e. there are no small, highly connected groups of nodes. This is a necessary simplification to derive these models, but is unrealistic. Real social networks often have high levels of clustering [167]. Although it can be shown that these models place an upper bound on the true expected behaviour [80], future research should strive to develop exact models where clustering is present. As the inspiration for MP methods came from percolation theory, new models could begin from the work of Serrano et al. [147]; who developed the theory for percolation in networks with community structure.

Additionally, it could be refined to account for dynamic or adaptive contacts. Dynamic networks have already been incorporated in edge-based modelling in the purely Markovian setting [119], and it may be possible to extend this to a more general framework to allow for a more unified treatment of models that include the concurrent spread of the disease and link turnover.

Acknowledgements

N. Sherborne acknowledges funding for his PhD studies from the EPSRC (Engineering and Physical Sciences Research Council), EP/M506667/1, and the University of Sussex.

Chapter 5

Paper 4: Bursting endemic bubbles with adaptive rewiring on networks

N. Sherborne[1], K.B. Blyuss[1] and I.Z. Kiss[1]

[1]Department of Mathematics, School of Mathematical and Physical Sciences, University of Sussex, Brighton, BN1 9QH, UK

5.1 Abstract

The spread of an infectious disease is known to change people's behaviour, which in turn affects the spread of disease. Adaptive network models that account for both epidemic and behaviour change have found oscillations, but in an extremely narrow region of the parameter space, which contrasts with intuition and available data. In this Chapter we propose a simple SIS epidemic model on an adaptive network with time-delayed rewiring, and show that oscillatory solutions are now present in a wide region of the parameter space. Altering the transmission or rewiring rates reveals the presence of an endemic bubble - an enclosed region of the parameter space where oscillations are observed.

5.2 Introduction

The spread of an infectious disease changes the behaviour of individuals, and this, in turn, affects the spread of the disease [52]. Broadly speaking, responses to an epidemic fall into two categories: coordinated and uncoordinated. Coordinated responses include vaccination and quarantine schemes, travel restrictions, and information spread through mass media. Uncoordinated responses cover individuals adapting their behaviour based on their own perceived risk, this includes improved hygiene regimens and avoiding crowded places and public transport during outbreaks. Surveys consistently identify such precautionary measures taken by individuals during epidemic outbreaks [57, 144]. Fear of becoming infected during the 2003 SARS epidemic in Hong Kong caused huge behavioural shifts; air travel into Hong Kong dropped by as much as 80% [48]. Responses to a large study covering numerous European and Asian regions revealed that, in the event of an influenza pandemic, 75% of people would avoid public transport, and $20-30\%$ would try to stay indoors [145]. These behavioural shifts change the potential routes for transmission and can alter the size and time-scale of an epidemic [53].

In the context of epidemic models on networks, perhaps, the most widespread approach to couple epidemics and behaviour is by using adaptive networks, where behavioural changes are captured by link rewiring based on the disease status of nodes [63, 53]. Gross et al. [64, 65] considered a simple SIS model with rewiring, in which susceptible nodes disconnect from infected neighbours at rate ω, and immediately reconnect to a randomly chosen susceptible node. This simple model led to bistability and

to oscillatory solutions, albeit with oscillations limited to an extremely narrow region of the parameter space. This rewiring procedure has since been extended to consider scenarios where both the susceptible and infected nodes can rewire, and diseases with a latent period [139]. Zhang et al. [172] presented a further alternative, where news about past prevalence influences whether nodes choose to disconnect edges. The authors found an estimate of the critical delay that induces a Hopf bifurcation, thus causing periodicity. Tunc et al. [158] studied a network model with temporary deactivation of edges between susceptible and infected individuals. On a growing network, Zhou et al. [173] showed that cutting links between susceptible and infected individuals can lead to epidemic re-emergence, with long periods of low disease prevalence punctuated by large outbreaks.

Periodic cycles and disease re-emergence are evident in real-world data. Many diseases are subject to seasonal peaks, which have been studied extensively [3, 59]. Often a sinusoidal or other form of time-varying transmission parameter is used to imitate seasonality, which can lead to multiennial peaks [95]. A number of models have identified other possible causes of periodicity in epidemic dynamics. To give one example, Hethcote at al. [67] showed that in a well-mixed population temporary immunity in SIRS- or SEIRS-type models as represented by a time delay can result in the emergence of periodic solutions when the immunity period exceeds some critical value.

One should note that seasonality alone cannot explain all cases of oscillations. In both the UK and the USA, the 2009 H1N1 pandemic occurred in two distinct waves separated by a few months [27, 76]. Other diseases have shown more long-term trends. Incidence reports of mycoplasma pneumonia have found evidence of epidemic cycles in many different countries, with periodicity of 3 to 5 years [74, 164]. Recently, it has been suggested that syphilis exhibits periodic cycling [60], although these findings have been subsequently questioned [22]. Whilst it is difficult to pinpoint the specific causes of periodicity in the dynamics of these diseases, if syphilis epidemics are indeed cyclical, then changes in human behaviour have been proposed as the likely explanation [2].

Intuitively, and as shown by empirical observations, one would expect oscillations to appear in epidemic models where behaviour is considered. If an individual is aware of the state of their neighbours and responds accordingly, then times of high prevalence will be associated with greater caution, curbing further spread. Conversely, without advance warning, behaviour will return to normal as prevalence wanes, enabling a second wave of the epidemic. Despite this intuition, adaptive network models have so far not been able

to show such robust oscillations over reasonable regions of the parameter space. This means that, in situations where adaptive behaviour is expected, modelling is unlikely to identify the risk of oscillations in prevalence. As a result policymakers and healthcare services will have a poor, and potentially misleading prediction of the expected pattern of an impending epidemic outbreak. Clearly, this could have severe consequences.

To tackle this problem, we introduce a simple SIS model on an adaptive network with N nodes. Infected nodes transmit the disease to susceptible neighbours at rate β across links, and recover and become susceptible again at rate γ, independently of the network. Susceptible nodes cut links that connect them to infected neighbours at rate ω and, after a fixed time delay of length τ, reconnect to susceptible nodes chosen uniformly at random from all such available nodes. The delay between cutting and reconnecting is crucial. It is unrealistic to expect that alternative contacts can be identified and established arbitrarily quickly. The delay represents both people's hesitance to make new contacts and also the potential lack of availability of such new contacts when an epidemic is spreading thorough a population [145].

5.3 Model derivation

To construct the mean-field model, we use the pairwise approximation method [82]. The number of nodes in the susceptible or infected state at time t is denoted by $[S]$ and $[I]$, respectively; $[SS]$, $[SI]$ and $[II]$ denote the number of connected pairs of nodes in the respective states, with all pairs being doubly counted. The explicit dependence on time is dropped for simplicity. For the moment closure approximation we use the assumption that once a node is fixed, typically a susceptible node, then the states of the neighbours are Poisson-distributed [135]. This leads to:

$$[XYZ] = \frac{[XY][YZ]}{[Y]}, \quad X, Y, Z \in \{S, I\}, \tag{5.1}$$

to express the number of connected triples [64, 82].

The delay before an $S-I$ edge is rewired to an $S-S$ edge introduces a complication to the modelling, as not all newly formed edges will be between two susceptible nodes. To see this, consider an example of a susceptible node with two or more infected neighbours. At some time t_1 it disconnects from one of these neighbours. Then, in the interval $(t_1, t_1+\tau)$ another infected neighbour transmits the disease to it. If it then remains infected until time $t_1+\tau$, the new edge will be of an $I-S$ type rather

than $S-S$. To deal with this issue we use a technique similar to that used by Kiss et al. [92] for a pairwise model with an infectious period of fixed length. Consider $y_p(t)$ to be the cohort of susceptible nodes that have cut a link at time $t-\tau$ and are waiting to reconnect. The expected number of infected neighbours a susceptible node has is approximated by $[SI]/[S]$. Therefore, the rate at which nodes in the cohort become infected over the interval $(t-\tau, t)$ is

$$\dot{y}_p = -\beta y_p \frac{[SI]}{[S]}.$$

The solution to this ODE is

$$y_p(t) = \omega[SI](t-\tau)\exp\left(-\beta \int_{t-\tau}^{t} \frac{[SI](u)}{[S](u)}\, du\right), \tag{5.2}$$

since $y_p(t-\tau) = \omega[SI](t-\tau)$.

A member of the cohort infected at some time $u \in (t-\tau, t)$ may recover before time t. To ensure that we only consider nodes which remain infected, we must include the probability that a node infected at time u remains infected until time t in the integral term of (5.2). This is the survival probability of the recovery process, and it is given by $e^{-\gamma(t-u)}$. Therefore, the rate at which new $S-S$ edges are formed is,

$$y(t) := \omega[SI](t-\tau)\exp\left(-\beta \int_{t-\tau}^{t} \frac{[SI]}{[S]} e^{-\gamma(t-u)}\, du\right). \tag{5.3}$$

If the exponential term in (5.3) is denoted by $x(t)$, the rate at which new $I-S$ edges are formed is $\omega[SI](t-\tau)(1-x(t))$. With this in mind, the mean-field model is

$$\begin{aligned}
[\dot{S}] &= -\beta[SI] + \gamma[I], \\
[\dot{I}] &= \beta[SI] - \gamma[I], \\
[\dot{SS}] &= 2\gamma[SI] - 2\beta\frac{[SS][SI]}{[S]} + 2\omega[SI](t-\tau)x(t), \\
[\dot{SI}] &= -(\beta+\gamma+\omega)[SI] + \beta[SI]\left(\frac{[SS]}{[S]} - \frac{[SI]}{[S]}\right) \\
&\qquad + \gamma[II] + \omega[SI](t-\tau)(1-x(t)), \\
[\dot{II}] &= -2\gamma[II] + 2\beta\left(\frac{[SI][SI]}{[S]} + [SI]\right), \\
\dot{x} &= -x\left\{\gamma \ln x + \beta\left(\frac{[SI]}{[S]} - \frac{[SI](t-\tau)}{[S](t-\tau)} e^{-\gamma\tau}\right)\right\},
\end{aligned} \tag{5.4}$$

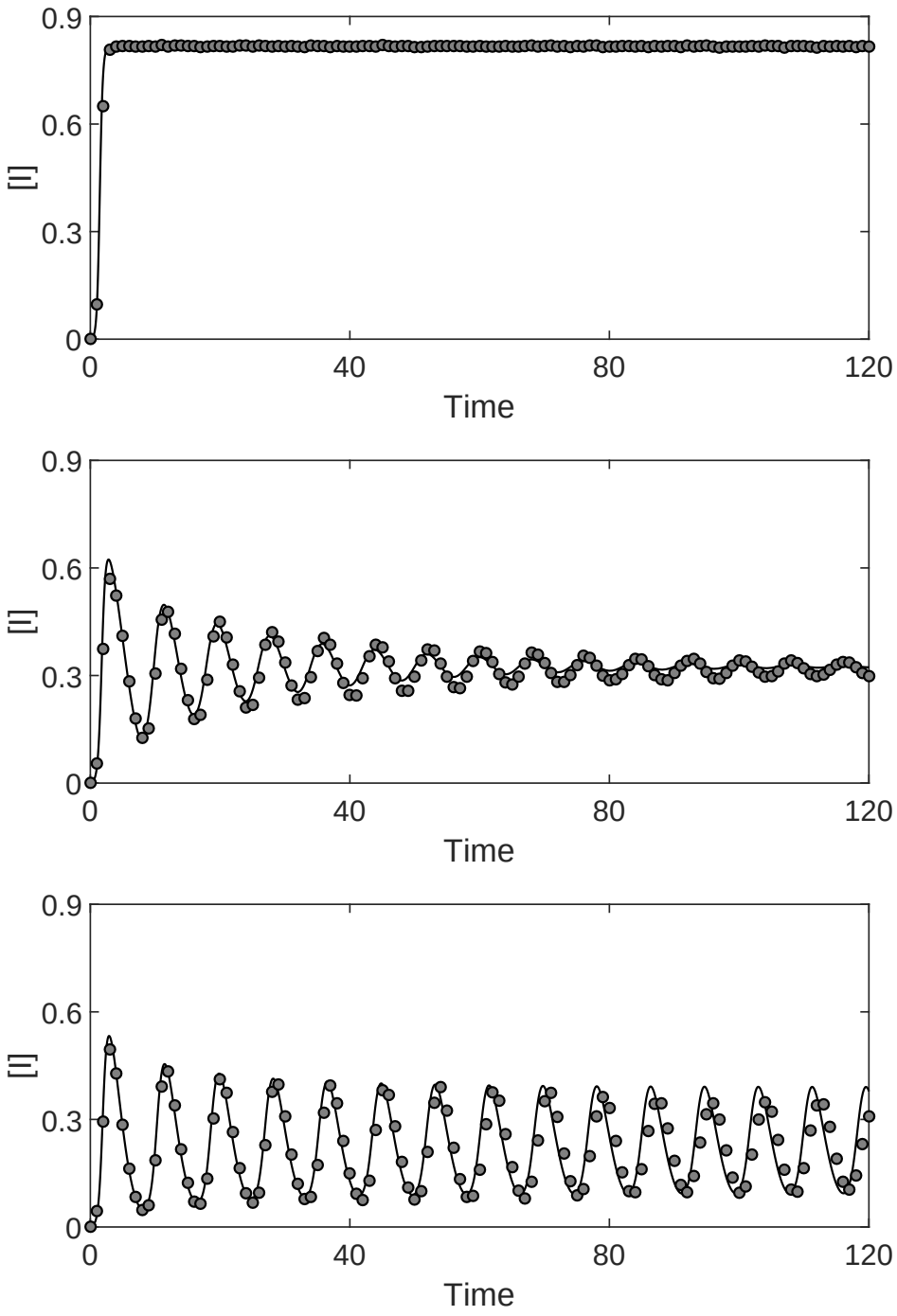

Figure 5.1: Comparison between the solution of (5.4) and numerical simulation. Three sets of results are shown, $\omega = 0$ (top), $\omega = 1$ (middle) and $\omega = 1.4$ (bottom). Other parameters are $\beta = 0.6$, $\gamma = 1$, $\tau = 6$ and $\langle k \rangle = 10$. Simulation results are averaged across 100 iterations on random networks of 1000 nodes. All simulations begin by randomly selecting a node to infect at time $t = 0$. Simulation runs which die out are discarded and performed again.

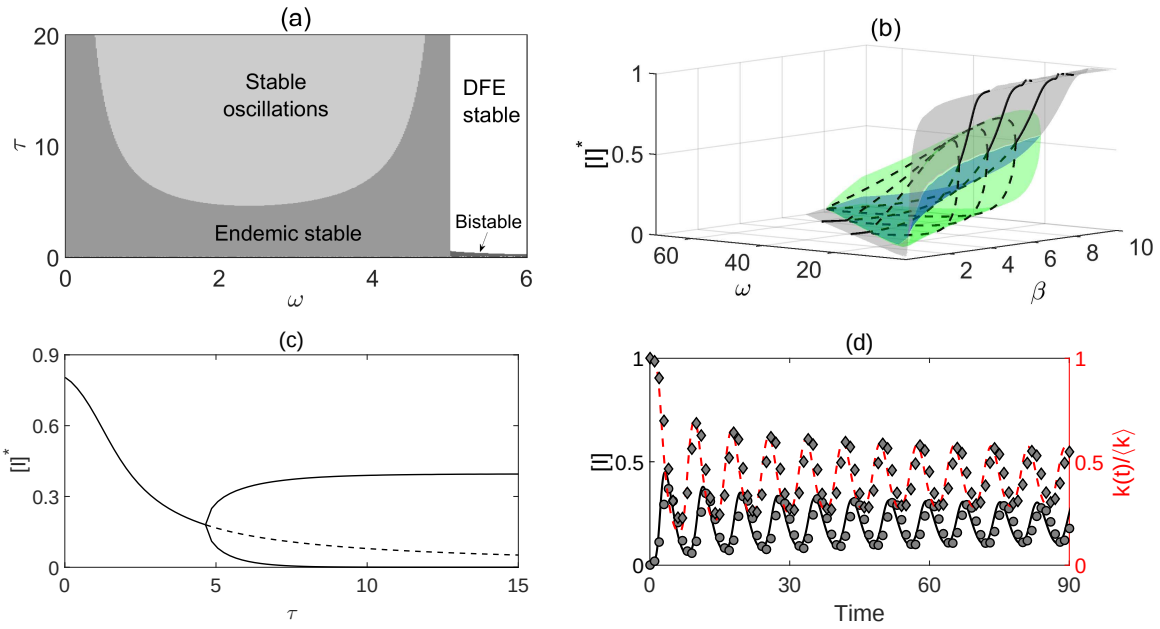

Figure 5.2: (a) shows a two-parameter bifurcation diagram indicating different dynamical regimes in the behaviour of model (5.4) with $\beta = 0.6$. (b) shows the *endemic bubble* for model (5.4) for $\tau = 6$. The endemic equilibrium is stable on the grey surface and unstable on the green. Green surface is constructed using the minima and maxima of oscillations and shows the shape of the *endemic bubble*. In (c) the value of the endemic equilibrium is plotted against the rewiring delay τ for $\beta = 0.6$ and $\omega = 2$. Increasing τ decreases the expected number of infected individuals at endemic equilibrium until the Hopf bifurcation point, beyond which the amplitude of oscillations grows. In (d) the average behaviour from 100 numerical simulations on random networks of 1000 nodes is compared to the mean-field model (5.4). The solid black line (circles) denote the prevalence of the disease in the mean-field model (simulations), and the red dashed line (diamonds) denotes the normalized mean degree calculated from (5.6). Parameter values are $\beta = 0.55$, $\omega = 1.5$, $\tau = 5.5$, $\gamma = 1$, $\langle k \rangle = 10$. Simulations in which epidemic outbreaks died out were discarded and performed again.

where $x(t) = 1$ for $t \leq 0$. When $\tau = 0$, the dynamics of (5.4) are equivalent to the well-known model of Gross et al [64].

Fig. 5.1 shows a comparison between the solution of the new model (5.4) and numerical simulation. The agreement is excellent despite the simplicity of the model and the fact that the moment closures do not reflect the changing network structure. In particular, both the solution and simulation results exhibit similar oscillatory behaviour for the same parameter values. These results validate the model and allow us to analyse

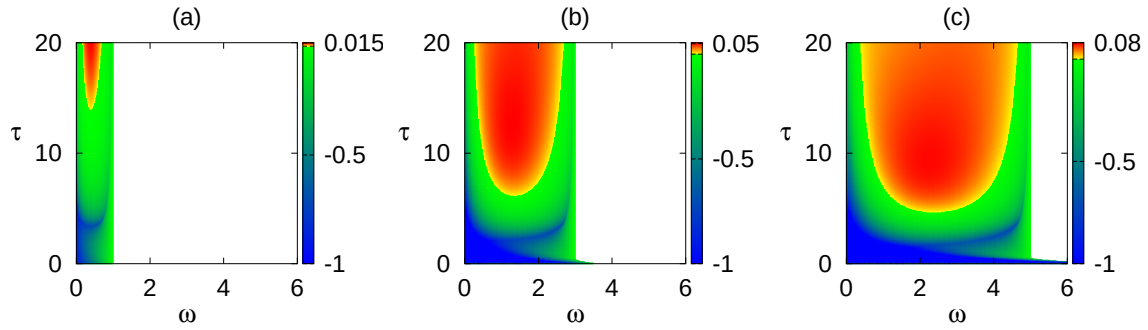

Figure 5.3: Real part of the maximum characteristic eigenvalue of the endemic equilibrium of (5.4) for $\beta = 0.2$ (a), 0.4 (b), and 0.6 (c). Other parameters are the same as in Fig. 5.2 (a). The endemic equilibrium is unstable in the red/yellow region, stable in the green/blue region, and biologically infeasible in the white region.

its behaviour.

5.4 Results

Firstly, consider the basic reproductive ratio, R_0, defined as the expected number of secondary infections caused by a single typical infectious node in an otherwise wholly susceptible population. One can find R_0 for the delayed rewiring model (5.4) via linear stability analysis near the disease-free equilibrium (DFE), $([S]^*, [I]^*, [SS]^*, [SI]^*, [II]^*, x^*) = (N, 0, \langle k \rangle N, 0, 0, 1)$. Performing this analysis gives

$$R_0 = \frac{\beta \langle k \rangle}{\gamma + \omega}. \tag{5.5}$$

Note that increasing the rewiring rate decreases the epidemic threshold R_0, but the length of the delay, τ, has no effect on the threshold. However, as we will show later, it does affect the final outcome of the epidemic.

System (5.4) also has an endemic steady state, but its value is determined by a transcendental equation which can only be solved numerically. Using this result in the numerical linear stability analysis of (5.4) allows us to analyse the stability of the endemic equilibrium. As shown in Fig. 5.2 (a), changes to both τ and ω are capable of destabilising the endemic equilibrium. Regardless of the value of τ, eventually high values of the rewiring rate make the DFE stable again. For most values of τ this coincides with the point where the endemic steady state becomes biologically infeasible (less than or equal to zero), leaving the DFE as the only plausible steady state for the

system. However, for sufficiently small values of τ, the endemic steady state remains feasible, and there is a small region of bistability. Qualitatively, this behaviour is the same for any choice of the other parameters, as long as the endemic steady state remains biologically feasible, as illustrated for different values of β in Fig. 5.3. This figure shows that increasing the disease transmission rate results allows the endemic steady state to be feasible for a wider range of link-cutting rate ω, and it also lowers the critical time delay τ, at which this steady state becomes unstable.

Figure 5.2 (b) shows the endemic equilibrium, as well as the minima and maxima of oscillations for a range of β and ω values, with oscillations being observed in a significant part of the parameter space. One can clearly see the formation of an *endemic bubble* that has been discovered earlier in other epidemic models [94, 101]. Interestingly, both ω and β appear to play similar roles in the formation of endemic bubble, namely they open it through a supercritical Hopf bifurcation of the endemic equilibrium and then close it through a subcritical Hopf bifurcation.

Increasing the length of the delay can only induce a supercritical Hopf bifurcation, resulting in the emergence of stable oscillations, beyond which point larger values of τ only increase the amplitude of oscillations until it settles on some steady level, as shown in Fig. 5.2 (c). One should note that the minima of oscillations get closer to zero for larger τ, suggesting that for large rewiring times, there are periods of time with negligible disease prevalence, followed by major outbreaks, as illustrated in Fig. 5.2 (d). In the limit $\tau \to \infty$, disconnected edges are never redrawn and the epidemic dies out, partially due to the network becoming sparser.

For the case without time delay, Gross et al. [64] found bistability in a large region of the parameter space, and periodic oscillations in a much smaller region. By contrast, results shown in Fig. 5.2 demonstrate a large region in the parameter space with oscillatory behaviour. DDEs are known to often produce oscillatory dynamics, and bubbles similar to those shown in Fig. 5.2 (b) have been reported in other biological and epidemic models [94, 101].

Let us now discuss the oscillatory behaviour in our model. The delay between disconnecting an edge and drawing a new one means that the total number of edges, and thus also the mean degree, is not constant. Whenever a susceptible node chooses to rewire, the total number of edges in the network decreases by two (since all edges are bidirectional) until time τ passes, and the edge is redrawn. The mean degree $k(t)$

at any time t can be calculated directly from this argument as follows,

$$k(t) = \langle k \rangle - 2\omega \int_{t-\tau}^{t} [SI](u)\, du. \tag{5.6}$$

Figure 5.2 (d) shows that oscillations are the result of the influence that the dynamics of $k(t)$ and $[I](t)$ have on each other. During the early stages of an outbreak with a high rewiring rate $k(t)$ falls rapidly, as susceptible nodes cut links in response to the propagation of the disease. If the value of τ is large enough, then after a certain time the number of edges in the network is small enough to effectively starve the disease of transmission routes, and prevalence falls. These edges are then redrawn at the same rate as they were cut τ time ago, and $k(t)$ grows, which allows the disease to spread again. Figure 5.2 (d) illustrates this behaviour both in simulation and in the mean-field model (5.4), showing how after the initial outbreak each new wave of infection is preceded by the recovery of network connectivity.

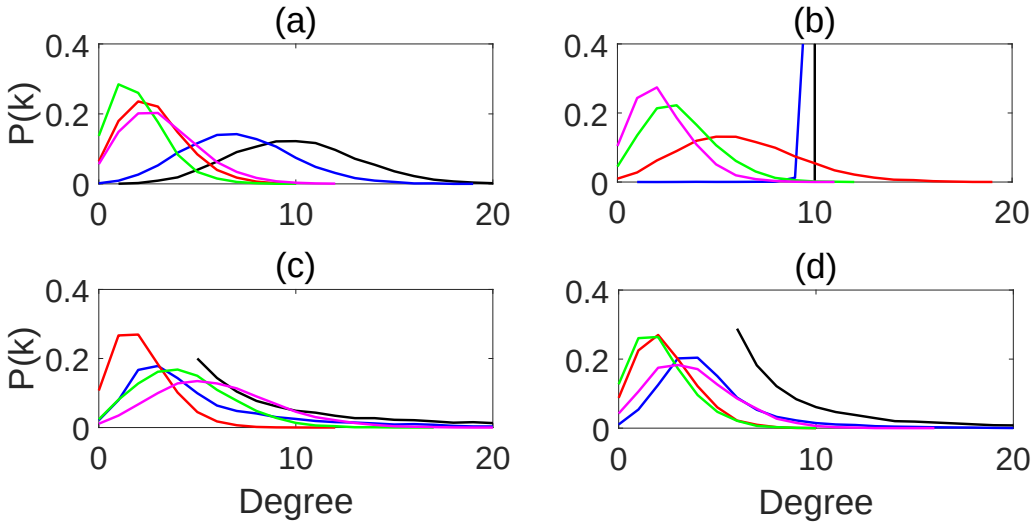

Figure 5.4: Snapshots of the degree distribution for networks of 10^4 nodes. In each plot the solid black solid is the initial degree distribution, the blue line is for the early growth phase, red shows the degree distribution at the initial peak of disease prevalence, and green and magenta later snapshots. Disease parameters are $\beta = 0.6$, $\gamma = 1$, $\omega = 1.4$, $\tau = 6$. (a) Erdős-Rényi network with $\langle k \rangle = 10$. (b) Homogeneous network with $k = 10$ for all nodes. (c), (d) Truncated scale-free networks with the scaling exponents $\alpha = 2$ and $\alpha = 3$, respectively.

The effect of oscillatory interactions between network connectivity and the propagating disease may be more pronounced in network simulations. Gross et al. [64] found

that adaptive rewiring without delay can lead to the formation of highly connected clusters of susceptible nodes that are vulnerable to disease once any one node becomes infected. Since the model (5.4) does not account for changes in network structure, i.e. the closure is the same for all times and it does not depend on the average degree or degree distribution, this can potentially explain the small discrepancy between the solution of the deterministic and simulation models observed in Fig. 5.1.

To get a better understanding of the interplay between network topology and dynamics, it is worth looking at how delayed rewiring alters degree distribution. Time snapshots of several large networks in Fig. 5.4 show the evolution of the degree distribution at various key points of an epidemic in an oscillatory regime. The initial network topology (black lines) is quickly reorganised to a peaked distribution. The oscillations in prevalence cause slight but repeated changes in the degree distribution. Unsurprisingly, when prevalence is at or near its peak, nodes with a lower degree are more common. When the prevalence falls, the distribution curves shift to the right, and the shape of the distribution flattens slightly. When the endemic steady state is stable, the degree distribution stabilises to a peaked distribution between the two extremes of the oscillatory regime. A very important observation is that irrespective of the initial network topology, due to rewiring different networks eventually settle on a very similar skewed degree distribution. This implies that earlier conclusions derived for the specific closure (5.1) appropriate for Erdős-Rényi graphs are actually applicable to modelling long-term dynamics of different types of networks, for which the influence of the initial topology is low since significant amount of rewiring has already taken place.

5.5 Discussion

The particular strength of this model lies in its ability to exhibit rich behaviour from a simple system of DDEs. Time delay captures the fact that finding alternative contacts takes time, and also during an epidemic many people try to temporarily reduce the number of their contacts. Such behaviour can be modelled using this delayed rewiring process. Previous work separated the processes of edge destruction and creation, and with edge creation occurring at a fixed rate, the number of edges in the network was bounded only by the network size [2, 72]. In the new model presented above, edge creation is reduced to replenishing global network connectivity towards its original level. Therefore, this model is fundamentally different to those earlier models, even

when parameters are matched.

During the initial growth phase it is the rate at which potential transmission is avoided by cutting a link, not the delay before drawing a new edge, that determines whether a major outbreak will occur. Although the delay does not affect the basic reproductive ratio R_0, it does impact the outcome of the epidemic (see Fig. 5.2 c). The result of introducing the delay is that oscillations occur in a large region of the parameter space. This happens due to the interplay between the spread of the disease and the behavioural changes in response to the epidemic. When the length of the delay is significant, the network becomes more sparse, healthy individuals are at lower risk of infection, and over time the prevalence falls. When the new edges are then formed, the disease is once again able to spread, and the cycle repeats.

Understanding the nature and cause of oscillations may provide opportunities to eradicate the disease. For example, if public awareness campaigns can lead to an increase in the length of the delay, the prevalence of the disease will naturally fall close to zero, at which time a relatively minor intervention, such as quarantining those who remain infected, may be enough to eradicate the disease from the population entirely.

Currently, the model assumes that only susceptible nodes rewire. However, in reality, infected nodes are also likely to change their behaviour. Risau-Gusman and Zanette [139] considered a model of rewiring where infected nodes rewire with a given probability. It would be of great value to examine a similar situation under delayed rewiring, with time delay representing the time for which infected nodes partially isolate themselves before rewiring, in accordance with advice given by public health authorities. This would alter the nature of the variable $x(t)$ in the model. For example, if only infected nodes rewire, $x(t) \approx e^{-\gamma\tau}$. Preliminary tests of this rewiring scheme show behaviour similar to the present model.

In addition to changing who rewires it would also be worthwhile to examine distributed delay models. One relatively straightforward approach would be to introduce a multi-stage approach. Once cut, an edge would change its state so that it is no longer active in the spread of the pathogen. It would then progress through some prescribed number of stages, W, according to some chosen rate. At the end of which, the edge would be rewired at random in the same manner described previously. The effect would be a gamma-distributed waiting time between edge deletion and rewiring similar to the gamma distributed infectious period achieved in Chapters 2 and 3 of this thesis. The limit of this would be either the model of Gross et al. [64] where rewiring is immediate

($W = 0$) or the system (5.4) ($W \to \infty$). Other distributions can be modelled with distributed delay differential equations. Any novel distribution for the waiting time should be chosen based on evidence from real-world data on behaviour modification.

Numerical simulations have shown that a similar oscillatory behaviour is observed for other initial network topologies, including scale-free networks. Furthermore, since rewiring nodes choose their new neighbours uniformly at random from all unconnected susceptible nodes, the initial network topology itself is transient, as shown in Fig. 5.4, and, as a result, over time our model becomes more relevant. A more thorough examination of limiting network behaviour is needed. Our initial investigation was based on studying a handful of network snapshots taken at qualitatively different points of the epidemic (e.g. initial growth, decline, local extrema). One particularly interesting approach could be to construct a discrete time model based on the same assumptions. It should then be possible to look at changes to the network structure in more detail, and potentially at each individual time step.

Future work will look at how the degree distribution and oscillations are affected in the case when the network links are rewired not randomly but according to a preferential attachment or some fitness-based rule. This could result in some interesting new dynamics due to the competition between the increased probability of highly-connected nodes receiving new links, and the increased probability of infection.

Acknowledgements

The authors are grateful to anonymous reviewers for their helpful comments and suggestions. N. Sherborne acknowledges funding for his PhD studies from the EPSRC, EP/M506667/1, and the University of Sussex.

Chapter 6

Discussion

This thesis presented a contribution to the field of epidemiology focused on the spread of infectious disease on networks. Specifically, it dealt with the construction and analysis of models with non-Markovian dynamics. This final Chapter presents a review of the main results as well as possible extensions and areas for future research where they arise.

In Chapter 2, the research paper entitled "Dynamics of multi-stage infections on networks" we focused on a gamma-distributed infectious period characterised within the model by subdividing the infectious compartment into K stages. This is known as the $\mathrm{SI}^K\mathrm{R}$ model [103]. We began by summarising the known results for the case where the population is homogeneously well-mixed. This included the basic reproductive ratio and the final epidemic size, both of which do not depend on the number of infectious stages [73, 105]. To show the impact that K has on the dynamics of the spread we gave examples of how the trajectories change when K is changed but all other parameters remain identical, this was analytically reinforced by results for the early-stage epidemic growth rate which we summarised and verified [168].

We then moved on to network modelling. The new multi-stage pairwise model was constructed based on the classical structure and closures [84]. We used linear stability analysis to find a threshold parameter $\mathcal{R}$ and, using knowledge of the equivalent stochastic network model, we were able to link this to the transmissibility of the disease to give an intuitive result. Extending the work of Keeling [84], we were able to use first-integral relations to give a proof for the final epidemic size directly from the new model. Both of these quantities depend on K, with larger K increasing $\mathcal{R}$ and the final epidemic size. This result contrasts with the same model in homogeneous randomly mixing populations and highlights the importance of representing social structures.

The model was then used with numerical simulation to illustrate the importance of considering the shape of the infectious period distribution. Previous studies have used the gamma distribution to approximate the infectious period for numerous diseases [168]. Using these estimates we showed how the trajectory of an epidemic in a network using our model can be dramatically different than the classical Markovian models would predict. We also observed excellent agreement between the pairwise model and simulation.

Further extensions to this model may include considering the impact of a multi-stage approach in SIS models on networks and examining whether the threshold parameter is the same and how the endemic equilibrium is affected by changing the number of infectious stages. This would be particularly useful given the comparative lack of options for non-Markovian SIS models on networks. Another practical extension would be to consider a latent compartment comprised of multiple stages. This has been studied with well-mixed models [168]. However, we have shown that incorporating network structure can render findings based on well-mixed populations inaccurate and misleading. Thus, revisiting such studies could be beneficial.

In constructing the model we made several unrealistic assumptions, not least that the contact network was regular and unclustered. These are major simplifications, and ones which are often violated by real-world networks [167, 26, 99]. Therefore we decided to generalise the model to heterogeneous and clustered networks in Chapter 3, the research paper "Compact pairwise models for epidemics with multiple infectious stages on degree heterogeneous and clustered networks". While we were still able to recover a threshold parameter $\mathcal{R}$ the first integral relations previously used to find the final epidemic size break down under the new closure and thus we were unable to find an analytic expression. When clustering was introduced in the model the required size of the system grew from $2K+3$ equations to K^2+3K+4 due to the added complexity of the closures. We observed good agreement with numerical simulation for all degree distributions that we tested and for zero or low levels of clustering. In constructing the model we assumed that the degree distribution of susceptible nodes is linearly related to the overall degree distribution in order to derive the closures, an approach previously used for SIS dynamics [151]. The accuracy of this approximation cannot be guaranteed, although this was not significantly detrimental to the accuracy of the model. Analysis of closure approximations and their accuracy is crucial to improving our understanding and the quality of our models. Thorough studies on toy networks and motifs are a

fundamental part of this [133]. Despite clustering being ever-present in data collected on real networks [128, 66] it is relatively rarely studied. Future research must tackle this disparity.

In Chapter 4, the research paper titled "Mean-field models for non-Markovian epidemics on networks" we introduced a new EBCM and provided a full explanation of its construction. This model extends the original [119] to general independent transmission and recovery processes. The major result of the paper is the full proof that the new EBCM is equivalent to the MP method of Karrer and Newman [80]. A direct consequence is that the new model is exact on the ensemble of CM networks in the limit of infinite size. We also show that the well known final epidemic size result [126] can be retrieved directly from the EBCM.

We go on to impose an exponentially distributed transmission process and derive a pairwise-like model from the MP equations [169]. This is used as the basis for a model hierarchy where, under further conditions, many well known models are recovered. Not only does this validate many models which were originally constructed heuristically, it can also reconcile disparate modelling paradigms. There are many different models in existence and more are always being proposed. Efforts to identify model equivalences and hierarchies [70, 120, 169] should be encouraged, as we believe that it will lead to a more unified approach to tackling future problems and infectious disease threats. There are numerous valuable options for future research based on this work. The original EBCM was applied to dynamic networks [119] and we see no reason why this new model cannot also be extended in this manner. Furthermore, the model is limited to unclustered networks. Efforts have been made to quantify threshold parameters and final epidemic size using percolation theory on clustered networks [147, 115], and there may be scope to extend these to MP or EBCM methods. Another option would be to use muliplex networks, an upcoming paper applied the methods of the EBCM to a dual-layer network with a static clustered layer and an adaptively rewiring layer [12]. However, more work in this area needs to be done.

Considering the real-world causes and effects of behavioural changes led us to consider a delayed rewiring process in Chapter 5, entitled "Bursting endemic bubbles in an adaptive network". Here we imposed a fixed length delay in the rewiring process between a susceptible node disconnecting from an infectious neighbour and randomly selecting a susceptible to be a new neighbour, in contrast to previous work which has assumed that these processes occurred in the same instant [64, 65, 119]. Inspired by

Kiss et al. [92] we correctly modelled the potential for nodes waiting to rewire to be infected by an infectious neighbour they had not yet disconnected from. Model analysis found the threshold parameter and an analytical expression for the mean node degree at any time t. We were limited to numerical methods to analyse the stability of the endemic equilibrium. This analysis revealed the presence of enclosed regions of the parameter space where oscillations occur, known as endemic bubbles. Oscillatory behaviour is found in a much larger region of the parameter space when the delay is included in the model, we suggest this is due to total network connectivity decreasing in response to the disease. Although the model only directly applies to unclustered random graphs we showed that the network topology is transient due to the rewiring process, and thus initial network topology is only a factor in the early stages of the epidemic. The model was designed to be as simple as possible and as a result it can be extended or generalised in many different ways. More work should be done to study how the network topology evolves over time and, if possible, to try and find evidence of similar changes in real-world networks. It would be particularly useful to study general, distributed delays in the rewiring process and to consider documented behavioural changes and how long they last [144, 57, 145]. Such comparisons remain rare in the literature despite the increasing attention paid to the topic [161].

The model assumes that the level and rate of response remains constant, and individuals have perfect information on the state of all others in the network. These are both unlikely to be true. Other behaviours and influences on behaviour have been suggested, such as belief-based models where avoidance is based on the perceived threat or prevalence of disease, allowing media influence or hysteria to be explicitly considered; others have modelled disease awareness spreading through a network in a similar way to the disease itself. See Manfredi et al. [107] for examples. Within the delayed rewiring model, these approached could influence which nodes cut edges, and what they do afterwards.

Lastly, applying this approach to SIR dynamics could reproduce epidemics which feature multiple peaks before dying out, such as the recent H1N1 influenza outbreak [27].

Constructing and analysing non-Markovian models for the spread of infectious disease is likely to remain a challenge for years to come. Paradigms such as the EBCM or MP achieve success in this regard but still have limitations. Both models assume that the neighbours of a node can be considered independent of each other. Difficulties

arise when it comes to clustered networks, multiple paths between nodes violates the assumption of independence of neighbours. For now at least we are limited to approximate models or models with specific definitions of clustering. This assumption also breaks down when the disease confers no immunity or when immunity wanes. New modelling paradigms will likely be needed before exact SIS (and SIRS, etc.) models exist with the same generality.

Within the growing field of adaptive networks there are several issues which must be dealt with. For instance, the majority of models are constructed without using real data for validation or parametrization [161]. In many cases, the behavioural response may be influenced more by information spreading on a different network, such as social media, than the physical contact network.

Clearly, the main goal of modelling epidemic dynamics is to inhibit or even prevent major outbreaks of infectious disease. While they have not been explicitly discussed within this thesis, control procedures - such as vaccination, quarantining and ensuring improved hygiene - are the major part of this, and must be included in modelling scenarios. However, to make good decisions the models must represent reality as closely as possible. The models in this thesis show the importance of this, and highlight phenomena that are rare in the more established Markovian models.

A coordinated effort between modelling and data gathering, taking advantage of the latest tools for studying behaviour and tracking epidemic spread has the best chance of answering these questions and providing new insight when it comes to controlling and preventing future infectious disease epidemics.

Bibliography

[1] R. Albert and A.-L. Barabási. Statistical mechanics of complex networks. *Rev. Mod. Phys*, 74(1):47, 2002.

[2] B. M. Althouse and L. Hébert-Dufresne. Epidemic cycles driven by host behaviour. *J. R. Soc. Interface*, 11(99):20140575, 2014.

[3] S. Altizer, A. Dobson, P. Hosseini, P. Hudson, M. Pascual, and P. Rohani. Seasonality and the dynamics of infectious diseases. *Ecol. Lett.*, 9(4):467–484, 2006.

[4] D. Anderson and R. Watson. On the spread of a disease with gamma distributed latent and infectious periods. *Biometrika*, 67(1):191–198, 1980.

[5] D. F. Anderson. A modified next reaction method for simulating chemical systems with time dependent propensities and delays. *J. Chem. Phys.*, 127(21):214107, 2007.

[6] R. M. Anderson and R. M. May. *Infectious diseases of humans: dynamics and control*, volume 1. Oxford University Press, Oxford, 1991.

[7] V. Andreasen. The final size of an epidemic and its relation to the basic reproduction number. *Bull. Math. Biol*, 73(10):2305–2321, 2011.

[8] N. T. J. Bailey. A statistical method of estimating the periods of incubation and infection of an infectious disease. *Nature*, 174(4420):139–140, 1954.

[9] S. Bansal, B. T. Grenfell, and L. A. Meyers. When individual behaviour matters: homogeneous and network models in epidemiology. *J. R. Soc. Interface*, 4(16):879–891, 2007.

[10] S. Bansal, S. Khandelwal, and L. A. Meyers. Exploring biological network structure with clustered random networks. *BMC Bioinformatics*, 10(1):405, 2009.

[11] A.-L. Barabási and R. Albert. Emergence of scaling in random networks. *Science*, 286(5439):509–512, 1999.

[12] R. C. Barnard, I. Z. Kiss, L. Berthouze, and J. C. Miller. Edge-based compartmental modelling of an SIR epidemic on a dual-layer static-dynamic multiplex network with tunable clustering. *arXiv preprint arXiv:1801.01337*, 2018.

[13] M. Barrio, K. Burrage, A. Leier, and T. Tian. Oscillatory regulation of Hes1: discrete stochastic delay modelling and simulation. *PLoS Comput. Biol.*, 2(9):e117, 2006.

[14] C. T. Bauch, J. O. Lloyd-Smith, M. P. Coffee, and A. P. Galvani. Dynamically modeling SARS and other newly emerging respiratory illnesses: past, present, and future. *Epidemiology*, 16(6):791–801, 2005.

[15] E. A. Bender and E. R. Canfield. The asymptotic number of labeled graphs with given degree sequences. *J. Comb. Theory A*, 24(3):296–307, 1978.

[16] A. J. Black and J. Ross. Computation of epidemic final size distributions. *J. Theor. Biol*, 367:159–165, 2015.

[17] K. B. Blyuss and Y. N. Kyrychko. Stability and bifurcations in an epidemic model with varying immunity period. *Bull. Math. Biol*, 72(2):490–505, 2010.

[18] S. Boccaletti, V. Latora, Y. Moreno, M. Chavez, and D.-U. Hwang. Complex networks: Structure and dynamics. *Physics reports*, 424(4-5):175–308, 2006.

[19] M. Boguná, L. F. Lafuerza, R. Toral, and M. Á. Serrano. Simulating non-Markovian stochastic processes. *Phys. Rev. E*, 90(4):042108, 2014.

[20] B. Bollobás. A probabilistic proof of an asymptotic formula for the number of labelled regular graphs. *European J. Combin*, 1(4):311–316, 1980.

[21] D. Bratsun, D. Volfson, L. S. Tsimring, and J. Hasty. Delay-induced stochastic oscillations in gene regulation. *Proc. Natl. Acad. Sci. U.S.A*, 102(41):14593–14598, 2005.

[22] R. Breban, V. Supervie, J. T. Okano, R. Vardavas, and S. Blower. Is there any evidence that syphilis epidemics cycle? *Lancet Infect. Dis.*, 8(9):577–581, 2008.

[23] S. R. Broadbent and J. M. Hammersley. Percolation processes: I. crystals and mazes. *Math. Proc. Camb. Philos. Soc*, 53(3):629–641, 1957.

[24] D. Brockmann, L. Hufnagel, and T. Geisel. The scaling laws of human travel. *Nature*, 439(7075):462–465, 2006.

[25] T. L. Burr and G. Chowell. Signatures of non-homogeneous mixing in disease outbreaks. *Math. Comp. Model*, 48(1-2):122–140, 2008.

[26] G. Caldarelli, R. Marchetti, and L. Pietronero. The fractal properties of Internet. *Europhys. Lett*, 52(4):386–391, 2000.

[27] C. Campbell, O. Mytton, E. McLean, P. Rutter, R. Pebody, N. Sachedina, P. White, C. Hawkins, B. Evans, P. Waight, et al. Hospitalization in two waves of pandemic influenza A (H1N1) in England. *Epidemiol. Infect*, 139(10):1560–1569, 2011.

[28] E. Cator, R. Van de Bovenkamp, and P. Van Mieghem. Susceptible-infected-susceptible epidemics on networks with general infection and cure times. *Phys. Rev. E*, 87(6):062816, 2013.

[29] C. Cattuto, W. Van den Broeck, A. Barrat, V. Colizza, J.-F. Pinton, and A. Vespignani. Dynamics of person-to-person interactions from distributed RFID sensor networks. *PloS One*, 5(7):e11596, 2010.

[30] S. Cauchemez, F. Carrat, C. Viboud, A. Valleron, and P. Boelle. A Bayesian MCMC approach to study transmission of influenza: application to household longitudinal data. *Stat. Med*, 23(22):3469–3487, 2004.

[31] A. Chaintreau, P. Hui, J. Crowcroft, C. Diot, R. Gass, and J. Scott. Impact of human mobility on opportunistic forwarding algorithms. *IEEE Trans. Mob. Comp.*, 6(6):606–620, 2007.

[32] W.-Y. Chen and S. Bokka. Stochastic modeling of nonlinear epidemiology. *J. Theor. Biol*, 234(4):455–470, 2005.

[33] G. Chowell and H. Nishiura. Transmission dynamics and control of Ebola virus disease (EVD): a review. *BMC medicine*, 12(1):196, 2014.

[34] D. Cox and H. Miller. *The Theory of Stochastic Processes*. Chapman and Hall, London, 1965.

[35] L. Danon, A. P. Ford, T. House, C. P. Jewell, M. J. Keeling, G. O. Roberts, J. V. Ross, and M. C. Vernon. Networks and the epidemiology of infectious disease. *Interdisciplinary perspectives on infectious diseases*, 2011.

[36] O. Diekmann, M. De Jong, and J. A. J. Metz. A deterministic epidemic model taking account of repeated contacts between the same individuals. *J. Appl. Prob*, 35(2):448–462, 1998.

[37] O. Diekmann, H. Heesterbeek, and T. Britton. *Mathematical Tools for Understanding Infectious Disease Dynamics*. Princeton University Press, Princeton, 2012.

[38] O. Diekmann and J. Heesterbeek. *Mathematical epidemiology of infectious diseases: model building, analysis and interpretation*, volume 5. John Wiley & Sons, 2000.

[39] O. Diekmann and J. A. P. Heesterbeek. *Mathematical epidemiology of infectious diseases: model building, analysis and interpretation*, volume 5. John Wiley & Sons, 2000.

[40] K. Dietz and J. Heesterbeek. Daniel Bernoulli's epidemiological model revisited. *Math. Biosci*, 180(1-2):1–21, 2002.

[41] C. A. Donnelly, A. C. Ghani, G. M. Leung, A. J. Hedley, C. Fraser, S. Riley, L. J. Abu-Raddad, L.-M. Ho, T.-Q. Thach, P. Chau, et al. Epidemiological determinants of spread of causal agent of severe acute respiratory syndrome in Hong Kong. *Lancet*, 361(9371):1761–1766, 2003.

[42] R. Durrett. *Probability: theory and examples*. Cambridge University Press, 2010.

[43] K. T. Eames. Modelling disease spread through random and regular contacts in clustered populations. *Theor. Popul. Biol*, 73(1):104–111, 2008.

[44] K. T. Eames and M. J. Keeling. Modeling dynamic and network heterogeneities in the spread of sexually transmitted diseases. *Proc. Nat. Acad. Sci.*, 99(20):13330–13335, 2002.

[45] K. T. Eames and M. J. Keeling. Contact tracing and disease control. *Proc. R. Soc. B*, 270(1533):2565–2571, 2003.

[46] P. Erdős and A. Rényi. On random graphs I. *Publ. Math. Debrecen*, 6:290–297, 1959.

[47] Z. Feng. Final and peak epidemic sizes for SEIR models with quarantine and isolation. *Math. Biosci. Eng*, 4(4):675–686, 2007.

[48] N. M. Ferguson, D. A. Cummings, C. Fraser, J. C. Cajka, P. C. Cooley, and D. S. Burke. Strategies for mitigating an influenza pandemic. *Nature*, 442(7101):448, 2006.

[49] N. M. Ferguson, M. J. Keeling, W. J. Edmunds, R. Gani, B. T. Grenfell, R. M. Anderson, and S. Leach. Planning for smallpox outbreaks. *Nature*, 425(6959):681, 2003.

[50] B. S. Finkelman, C. Viboud, K. Koelle, M. J. Ferrari, N. Bharti, and B. T. Grenfell. Global patterns in seasonal activity of influenza A/H3N2, A/H1N1, and B from 1997 to 2005: viral coexistence and latitudinal gradients. *PloS One*, 2(12):e1296, 2007.

[51] D. V. Foster, J. G. Foster, P. Grassberger, and M. Paczuski. Clustering drives assortativity and community structure in ensembles of networks. *Phys. Rev. E*, 84(6):066117, 2011.

[52] S. Funk, E. Gilad, C. Watkins, and V. A. Jansen. The spread of awareness and its impact on epidemic outbreaks. *Proc. Natl. Acad. Sci*, 106(16):6872–6877, 2009.

[53] S. Funk, M. Salathé, and V. A. Jansen. Modelling the influence of human behaviour on the spread of infectious diseases: a review. *J. R. Soc. Interface*, 7(50):1247–1256, 2010.

[54] I. Gel'fand and G. Shilov. *Generalized Functions, Volume 1.* Academic Press, 1964.

[55] D. T. Gillespie. Exact stochastic simulation of coupled chemical reactions. *J. Phys. Chem.*, 81(25):2340–2361, 1977.

[56] J. O. Giraldo and D. H. Palacio. Deterministic SIR (Susceptible–Infected–Removed) models applied to varicella outbreaks. *Epidemiol. Infect*, 136(5):679–687, 2008.

[57] R. Goodwin, S. Haque, F. Neto, and L. B. Myers. Initial psychological responses to influenza A, H1N1 ("Swine flu"). *BMC Infectious Diseases*, 9(1):166, 2009.

[58] K. Gough. The estimation of latent and infectious periods. *Biometrika*, 64(3):559–565, 1977.

[59] N. C. Grassly and C. Fraser. Seasonal infectious disease epidemiology. *Proc. R. Soc. B*, 273(1600):2541–2550, 2006.

[60] N. C. Grassly, C. Fraser, and G. P. Garnett. Host immunity and synchronized epidemics of syphilis across the United States. *Nature*, 433(7024):417–422, 2005.

[61] D. M. Green and I. Z. Kiss. Large-scale properties of clustered networks: Implications for disease dynamics. *J. Biol. Dyn.*, 4(5):431–445, 2010.

[62] D. Greenhalgh, S. Rana, S. Samanta, T. Sardar, S. Bhattacharya, and J. Chattopadhyay. Awareness programs control infectious disease–multiple delay induced mathematical model. *Appl. Math. Comput*, 251:539–563, 2015.

[63] T. Gross and B. Blasius. Adaptive coevolutionary networks: a review. *J. R. Soc. Interface*, 5(20):259–271, 2008.

[64] T. Gross, C. J. D. D'Lima, and B. Blasius. Epidemic dynamics on an adaptive network. *Phys. Rev. Lett*, 96(20):208701, 2006.

[65] T. Gross and I. G. Kevrekidis. Robust oscillations in SIS epidemics on adaptive networks: Coarse graining by automated moment closure. *Europhys. Lett*, 82(3):38004, 2008.

[66] J. W. Grossman. The evolution of the mathematical research collaboration graph. *Congressus Numerantium*, 158:201–212, 2002.

[67] H. W. Hethcote, H. W. Stech, and P. Van Den Driessche. Nonlinear oscillations in epidemic models. *SIAM J. Appl. Math.*, 40(1):1–9, 1981.

[68] H. W. Hethcote and D. W. Tudor. Integral equation models for endemic infectious diseases. *J. Math. Biol*, 9(1):37–47, 1980.

[69] T. House and M. J. Keeling. Epidemic prediction and control in clustered populations. *J. Theor. Biol.*, 272(1):1–7, 2011.

[70] T. House and M. J. Keeling. Insights from unifying modern approximations to infections on networks. *J. R. Soc. Interface*, 8(54):67–73, 2011.

[71] T. House, J. V. Ross, and D. Sirl. How big is an outbreak likely to be? Methods for epidemic final-size calculation. *Proc. R. Soc. A*, 469(2150):20120436, 2013.

[72] C. Huepe, G. Zschaler, A.-L. Do, and T. Gross. Adaptive-network models of swarm dynamics. *New J. Phys*, 13(7):073022, 2011.

[73] J. M. Hyman, J. Li, and E. A. Stanley. The differential infectivity and staged progression models for the transmission of HIV12. *Math. Biosci*, 155(2):77–109, 1999.

[74] I. Ito, T. Ishida, M. Osawa, M. Arita, T. Hashimoto, T. Hongo, and M. Mishima. Culturally verified mycoplasma pneumoniae pneumonia in japan: a long-term observation from 1979–99. *Epidemiol. Infect*, 127(2):365–367, 2001.

[75] A. James, J. W. Pitchford, and M. J. Plank. An event-based model of superspreading in epidemics. *Proc. R. Soc. B*, 274(1610):741–747, 2007.

[76] M. A. Jhung, D. Swerdlow, S. J. Olsen, D. Jernigan, M. Biggerstaff, L. Kamimoto, K. Kniss, C. Reed, A. Fry, L. Brammer, et al. Epidemiology of 2009 pandemic influenza A (H1N1) in the United States. *Clin. Infect. Dis.*, 52(suppl_1):S13–S26, 2011.

[77] H.-H. Jo, M. Karsai, J. Kertész, and K. Kaski. Circadian pattern and burstiness in mobile phone communication. *New J. Phys*, 14(1):013055, 2012.

[78] P. W. Jones and P. Smith. *Stochastic processes: an introduction*. 2nd edn. CRC Press, 2017.

[79] E. H. Kaplan, D. L. Craft, and L. M. Wein. Emergency response to a smallpox attack: the case for mass vaccination. *Proc. Natl. Acad. Sci. U.S.A*, 99(16):10935–10940, 2002.

[80] B. Karrer and M. E. J. Newman. Message passing approach for general epidemic models. *Phys. Rev. E*, 82(1):016101, 2010.

[81] B. Karrer and M. E. J. Newman. Random graphs containing arbitrary distributions of subgraphs. *Phys. Rev. E*, 82(6):066118, 2010.

[82] M. Keeling, D. Rand, and A. Morris. Correlation models for childhood epidemics. *Proc. R. Soc. B*, 264(1385):1149–1156, 1997.

[83] M. Keeling and P. Rohani. Modeling infectious diseases in humans and animals. *Clin. Infect. Dis*, 47:864–6, 2008.

[84] M. J. Keeling. The effects of local spatial structure on epidemiological invasions. *Proc. R. Soc. B.*, 266(1421):859–867, 1999.

[85] M. J. Keeling and K. T. Eames. Networks and epidemic models. *J. R. Soc. Interface*, 2(4):295–307, 2005.

[86] M. J. Keeling and B. Grenfell. Disease extinction and community size: modeling the persistence of measles. *Science*, 275(5296):65–67, 1997.

[87] M. J. Keeling and B. T. Grenfell. Understanding the persistence of measles: reconciling theory, simulation and observation. *Proc. R. Soc. B*, 269(1489):335–343, 2002.

[88] E. Kenah and J. M. Robins. Second look at the spread of epidemics on networks. *Phys. Rev. E*, 76(3):036113, 2007.

[89] W. Kermack and A. McKendrick. A contribution to the mathematical theory of epidemics. *Proc. R. Soc. Lond. A*, 115(772):700–721, 1927.

[90] I. Z. Kiss, L. Berthouze, T. J. Taylor, and P. L. Simon. Modelling approaches for simple dynamic networks and applications to disease transmission models. *Proc. R. Soc. A*, 468(2141):1332–1355, 2012.

[91] I. Z. Kiss, J. C. Miller, and P. L. Simon. *Mathematics of epidemics on networks: from exact to approximate models*. Springer International Publishing, 2017.

[92] I. Z. Kiss, G. Röst, and Z. Vizi. Generalization of pairwise models to non-Markovian epidemics on networks. *Phys. Rev. Lett*, 115(7):078701, 2015.

[93] J. Koplan, M. Azizullah, and S. Foster. Urban hospital and rural village smallpox in Bangladesh. *Tropical and geographical medicine*, 30(3):355–358, 1978.

[94] T. Krisztin and E. Liz. Bubbles for a class of delay differential equations. *Qual. Theory Dynam. Sys.*, 10(2):169–196, 2011.

[95] Y. A. Kuznetsov and C. Piccardi. Bifurcation analysis of periodic SEIR and SIR epidemic models. *J. Math. Biol*, 32(2):109–121, 1994.

[96] Y. N. Kyrychko and K. B. Blyuss. Global properties of a delayed SIR model with temporary immunity and nonlinear incidence rate. *Nonlinear Anal*, 6(3):495–507, 2005.

[97] N. Lee, D. Hui, A. Wu, P. Chan, P. Cameron, G. M. Joynt, A. Ahuja, M. Y. Yung, C. Leung, K. To, et al. A major outbreak of severe acute respiratory syndrome in Hong Kong. *N. Engl. J. Med*, 348(20):1986–1994, 2003.

[98] R. S. Lee, J.-F. Proulx, D. Menzies, and M. A. Behr. Progression to tuberculosis disease increases with multiple exposures. *Eur. Respir. J*, 48(6):1682–1689, 2016.

[99] F. Liljeros, C. R. Edling, L. A. N. Amaral, H. E. Stanley, and Y. Åberg. The web of human sexual contacts. *Nature*, 411(6840):907–908, 2001.

[100] J. Lindquist, J. Ma, P. Van den Driessche, and F. H. Willeboordse. Effective degree network disease models. *J. Math. Biol*, 62(2):143–164, 2011.

[101] M. Liu, E. Liz, and G. Rost. Endemic bubbles generated by delayed behavioral response: global stability and bifurcation switches in an SIS model. *SIAM J. Appl. Math.*, 75(1):75–91, 2015.

[102] A. L. Lloyd. Destabilization of epidemic models with the inclusion of realistic distributions of infectious periods. *Proc. R. Soc. B*, 268(1470):985–993, 2001.

[103] A. L. Lloyd. Realistic distributions of infectious periods in epidemic models: changing patterns of persistence and dynamics. *Theor. Popul. Biol*, 60(1):59–71, 2001.

[104] A. L. Lloyd and R. M. May. How viruses spread among computers and people. *Science*, 292(5520):1316–1317, 2001.

[105] J. Ma and D. J. Earn. Generality of the final size formula for an epidemic of a newly invading infectious disease. *Bull. Math. Biol*, 68(3):679–702, 2006.

[106] N. MacDonald. *Time Lags in Biological Models*. Springer Berlin Heidelberg, 1978.

[107] P. Manfredi and A. D'Onofrio. *Modeling the interplay between human behavior and the spread of infectious diseases*. Springer Science & Business Media, 2013.

[108] N. Masuda, N. Konno, and K. Aihara. Transmission of severe acute respiratory syndrome in dynamical small-world networks. *Phys. Rev. E*, 69(3):031917, 2004.

[109] N. Masuda and L. E. Rocha. A Gillespie algorithm for non-Markovian stochastic processes. *SIAM Review*, 60(1):95–115, 2018.

[110] W. H. McNeill. *Plagues and peoples*. Anchor, 1976.

[111] J. McVernon, K. Mason, S. Petrony, P. Nathan, A. D. LaMontagne, R. Bentley, J. Fielding, D. M. Studdert, and A. Kavanagh. Recommendations for and compliance with social restrictions during implementation of school closures in the early phase of the influenza A (H1N1) 2009 outbreak in Melbourne, Australia. *BMC Infectious Diseases*, 11(1):257, 2011.

[112] M. I. Meltzer, I. Damon, J. W. LeDuc, and J. D. Millar. Modeling potential responses to smallpox as a bioterrorist weapon. *Emerg. Infect. Diseases*, 7(6):959, 2001.

[113] E. Miller, K. Hoschler, P. Hardelid, E. Stanford, N. Andrews, and M. Zambon. Incidence of 2009 pandemic influenza A H1N1 infection in England: a cross-sectional serological study. *Lancet*, 375(9720):1100–1108, 2010.

[114] J. C. Miller. Epidemic size and probability in populations with heterogeneous infectivity and susceptibility. *Phys. Rev. E*, 76:010101, 2007.

[115] J. C. Miller. Percolation and epidemics in random clustered networks. *Phys. Rev. E*, 80(2):020901, 2009.

[116] J. C. Miller. A note on the derivation of epidemic final sizes. *Bull. Math. Biol*, 74(9):2125–2141, 2012.

[117] J. C. Miller. Epidemics on networks with large initial conditions or changing structure. *PloS One*, 9(7):e101421, 2014.

[118] J. C. Miller and I. Z. Kiss. Epidemic spread in networks: Existing methods and current challenges. *Math. Model. Nat. Phenom*, 9(2):4–42, 2014.

[119] J. C. Miller, A. C. Slim, and E. M. Volz. Edge-based compartmental modelling for infectious disease spread. *J.R. Soc. Interface*, 9(70):890–906, 2012.

[120] J. C. Miller and E. M. Volz. Model hierarchies in edge-based compartmental modeling for infectious disease spread. *J. Math. Biol*, 67(4):869–899, 2013.

[121] R. G. Miller. *Survival analysis*, volume 66. John Wiley & Sons, 2011.

[122] M. Molloy and B. Reed. A critical point for random graphs with a given degree sequence. *Random structures & algorithms*, 6(2-3):161–180, 1995.

[123] M. Molloy and B. Reed. The size of the giant component of a random graph with a given degree sequence. *Comb. Probab. Comput*, 7(03):295–305, 1998.

[124] M. Newman. *Networks: an introduction*. Oxford university press, 2010.

[125] M. E. J. Newman. Assortative mixing in networks. *Phys. Rev. Lett*, 89(20):208701, 2002.

[126] M. E. J. Newman. Spread of epidemic disease on networks. *Phys. Rev. E*, 66(1):016128, 2002.

[127] M. E. J. Newman. Mixing patterns in networks. *Phys. Rev. E*, 67(2):026126, 2003.

[128] M. E. J. Newman, S. H. Strogatz, and D. J. Watts. Random graphs with arbitrary degree distributions and their applications. *Phys. Rev. E*, 64(2):026118, 2001.

[129] H. T. Nguyen and P. Rohani. Noise, nonlinearity and seasonality: the epidemics of whooping cough revisited. *J. R. Soc. Interface*, 5(21):403–413, 2008.

[130] L. Pasteur. On the extension of the germ theory to the etiology of certain common diseases. *Comptes Rendus de lAcademie des Sciences Paris*, pages 1033–44, 1880.

[131] R. Pastor-Satorras, C. Castellano, P. Van Mieghem, and A. Vespignani. Epidemic processes in complex networks. *Rev. Mod. Phys*, 87(3):925, 2015.

[132] R. Pastor-Satorras and A. Vespignani. Epidemic spreading in scale-free networks. *Phys. Rev. Lett*, 86(14):3200–3203, 2001.

[133] L. Pellis, T. House, and M. J. Keeling. Exact and approximate moment closures for non-Markovian network epidemics. *J. Theor. Biol.*, 382:160–177, 2015.

[134] P. Poletti, B. Caprile, M. Ajelli, and S. Merler. Uncoordinated human responses during epidemic outbreaks. In *Modeling the Interplay Between Human Behavior and the Spread of Infectious Diseases*, pages 79–91. Springer, 2013.

[135] D. A. Rand. *Advanced ecological theory: principles and applications*, chapter Correlation equations and pair approximations for spatial ecologies, pages 100–142. Oxford: Blackwell Science, 1999.

[136] P. Rattana, K. B. Blyuss, K. T. Eames, and I. Z. Kiss. A class of pairwise models for epidemic dynamics on weighted networks. *Bull. Math. Biol*, 75(3):466–490, 2013.

[137] P. Rattana, J. Miller, and I. Kiss. Pairwise and edge-based models of epidemic dynamics on correlated weighted networks. *Math. Model. Nat. Phenom*, 9(2):58–81, 2014.

[138] S. Riley, C. Fraser, C. A. Donnelly, A. C. Ghani, L. J. Abu-Raddad, A. J. Hedley, G. M. Leung, L.-M. Ho, T.-H. Lam, T. Q. Thach, et al. Transmission dynamics of the etiological agent of SARS in Hong Kong: impact of public health interventions. *Science*, 300(5627):1961–1966, 2003.

[139] S. Risau-Gusmán and D. H. Zanette. Contact switching as a control strategy for epidemic outbreaks. *J. Theor. Biol*, 257(1):52–60, 2009.

[140] M. Ritchie, L. Berthouze, T. House, and I. Z. Kiss. Higher-order structure and epidemic dynamics in clustered networks. *J. Theor. Biol*, 348:21–32, 2014.

[141] M. Ritchie, L. Berthouze, and I. Z. Kiss. Beyond clustering: Mean-field dynamics on networks with arbitrary subgraph composition. *J. Mat. Biol.*, 72(1):255–281, 2015.

[142] C. Rizzo, M. Fabiani, R. Amlôt, I. Hall, T. Finnie, G. J. Rubin, R. Cucuiu, A. Pistol, F. Popovici, R. Popescu, et al. Survey on the likely behavioural changes of the general public in four European countries during the 2009/2010 pandemic. In *Modeling the Interplay Between Human Behavior and the Spread of Infectious Diseases*, pages 23–41. Springer, 2013.

[143] G. Röst, Z. Vizi, and I. Kiss. Pairwise approximation for SIR-type network epidemics with non-Markovian recovery. *Proc. R. Soc. A*, 474(2210):20170695, 2018.

[144] G. J. Rubin, R. Amlôt, L. Page, and S. Wessely. Public perceptions, anxiety, and behaviour change in relation to the swine flu outbreak: cross sectional telephone survey. *BMJ*, 339:b2651, 2009.

[145] M. Z. Sadique, W. J. Edmunds, R. D. Smith, W. Jan Meerding, O. De Zwart, J. Brug, and P. Beutels. Precautionary behavior in response to perceived threat of pandemic influenza. *Emerg. Infect. Dis*, 13(9):1307–1313, 2007.

[146] F. Sélley, Á. Besenyei, I. Z. Kiss, and P. L. Simon. Dynamic control of modern, network-based epidemic models. *SIAM J. Appl. Dyn. Syst.*, 14(1):168–187, 2015.

[147] M. Á. Serrano and M. Boguñá. Percolation and epidemic thresholds in clustered networks. *Phys. Rev. Lett.*, 97(8):088701, 2006.

[148] K. J. Sharkey, C. Fernandez, K. L. Morgan, E. Peeler, M. Thrush, J. F. Turnbull, and R. G. Bowers. Pair-level approximations to the spatio-temporal dynamics of epidemics on asymmetric contact networks. *J. Math. Biol*, 53(1):61–85, 2006.

[149] N. Sherborne, K. B. Blyuss, and I. Z. Kiss. Dynamics of multi-stage infections on networks. *Bull. Math. Biol*, 77(10):1909–1933, 2015.

[150] M. S. Shkarayev, I. Tunc, and L. B. Shaw. Epidemics with temporary link deactivation in scale-free networks. *J. Phys. A*, 47(45):455006, 2014.

[151] P. L. Simon and I. Z. Kiss. Super compact pairwise model for SIS epidemic on heterogeneous networks. *J. Comp. Net.*, 4(2):187–200, 2016.

[152] R. H. Simpson et al. Infectiousness of communicable diseases in the household (measles, chickenpox, and mumps). *Lancet*, 260:549–554, 1952.

[153] T. Takaguchi, N. Masuda, and P. Holme. Bursty communication patterns facilitate spreading in a threshold-based epidemic dynamics. *PloS One*, 8(7):e68629, 2013.

[154] M. Taylor, P. L. Simon, D. M. Green, T. House, and I. Z. Kiss. From Markovian to pairwise epidemic models and the performance of moment closure approximations. *J. Math. Biol*, 64(6):1021–1042, 2012.

[155] T. J. Taylor and I. Z. Kiss. Interdependency and hierarchy of exact and approximate epidemic models on networks. *J. Math. Biol.*, 69(1):183–211, 2014.

[156] W. E. R. Team. Ebola virus disease in West Africa - The first 9 months of the epidemic and forward projections. *N. Engl. J. Med.*, 371(16):1481–1495, 2014.

[157] D. Thompson, P. Muriel, D. Russell, P. Osborne, A. Bromley, M. Rowland, S. Creigh-Tyte, and C. Brown. Economic costs of the foot and mouth disease outbreak in the united kingdom in 2001. *Revue scientifique et technique (International Office of Epizootics)*, 21(3):675–687, 2002.

[158] I. Tunc, M. S. Shkarayev, and L. B. Shaw. Epidemics in adaptive social networks with temporary link deactivation. *J. Stat. Phys.*, 151(1-2):355–366, 2013.

[159] P. Van den Driessche and J. Watmough. Reproduction numbers and sub-threshold endemic equilibria for compartmental models of disease transmission. *Math. Biosci*, 180(1-2):29–48, 2002.

[160] A. Vazquez, B. Rácz, A. Lukács, and A.-L. Barabási. Impact of non-Poissonian activity patterns on spreading processes. *Phys. Rev. Lett*, 98(15):158702, 2007.

[161] F. Verelst, L. Willem, and P. Beutels. Behavioural change models for infectious disease transmission: a systematic review (2010–2015). *J. R. Soc. Interface*, 13(125):20160820, 2016.

[162] E. Volz. SIR dynamics in random networks with heterogeneous connectivity. *J. Math. Biol*, 56(3):293–310, 2008.

[163] E. M. Volz, J. C. Miller, A. Galvani, and L. A. Meyers. Effects of heterogeneous and clustered contact patterns on infectious disease dynamics. *PLoS Comput. Biol.*, 7(6):e1002042, 2011.

[164] K. B. Waites and D. F. Talkington. Mycoplasma pneumoniae and its role as a human pathogen. *Clin. Microbiol. Rev.*, 17(4):697–728, 2004.

[165] W. Wang, M. Tang, H.-F. Zhang, H. Gao, Y. Do, and Z.-H. Liu. Epidemic spreading on complex networks with general degree and weight distributions. *Phys. Rev. E*, 90(4):042803, 2014.

[166] S. Wasserman and K. Faust. *Social network analysis: Methods and applications*. Cambridge university press, 1994.

[167] D. J. Watts and S. H. Strogatz. Collective dynamics of small-world networks. *Nature*, 393(6684):440–442, 1998.

[168] H. J. Wearing, P. Rohani, and M. J. Keeling. Appropriate models for the management of infectious diseases. *PLoS Medicine*, 2(7):e174, 2005.

[169] R. R. Wilkinson, F. G. Ball, and K. J. Sharkey. The relationships between message passing, pairwise, Kermack–McKendrick and stochastic SIR epidemic models. *J. Math. Biol*, 75(6-7):1563–1590, 2017.

[170] R. R. Wilkinson and K. J. Sharkey. Message passing and moment closure for susceptible-infected-recovered epidemics on finite networks. *Phys. Rev. E*, 89(2):022808, 2014.

[171] J. A. Yorke, H. W. Hethcote, and A. Nold. Dynamics and control of the transmission of gonorrhea. *Sex. Transm. Dis*, 5(2):51–56, 1978.

[172] H. Zhang, M. Small, X. Fu, G. Sun, and B. Wang. Modeling the influence of information on the coevolution of contact networks and the dynamics of infectious diseases. *Physica D*, 241(18):1512–1517, 2012.

[173] J. Zhou, G. Xiao, S. A. Cheong, X. Fu, L. Wong, S. Ma, and T. H. Cheng. Epidemic reemergence in adaptive complex networks. *Phys. Rev. E*, 85(3):036107, 2012.